INFORMATION TO USERS

This manuscript has been reproduced from the microfilm master. UMI films the text directly from the original or copy submitted. Thus, some thesis and dissertation copies are in typewriter face, while others may be from any type of computer printer.

The quality of this reproduction is dependent upon the quality of the copy submitted. Broken or indistinct print, colored or poor quality illustrations and photographs, print bleedthrough, substandard margins, and improper alignment can adversely affect reproduction.

In the unlikely event that the author did not send UMI a complete manuscript and there are missing pages, these will be noted. Also, if unauthorized copyright material had to be removed, a note will indicate the deletion.

Oversize materials (e.g., maps, drawings, charts) are reproduced by sectioning the original, beginning at the upper left-hand corner and continuing from left to right in equal sections with small overlaps.

Photographs included in the original manuscript have been reproduced xerographically in this copy. Higher quality 6" x 9" black and white photographic prints are available for any photographs or illustrations appearing in this copy for an additional charge. Contact UMI directly to order.

Bell & Howell Information and Learning
300 North Zeeb Road, Ann Arbor, MI 48106-1346 USA
800-521-0600

EFFECT OF HIGH-STRENGTH CONCRETE ON THE PERFORMANCE OF SLAB-COLUMN SPECIMENS

by

Carla M. Ghannoum

November 1998

Department of Civil Engineering and Applied Mechanics

McGill University

Montréal, Canada

A thesis submitted to the Faculty of Graduate Studies
and Research in partial fulfilment of the requirements
for the degree of Master of Engineering

To My Mom and Dad

Abstract

The behaviour of interior slab-column connections in flat plates is investigated. The first part of this thesis discusses six two-way slab-column specimens which were designed such that they would fail in punching shear. The parameters investigated were the use of high-strength concrete and the concentration of the slab flexural reinforcement in the immediate column region. The effects of these parameters on the punching shear capacity, negative moment cracking, and stiffness of the two-way slab specimens are investigated.

The second part of this thesis is a comparison of the test results obtained from this experimental program with the punching shear predictions of the Canadian CSA A23.3-94 Standard and the American ACI 318-95 Code. Some comparisons of the punching shear strength provisions of the British BS 8110-85 Standard and the European CEB-FIP 1990 Model Code are also carried out. Furthermore, the CSA Standard and the ACI Code predictions are compared to the experimental results obtained from some slab-column connections tested in this experimental program and tested by various investigators.

The beneficial effects of the use of high-strength concrete and of the concentration of flexural reinforcement in the immediate column vicinity are demonstrated. It is also concluded that the punching shear strength of slab-column connections is a function of the flexural reinforcement ratio and that the shear design of slabs according to the current Canadian and American codes can be unconservative under certain conditions. It is recommended that the punching shear expressions of the CSA Standard and the ACI Code be modified to include the effect that the flexural reinforcement ratio has on the shear capacity of slab structures.

Résumé

Le comportement d'assemblages dalle-colonne est étudié. La première partie de cette thèse décrit le comportement de six assemblages dalle-colonne dimmensionés pour une défaillance par poinçonnement en cisaillement. Les paramètres étudiés comprennent l'utilisation du béton à haute résistance et la quantité d'armature flexionnelle dans la dalle à proximité de la colonne. L'étude porte sur l'influence de ces paramètres sur la résistance à la contrainte de poinçonnement, la fissuration en flexion négative et la rigidité des spécimens.

La deuxième partie de cette thèse est une comparaison des résultats obtenus de ce programme expérimental avec les prédictions de la résistance à la contrainte de poinçonnement du Code Canadien CSA A23.3-94 et du Code Américain ACI 318-95. Quelques comparaisons avec le Code Britannique BS 8110-85 et le Code Européen CEB-FIP 1990 sont aussi effectuées. De plus, les prédictions du Code Canadien et du Code Américain sont comparées aux résultats expérimentaux obtenus de dalles testées dans ce programme expérimental et testées par d'autres investigateurs.

Les bénéfices de l'usage du béton à haute résistance et de la concentration de l'armature de la dalle autour de la colonne sont démontrés. Les résultats de l'étude indiquent que la résistance à la contrainte de poinçonnement est dépendante de la quantité d'armature et que la conception au cisaillement des dalles d'après le Code Canadien et le Code Americain peut être non sécuritaire sous certaines conditions. Il est recommandé que les expressions du code CSA Canadien et du code ACI Américain pour l'évaluation de la résistance à la contrainte de poinçonnement des dalles soit modifiées pour prendre en considération l'effet de la quantité d'armature sur la capacité en cisaillement des dalles.

Acknowledgements

The author would like to express her utmost gratitude to Professor Denis Mitchell for his expert guidance and his continued encouragement and support throughout this research programme. The author would also like to thank Dr. William Cook for his encouragement and assistance.

The research was carried out in the Jamieson Structures Laboratory at McGill University. The author wishes to thank Ron Sheppard, Marek Przykorski, John Bartczak and Damon Kiperchuk for their assistance in the laboratory. Special thanks is extended to Peter McHarg and Stuart Bristowe for all their time and helpful suggestions. The author would also like to thank Wassim Ghannoum, Pierre Koch, Hanaa Issa, Bryce Tupper, Emmet Poon, Pedro Da Silva, Robert Zsigo, Johnathan Vise and Kevin Li for their assistance.

The completion of this project would not have been possible without the patience and valuable help of the secretaries of the Civil Engineering Department, particularly Ann Bless, Sandy Shewchuk-Boyd, Lilly Nardini and Donna Sears.

The author would also like to express her deepest gratitude to her parents, her sister Nadyne, and her brother Wassim for their constant support, patience and understanding. Finally, the author would like to thank her friends Maya Sawaya, Walt Woo, Loubna Sawaya, Richard Hum and Mark Kim for their continuous encouragement's and support over her years at McGill.

Carla Ghannoum
November, 1998

Table of Contents

List of Figures

List of Tables

List of Symbols

a	depth of equivalent rectangular stress block
A_c	area of concrete
A_s	area of reinforcement
b	perimeter of loaded area
b_o	perimeter of critical section for shear
c	size of rectangular or equivalent rectangular column
d	distance from extreme compression fibre to centroid of tension reinforcement
d_b	nominal bar diameter
f_c'	specified compressive strength of concrete
f_r	modulus of rupture of concrete
f_y	specified yield strength of reinforcement
h	overall thickness of slab
jd	effective depth of slab
l_n	length of clear span measured face-to-face of supports
M_f	factored moment
M_r	factored moment resistance
n	ratio of tension steel through loaded area to total area of tension steel in slab
P_{calc}	calculated ultimate load of column
s	spacing of tension reinforcement
v	nominal shear strength
v_c	factored shear stress resistance provided by concrete
v_f	factored shear stress
v_r	factored shear stress resistance
V	shear force
V_c	factored shear force resistance attributed to the concrete
V_f	factored shear force at section
V_n	nominal shear force resistance
V_{sc}	shear transmitted to column due to specified loads, not less than twice self-weight of slab
w_f	factored load per unit area of slab
α_1	ratio of average stress in rectangular compression block to the specified concrete strength
ε_{sh}	steel strain at strain hardening
ϕ_c	resistance factor for concrete
ϕ_s	resistance factor for reinforcement
ϕ_o	ratio of ultimate load to the load at which flexural failure should occur
γ_c	partial safety factor
λ	factor to account for concrete density
ρ	ratio of tension reinforcement
ρ'	ratio of compression reinforcement
ξ	$1+(200/d)^{1/2}$ (size effect term)

Chapter 1

Introduction and Literature Review

1.1 Introduction

The design of flat plate structures is generally governed by serviceability limits on deflection or by ultimate strength of the slab-column connections. Failure of the connection, usually referred to as punching failure, is of special concern to engineers because of its catastrophic consequences. A failure of this type is undesirable since, for most practical design cases, an overall yielding mechanism will not develop before punching. The current building code design procedure for the punching strength of slab-column connections is empirically based and there is justifiable concern that, as building techniques and materials change, this procedure may not always ensure safe structures. Establishing reliable design procedures that would take into account the use of these new techniques and materials is hence of great importance.

The objectives of this research program were to investigate the punching shear behaviour of slab-column connections in flat plates. More specifically, this experimental program investigated the effects of concentrating the flexural reinforcement in the vicinity of the column and the use of high-strength concrete on the punching shear capacity of slab structures.

This chapter will give a brief overview of the previous research on punching shear resistance of two-way slabs. The current punching shear strength provisions used in the various codes will also be discussed.

1.2 Punching Shear Resistance of Two-Way Slabs

Researchers have long attempted to understand the effect of concentrating the flexural reinforcement in the vicinity of the column on the shear strength of slabs. Previous research has resulted in conflicting results with respect to whether or not concentrating flexural reinforcement near the column had any beneficial effect on the performance of slabs. The following section outlines some of the previous research that has had an impact on current design practice and which is related to this research program.

1.2.1 Previous Research

In the early 1900's, the German investigator E. Mörsch contributed extensively to the understanding of the behaviour of reinforced concrete structures with his work on shear. In his 1906 and 1907 papers, Mörsch proposed an equation for the nominal shearing stress, v. The equation is as follows:

$$v = \frac{V}{bjd} \tag{1.1}$$

where V is the applied shear force,

b is the perimeter of the loaded area, and,

jd is the effective depth.

The shear stress from Mörsch's equation is calculated along the perimeter, b, of the loaded area. For a uniformly loaded slab, the shear stress is therefore evaluated at the perimeter of the column.

Talbot (1913) presented a report of 83 column footings tested to failure. Of these footings, twenty failed in shear. They exhibited failure surfaces that were at an angle of approximately 45° to the vertical and that extended from the bottom face of the slab at its intersection with the column, reaching the level of the reinforcement at a distance d from the column face. From these test findings, Talbot concluded that it would be reasonable to take the vertical section located at a distance d from the face of the column as the critical shear section. He, therefore, proposed the following formula, which is similar to Mörsch's, except that the critical section was moved from the face of the column to a distance d from

the face:

$$v = \frac{V}{4(c + 2d)jd} \tag{1.2}$$

where c is the length of one face of a square column.

Talbot also studied the effect that the disposition of reinforcing bars had on shear strength. He concluded that increasing the percentage of flexural reinforcement resulted in an increase in the shearing capacity of slabs.

The joint committee of 1924 (appointed by a number of professional American societies) reported that the diagonal shear stress appeared to be critical at a distance (h-1.5 in.) from the periphery of the loaded area, where h is the slab thickness. Furthermore, the committee recommended that the shear stress, which is a working stress limit, be limited to:

$$v = 0.02f_c'(1 + n) \leq 0.03f_c' \tag{1.3}$$

where f_c' is the concrete compressive strength in MPa, and,

n is the area of steel in the loaded region divided by the total area of steel in the slab.

Graf (1933) examined the shear strength of slabs that were subjected to concentrated loads near the supports. He concluded that the shear capacity decreases as the loads move away from the supports and that flexural cracking had some effect on shearing strength. Graf also proposed the following expression for the shearing stress:

$$v = \frac{V}{4ch} \tag{1.4}$$

where h is the thickness of the slab.

Richart (1948) presented a report on a number of reinforced concrete footing tests. He reported that high tensile stresses in the flexural reinforcement lead to extensive cracking in the footings. This cracking reduced the section resisting shear, resulting in the footings failing at lower shearing stresses than expected. Richart also noted that although

the use of a critical shear section a distance d away from the face of the column compared reasonably well with test results, the use of some other section might be equally justified.

Elstner and Hognestad (1956) reported on thirty-four 6 feet square slabs that exhibited punching shear modes of failure. In two of these slabs, 50% of the flexural reinforcement was concentrated over the column. These slabs were then compared to two others that were similar except that the flexural reinforcement was uniformly distributed throughout the width of the slabs. Test findings indicated that concentrating the flexural reinforcement near the column did not result in any increase in the punching shear strength of the slab specimens. Elstner and Hognestad also revised a formula initially proposed by Hognestad in 1953, to evaluate the ultimate shear strength of slabs. The revised expression is as follows:

$$v = \frac{V}{\frac{7}{8} bd} = 2.3 + 0.046 \frac{f_c'}{\phi_o} \quad \text{(N and mm)} \qquad (1.5)$$

where ϕ_o is the ratio of the ultimate load to the load at which flexural failure should occur.

Whitney (1957) studied the failure mechanisms of a number of flat slabs with varying steel ratios and concrete strengths. Some of these slabs exhibited a sudden type of failure that he believes was actually a bond failure. This involves the splitting of concrete after loss of anchorage of the steel reinforcement, either due to insufficient embedment length or because the bars were too closely spaced. Whitney, then reviewed the results of slab tests by Richart, Elstner and Hognestad and reported that in these tests the slab specimens that had a high percentage of reinforcement probably also failed due to bond failure and not shear. Furthermore, Whitney proposed an ultimate shear strength theory and concluded that the shear strength is primarily a function of the "pyramid of rupture", which is a pyramid with surfaces sloping out from the column at angles of 45°.

The 1956 ACI Building Code recommended two different limits for shear stresses in slabs. The limits are for stresses evaluated at a distance d away from the periphery of the loaded area and are as follows:

$$v \leq 0.03\, f_c' \leq 0.69 \text{ MPa},$$

if more than 50% of the flexural reinforcement passes through the periphery; or

$$v \leq 0.025\, f_c' \leq 0.59 \text{ MPa},$$

if only 25% of the flexural reinforcement passes through the periphery.

Kinnunen and Nylander (1960) proposed a rational model for predicting punching shear behaviour in slabs. Basically, in this model the slab is divided into rigid radial segments, each bounded by two radial crack lines, the periphery of the column or loaded area where the initial circumferential crack usually forms and the slab boundary. Before failure occurs, the main deformation of each radial segment is a rotation around a centre of rotation (C.R.) located at the periphery of the column and at the level of the neutral axis. Failure takes place when the frontal part of the radial segment fails to support the force at the column face, that is the concrete crushes in the tangential direction.

Moe (1961) tested forty-three 6 foot square slab specimens and reviewed test findings from 260 slabs and footings tested by previous investigators. He suggested that the flexural strength had some influence on the shear strength of slabs. Moe also concluded that the concentration of the flexural reinforcement does not result in an increase in the shear strength but that it does increase the stiffness of the load-deformation response and the load at which initial yielding occurs. He proposed the following expression for evaluating the ultimate shear strength of slabs:

$$v_u = \frac{V_u}{bd} = \left[15\left(1 - 0.075\,\frac{c}{d}\right) - 5.25\phi_o\right]\sqrt{f_c'} \quad \text{(N and mm)} \qquad (1.6)$$

Regan (1974) reviewed previous research by various investigators on the punching shear strength of slabs. He noted that the shear strength increases with increasing reinforcement ratios and concrete strengths, but the effect is less than linear. Hence, the rate of increase of shear strength should decrease at higher reinforcement ratios and concrete strengths.

Hawkins, Mitchell and Hanna (1975) tested slab specimens in which the flexural reinforcement was concentrated within a distance of 1.5 times the slab thickness, h, either side of the column. They concluded that the concentration of the reinforcement resulted in

an improvement of the behaviour of the slab-column connections, especially for slabs with low reinforcement ratios.

Hawkins and Mitchell (1979) reported that in a punching shear failure the shear strength is dependent on the flexural capacity of the slab and that it will decrease as the stiffness of the connection decreases. Accordingly, the ultimate shear strength of connections transferring shear will decrease if significant yielding of the flexural reinforcement takes place. Hawkins and Mitchell also noted that concentrating flexural reinforcement in the immediate column region slightly increased the capacity of the connection but decreased its ductility.

Rankin and Long (1987) proposed a method for determining the punching shear strength of conventional slab-column connections based on rational concepts of the modes of failure of these connections. They proposed the following punching shear strength expression:

$$P_{vs} = 1.66\sqrt{f_c'}(c + d) \times d \times \sqrt[4]{100\rho} \quad \text{(N and mm)} \qquad (1.7)$$

where f_c' is the compressive strength in MPa,

ρ is the reinforcement ratio, As/bd, and,

P_{vs} is the punching shear strength.

Alexander and Simmonds (1988) note that although the CSA Standard (1984) recognizes that shear strength is sensitive to the amount of flexural reinforcement, it only treats this important parameter indirectly through detailing requirements (the 1984 CSA Standard requires that a large portion of the flexural reinforcement pass through or near the column). They believe that these detailing requirements give little indication as to how the amount of reinforcement actually affects punching shear strength and that a better approach would be for the CSA Standard to include the beneficial effect of the flexural reinforcement in its calculations for the shear strength capacity.

Shehata and Regan (1989) proposed a mechanical model to estimate the punching resistance of slabs. The model was based on test observations as well as numerical analyses. The authors believe that their model was an improvement over that of Kinnunen and

Nylander (1960) as it includes the influence of the deformation of the part of the slab on the top of the column and bounded by the shear crack. Furthermore, they suggest that their model provides a more complete definition of failure. Shehata and Regan also performed a parametric study of their theoretical model and of the American Code and the British Standard approaches. This study revealed that the British Standard results were closer to their theory in accounting for the steel ratio, which the ACI Code ignores.

Alexander and Simmonds (1992) reported that increasing the amount of reinforcement passing through the column region could lead to anchorage failures which are not distinguishable from punching shear failures on the basis of external appearances only. Anchorage failures also exhibit the classical pyramid shaped punching failure. They believe that this led investigators such as Moe, Elstner and Hognestad to wrongly diagnose the mode of failure in many of their tests and that it prevented them from observing an improvement in the shear capacity of slabs with the concentration of the flexural reinforcement near the column.

Gardner and Shao (1996) presented experimental results for the punching shear of a two-bay by two-bay reinforced concrete structure. They reviewed the code provisions of the ACI 318-89 Code, the BS 8110-85 Standard, and the CEB-FIP 1990 Model Code, and compared these predicted values to previous experimental research from various investigators. They concluded that the code equations that considered size effects and reinforcement ratios (such as the BS 8110-85 and CEB-FIP Model Code equations) had smaller coefficients of variation than the ACI expressions. They also noted that a parametric study by Shehata and Regan showed that the punching shear strength is approximately proportional to the cube root of the concrete strength, steel ratio, and steel yield stress. This led them to derive a shear stress expression that includes these various parameters. The equation is as follows:

$$v_u = \frac{V_u}{b_o d} = 0.79 \times \sqrt{1 + (200 / d)} \times \sqrt[3]{\rho f_y} \times \sqrt[3]{f_{cm}} \times \sqrt{(d / b_o)} \text{ (N and mm)} \quad (1.8)$$

where f_{cm} is the mean concrete strength, in MPa, and b_o is the perimeter of the loaded area. Gardner and Shao also cautioned that although increasing the amount of

flexural reinforcement increases the punching shear capacity of the slab-column connection, it results in a more brittle behaviour.

Sherif and Dilger (1996) reviewed the CSA A23.3-94 punching shear strength provisions for interior slab-column connections. After comparing these provisions to results from previous research experiments, they concluded that these provisions can be unsafe under certain conditions, particularly for slabs with low reinforcement ratios ($\rho < 1\%$). They also note that since most slab designs have a reinforcement ratio, ρ, of less than 1% it is important that the code equations for the shear strength be modified to include ρ. They recommend the following design equation for the punching shear stress at failure:

$$v_c = 0.7 \times \sqrt[3]{100\rho f_c'} \quad \text{(N and mm)} \qquad (1.9)$$

Sherif and Dilger do not recommend including the yield strength of the flexural reinforcement as a factor affecting punching shear strength.

1.3 High-Strength Concrete

In recent years, the use of high-performance concrete (HPC) or high-strength concrete (HSC) has become more widespread throughout the world. The performance of structural elements made with HSC has, therefore become a major concern and a significant amount of research is currently underway to ensure that high-strength concrete structures are both cost-effective and safe. A number of national scale research programs have been established to investigate the possible advantages of this new material. These include the Centre for Science and Technology for Advanced Cement-Based Materials (ACBM- United States), the Strategic Highway Research Program (SHRP- United States), Concrete Canada a Network of Centers of Excellence (NCE) Program, the Royal Norwegian Council for Scientific and Industrial Research Program, the Swedish National Program on HPC, the French National Program called "New Ways for Concrete" and the Japanese New Concrete Program.

However, although a lot of research has been done on high-strength concrete, a very small portion of it has been dedicated to investigating the structural behaviour of high-

strength two-way slabs or the punching characteristics of high-strength concrete slabs. The present code specifications for shear strength of reinforced concrete slabs are based on test results of slabs made with relatively low compressive strengths, varying mostly from 14 to 40 MPa. It is therefore necessary to re-evaluate the current shear design procedures when applied to high-strength concrete. A brief outline of the previous research on the influence of concrete strength on the punching shear resistance of slabs is presented below.

1.3.1 Previous Research

Graf (1933) studied the shear strength of slabs. He reported that the shear strength increased with increasing concrete strength but that test results indicated that the increase was not directly proportional to the increase in the concrete compressive strength.

Moe (1961) reported that the shear strength of slab-column connections is a function of $\sqrt{f_c'}$. He believed that shear failure is primarily controlled by the tensile-splitting strength, which is assumed proportional to $\sqrt{f_c'}$. He proposed Equation (1.6) to evaluate the shear strength.

The joint ASCE-ACI Committee 426 (1974), after reviewing the work of a number of investigators noted that the cube root relation between shear strength and compressive strength developed by Zsutty in 1968 for beams also seemed to be adequate for slabs with f_c' values greater than 28 MPa.

Marzouk and Hussein (1991) studied the effect that concrete strength has on the punching shear behaviour of seventeen reinforced concrete slabs. They concluded that increasing the compressive strength does increase the ultimate punching shear strength, but at a rate less than that of $\sqrt{f_c'}$. Therefore, North American codes whose shear provisions are mainly derived from Moe's square-root expression overestimate the influence of the concrete strength on the ultimate shear capacity. Marzouk and Hussein believe that the cube-root expressions used in the British and European codes better predict the punching shear capacity of high-strength concrete slabs. Furthermore, their test results revealed that the rational model proposed by Kinnunen and Nylander in 1960 remains the best means of predicting the punching shear strength of slabs. Therefore, Marzouk and Hussein proposed a model based on the Kinnunen and Nylander model but modified to include high strength

concrete. They also observed that in general, high-strength concrete slabs exhibit a more brittle failure than normal-strength concrete slabs.

Gardner and Shao (1996) reviewed the provisions of the ACI 318-89 Code, the BS 8110-85 Standard, and the CEB-FIP 1990 Model Code, and compared these predicted values to results from earlier tests conducted by various investigators. They concluded that punching shear strength is approximately proportional to the cube root of concrete strength, steel ratio, and steel yield stress and proposed equation (1.8) for the shear strength of slabs.

Sherif and Dilger (1996) conducted a parametric study based on test results by Elstner and Hognestad who systematically varied the concrete strength and the reinforcement ratio in their study of punching shear. They concluded that for reinforcement ratios less than 1.5%, that is for conventional slab designs, the function $\sqrt[3]{f_c'}$ seems to best represent the effect of the concrete strength on the shear capacity of slabs. Sherif and Dilger note that both the BS 8110-85 Standard and the CEB-FIP 1990 Model Code use this cube-root function, and that the ACI-ASCE Committee 352 (1988) recommend the use of the square root relationship for concrete strengths of 40 MPa or less, and the cube-root relation for concrete strengths exceeding 40 MPa. The authors, therefore, strongly recommended that the CSA A23.3-94 Standard uses the relationship $v_u \propto \sqrt[3]{f_c'}$ and proposed equation (1.9) for the shear strength of slabs.

1.4 Current Code Provisions for Punching Shear Strength of Two-Way Slabs

The current understanding of the mechanisms involved in the punching shear failures in flat slab structures is based mainly on experimental research programs conducted to investigate the behaviour and strength of conventional slab-column connections. Hence, the design provisions adopted in the different building codes are directly derived from empirical methods that are based on the test results of these experimental studies. Consequently, there exists a significant variation in the methods of evaluation of the punching shear capacity of slabs in the concrete codes of North America, Europe, and Britain. The American ACI Code and Canadian CSA Standard are largely based on the work of the German investigator Moe, while the European and British codes are primarily based on Regan's work. The equations used to determine the nominal shear strength in the

CSA Standard, the ACI Code, the BS Standard and the CEB-FIP Model Code are compared in Table 1.1.

Table 1.1 Comparison of code provisions for nominal shear strength

Code	Critical Periphery	Nominal Shear Strength
CSA A23.3-94 ACI 318-95	$b_o = 4\,(c + d)$	$v = (0.33 \times \sqrt{f_c'})$
BS 8110-85	$b_o = 4\,(c + 3d)$	$v = 0.79 \times \sqrt[3]{100\rho} \times \sqrt[4]{400 / d}$ where, ρ = ratio of steel within 1.5d of column face. For $f_c' > 25$ MPa , v may be multiplied by $\sqrt[3]{f_c'/25}$. The value of f_c' should not be taken as greater than 40 MPa.
CEB-FIP 1990	$b_o = 4\,(c + \pi d)$	$v = \dfrac{0.12 \times \xi \times \sqrt[3]{100\rho f_c'}}{\gamma_c}$ where, $\xi = 1 + \sqrt{200 / d}$ γ_c = partial safety factor = 1.5 (taken as 1.0 for nominal) The value of f_c' should not be taken as greater than 50 MPa.

The main differences between the various codes with regard to the punching shear strength of slabs are as follows:

- The ACI Code (1995) does not include the amount of flexural reinforcement in its shear strength calculations. The current CSA Standard (1994) requires that half of the flexural reinforcement needed in the column strip be placed within 1.5 times the slab thickness, h, either side of the column face, but does not give beneficial effects for this distribution in the calculation of the shear strength. Both the American and the Canadian codes do not include a size effect term in their expressions for shear strength

and use the relation $v \propto \sqrt{f_c'}$. It is noted that the 1994 CSA Standard uses a factored shear stress at failure of $0.4\ \phi_c\ \sqrt{f_c'}$, where ϕ_c is the material resistance factor for concrete, equal to 0.60. The factor of 0.4 in this expression was increased from 0.33 to 0.4 to account for the low value of ϕ_c. Hence, the nominal resistance should be taken as $0.33\ \sqrt{f_c'}$.

- The CEB-FIP Code (1990) and the BS Standard (1985) include the flexural reinforcement concentration and a size effect term in their calculations of the shear resistance of the connection. They both use the relation $v \propto \sqrt[3]{f_c'}$. In addition the British standard limits f_c' to 40 MPa in computing the shear strength and the CEB-FIP Code sets its limit on f_c' to 50 MPa.

1.5 Research Objectives

The objectives of this research program were to investigate the effects of concentrating the slab flexural reinforcement near the column and the effects of using high-strength concrete on the punching shear capacity, the cracking on the top surface of the slab and the stiffness of interior two-way slab-column connections.

Six full-scale, high-strength concrete slab-column connections were constructed. Three of these slab specimens were designed and detailed according to the CSA A23.3 Standard (1994), with half of their flexural reinforcement being concentrated within a distance of 1.5 times the slab thickness, h, either side of the column. The other three slabs were designed according to the ACI 318-95 Standard (1995), with the flexural reinforcement being uniformly distributed throughout the slabs widths. All specimens were instrumented to enable their various behavioural aspects to be studied as each test was carried out.

The behaviour of these six slab column specimens was compared to the behaviour of normal strength concrete slabs which were tested under a similar experimental study by McHarg (1997). Also, the test results obtained from this experimental program were compared to the ACI Code and the CSA Standard predictions for the punching shear strength of two-way slabs.

Chapter 2

Experimental Programme

2.1 Description of Prototype Structure

The slab-column connections tested in this study were full-scale models of the typical flat-plate prototype structure shown in Fig. 2.1. This prototype consisted of a four bay by four bay flat plate with 4.75 m x 4.75 m bays and was designed for assembly area use as specified by the National Building Code of Canada (NBCC, 1995). The design and loading details of the test specimens were based on the analysis of this prototype structure. The slab was designed for a superimposed dead load of 1.2 kPa and a specified live load of 4.8 kPa. The slab thickness was 150 mm with a 25 mm clear cover on both the top and bottom steel reinforcement. The interior columns were 225 mm square with a 30 mm clear concrete cover on the column ties. As the objective of this research program was to investigate the punching shear behaviour of slabs, the prototype structure was designed with relatively small columns and a high live load to produce high punching shear stresses in the slab around the column.

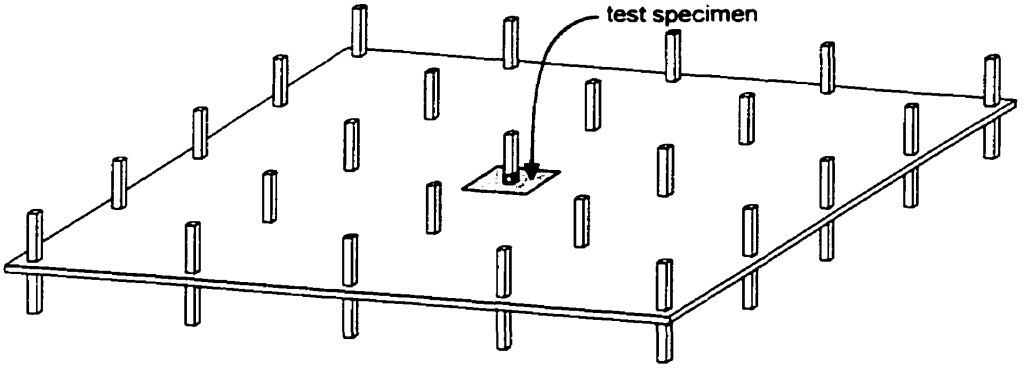

Figure 2.1 Prototype flat plate structure (4.75 m x 4.75 m bays)

2.2 Details of Test Specimens

Six, full-scale two-way slab specimens were constructed and tested to failure in the Structures Laboratory in the Department of Civil Engineering at McGill University. The tested specimens are interior slab-column connections representing the column strip regions of the prototype structure (see shaded region in Fig. 2.1). The test specimens, shown in Fig. 2.2, consist of a flat plate that is 150 mm thick and 2.3 m square with 225 mm square reinforced concrete column stubs extending 300 mm above and below the plate. The bottom stub columns were cast monolithically with the slab.

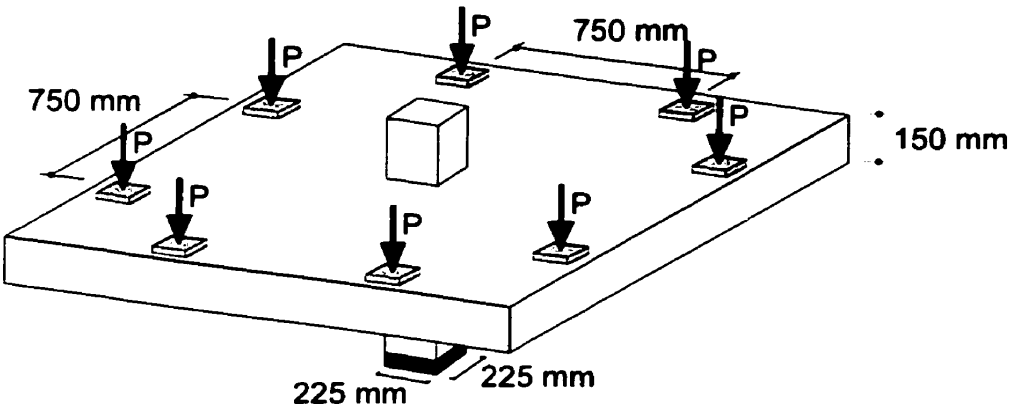

Figure 2.2 Slab-column test specimen (2.3 m x 2.3 m)

The prototype structure's design was carried out using the computer program ADOSS (CPCA, 1991) and was in accordance to the ACI Code (ACI, 1995) and the CSA Standard (CSA, 1994). The specimens were designed to investigate the effect of concrete strength and reinforcement ratio on the punching shear behaviour of high-strength concrete slabs. To ensure a shear failure the columns were chosen to be relatively small and the amount of reinforcement obtained from ADOSS was distributed such that the slabs would have sufficient flexural strength to meet the codes requirements and avoid a flexural failure.

The reinforcement was distributed both uniformly throughout the width of the slab and in a banded manner where the reinforcement was concentrated in the vicinity of the column. The uniform distribution was in conformance with the shear design provisions of

the 1995 ACI Building Code (ACI, 1995), while the banded distribution was in accordance to the requirements of the CSA Standard (CSA, 1994). Both top bar reinforcement layouts contained 14-No.15 bars in the strong direction and 16-No.15 bars in the weak direction. The two additional bars in the weak direction were placed to improve the slabs flexural strength in that direction and to thus ensure that even at higher concrete strengths the slabs will exhibit a shear mode of failure. Steel plates, 50 mm square, were welded to the ends of every other top bar to ensure that the reinforcement was properly anchored. The top mat reinforcement layout for both the uniform and the banded distributions is summarised in Fig. 2.3. The layout of the bottom reinforcement was, for all specimens as shown in Fig. 2.4. In order to satisfy the structural integrity requirements of the 1994 CSA Standard, three of the No. 10 bottom reinforcing bars were made continuous through the column. The column reinforcement consisted of four vertical No. 15 bars and two No. 10 hoops above and below the slab. Figure 2.5 shows the reinforcement of the slab-column specimens.

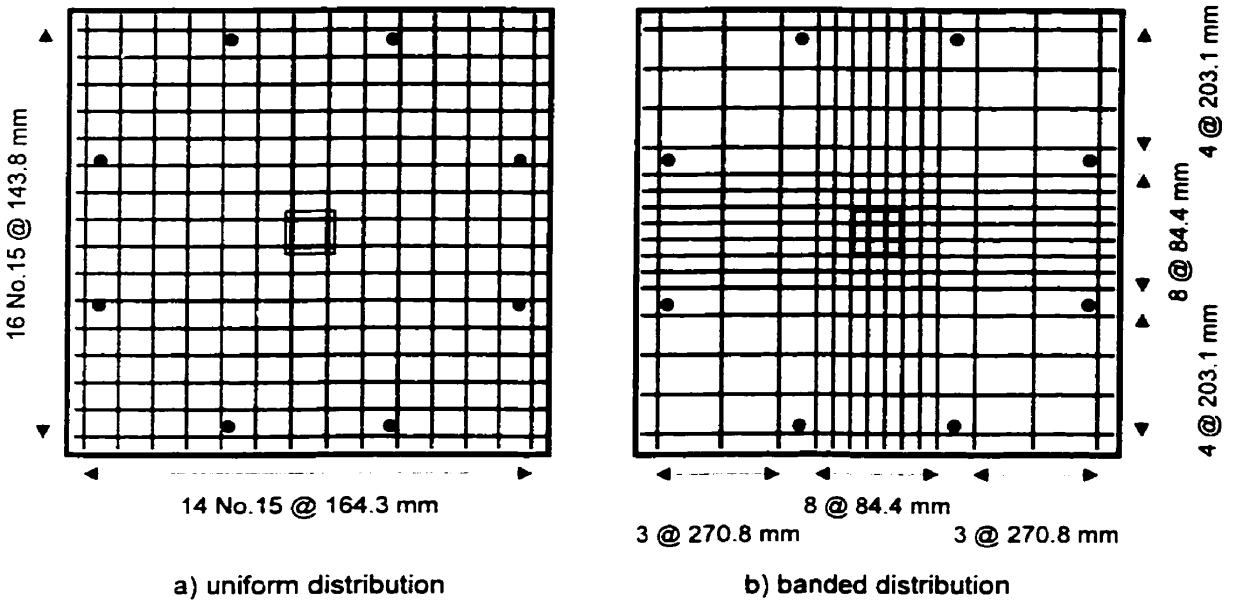

Figure 2.3 Distribution of top No. 15 bars

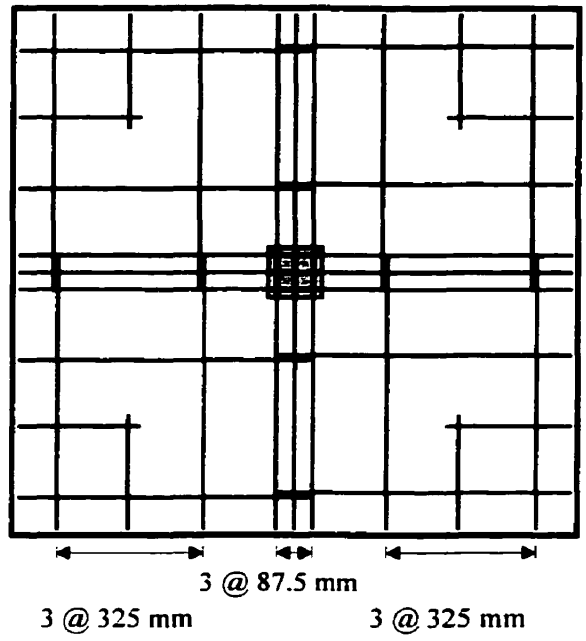

Figure 2.4 Layout of bottom No. 10 bars

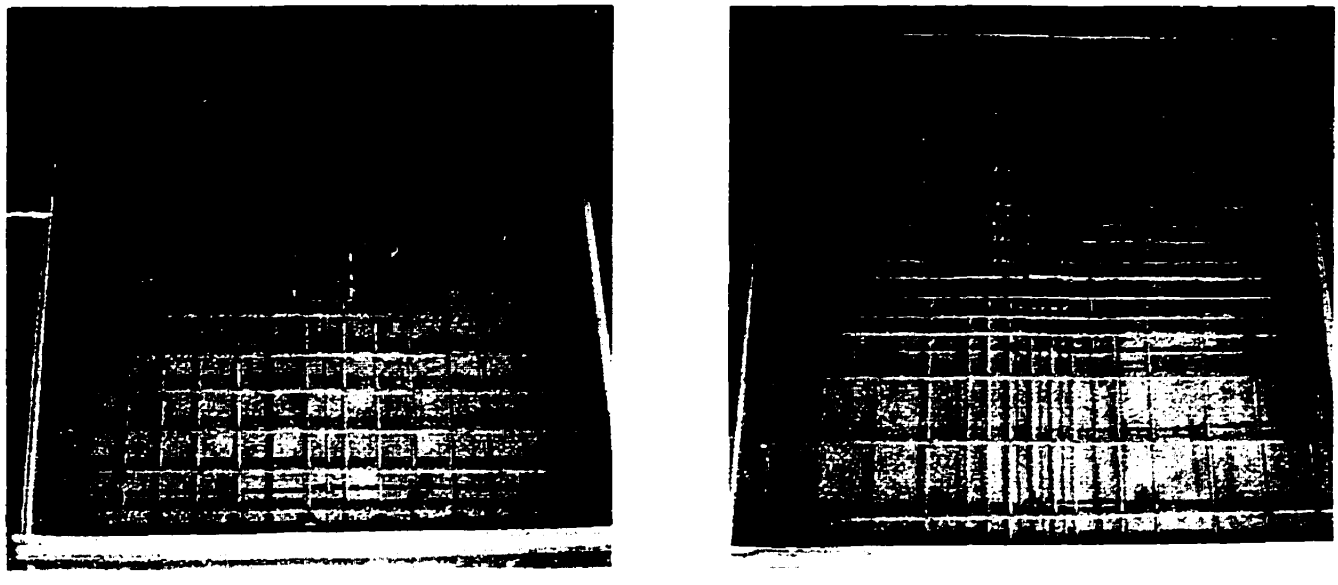

a) uniform specimens

b) banded specimens

Figure 2.5 Slab reinforcement

The testing program consisted of six slab-column test specimens divided into three series. Each series had a different concrete compressive strength and included one slab with a uniform distribution (U) of top bars in conformance with current U.S. practice (ACI, 1995) and one slab with a banded distribution (B) of the top reinforcement in conformance with the recent changes to Canadian design practice (CSA, 1994). The different series were identified as follows:

S1 Series: Specimens S1-U and S1-B,
with a concrete compressive strength of 37.2 MPa.

S2 Series: Specimens S2-U and S2-B,
with a concrete compressive strength of 57.1 MPa.

S3 Series: Specimens S3-U and S3-B,
with a concrete compressive strength of 67.1 MPa.

2.3 Material Properties

2.3.1 Reinforcing Steel

The steel reinforcement in all specimens consisted of hot-rolled deformed bars with a minimum specified yield stress of 400 MPa. Table 2.1 summarises the material properties of these bars. The values reported are the averages of values obtained from tension tests performed on sample coupons taken from three random bars. Figure 2.6 shows typical stress-strain responses of the reinforcing bars.

Table 2.1 Reinforcing steel properties

Size Designation	Area (mm^2)	f_y (MPa) (std. deviation)	f_u (MPa) (std. deviation)	ε_y (%)	ε_{sh} (%)	Function
No.10	100	454 (4.0)	676 (6.0)	0.34	0.43	bottom flexural reinforcement & column hoops
No. 15	200	445 (3.5)	588 (5.0)	0.23	1.95	top flexural reinforcement & column bars

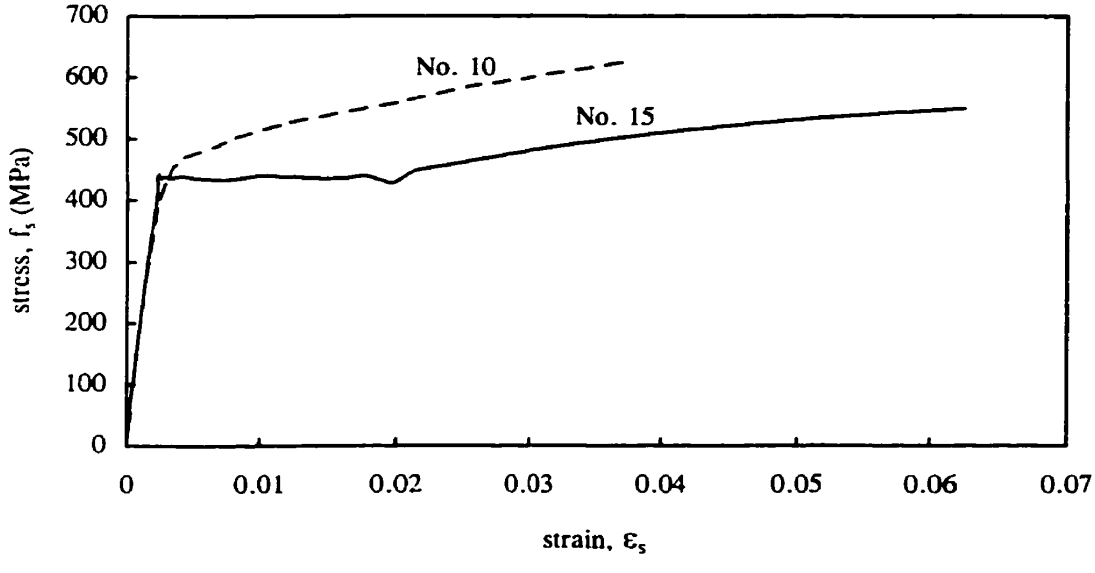

Figure 2.6 Typical tensile stress-strain curves for reinforcing steel

2.3.2 Concrete

The concrete used to build all specimens was normal weight concrete and was obtained from a local ready-mix supplier. The three different concrete mix designs used for series S1, S2 and S3 are summarised in Table 2.2. Their target concrete strengths were of 40, 50 and 70 MPa, respectively. Standard 150 mm x 300 mm compression cylinder and split cylinder tests were conducted on all mixes to determine values of the concrete compressive strength, f'_c and of the splitting tensile strength, f_{sp}. Also, standard 150 x 150 x 450 mm flexural beam, four point loading tests were carried out on all mixes to evaluate the modulus of rupture, f_r. At least three tests were carried out in order to determine the mean values of these material properties. The results obtained are summarised in Table 2.3. Figures 2.7 and 2.8 show respectively the typical stress-strain responses and the shrinkage readings for the three series, S1, S2 and S3.

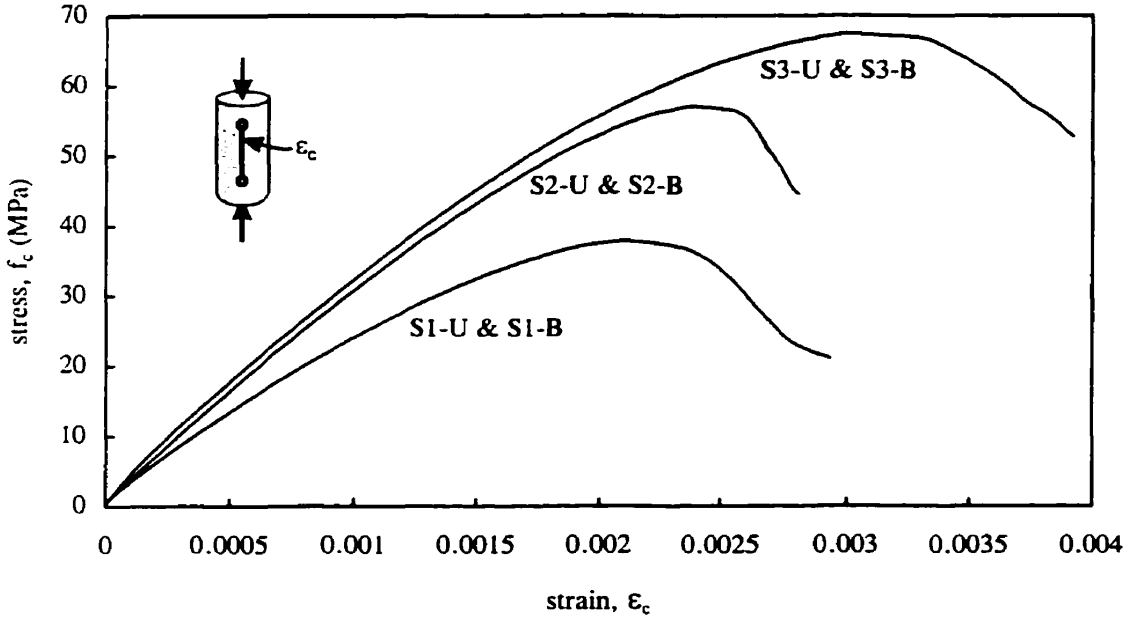

Figure 2.7 Typical compressive stress-strain curves of concrete

Table 2.2 Concrete mix designs

Characteristics	40 MPa	50 MPa	70 MPa
cement (Type 10), kg/m^3	-	-	480[1]
cement (Type 30), kg/m^3	440	460	-
fine aggregates (sand), kg/m^3	720	725	803
coarse aggregates (10 mm), kg/m^3	262*	-	1059**
coarse aggregates (14 mm), kg/m^3	367*	-	-
coarse aggregates (20 mm), kg/m^3	419*	1109**	-
total water[2], kg/m^3	155	140	135
water-cement ratio	0.35	0.3	0.28
water-reducing agent, ml/m^3	1377	1440	1502
superplasticizer, L/m^3	3.5	6	13
air-entraining agent, ml/m^3	460	874	-
slump, mm	150	175	210
air content, %	8.5	8.5	-
density, kg/m^3	2368	2442	2491

1 Type 10SF (Silica Fume)
2 Includes the water in admixtures
* Limestone (Demix Terrebonne)
** Limestone (St - Thimoteé, Dolomite)

Table 2.3 Average concrete properties for all series

Specimen	Average f'_c (MPa) (std. deviation)	Average ε_c' x 10^{-6} (std. deviation)	Average f_r (MPa) (std. deviation)
S1-U & S1-B	37.2 (1.7)	2248 (743)	3.50 (0.33)
S2-U & S2-B	57.1 (0.1)	2362 (30)	5.69 (0.28)
S3-U & S3-B	67.1 (0.9)	2857 (141)	6.30 (0.34)

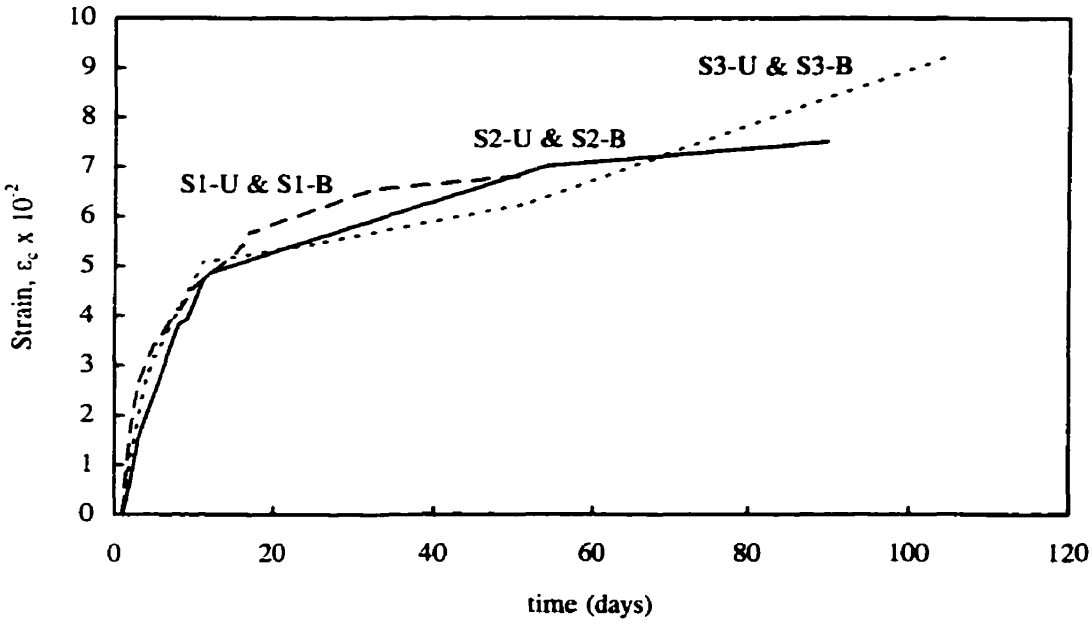

Figure 2.8 Shrinkage readings for concretes

2.4 Testing Procedure

2.4.1 Test Setup and Loading Apparatus

The lower column stub of the slab-column connection was placed on a steel supporting block and the slabs were loaded with eight equal concentrated loads around the perimeter to simulate a uniformly distributed load on the test specimens (see Fig. 2.9). From the analysis of the prototype structure, the points of inflection of the slab were determined to be approximately 900 mm from the face of the column. Thus, in order to obtain similar moment-to-shear ratios on the test specimen, pairs of load points were located 887.5 mm from the face of the square column. For each pair of loading points a steel load distribution beam that spans 750 mm was attached below the slab. Four hydraulic jacks connected to a common hydraulic pump were used to load these beams as seen in Fig. 2.9. Figure 2.10 shows a photograph of the test setup for the two-way slab specimens.

The load was applied monotonically in small increments with loads, deflections and strains being recorded at each increment. At key load stages, the crack pattern and crack widths were recorded.

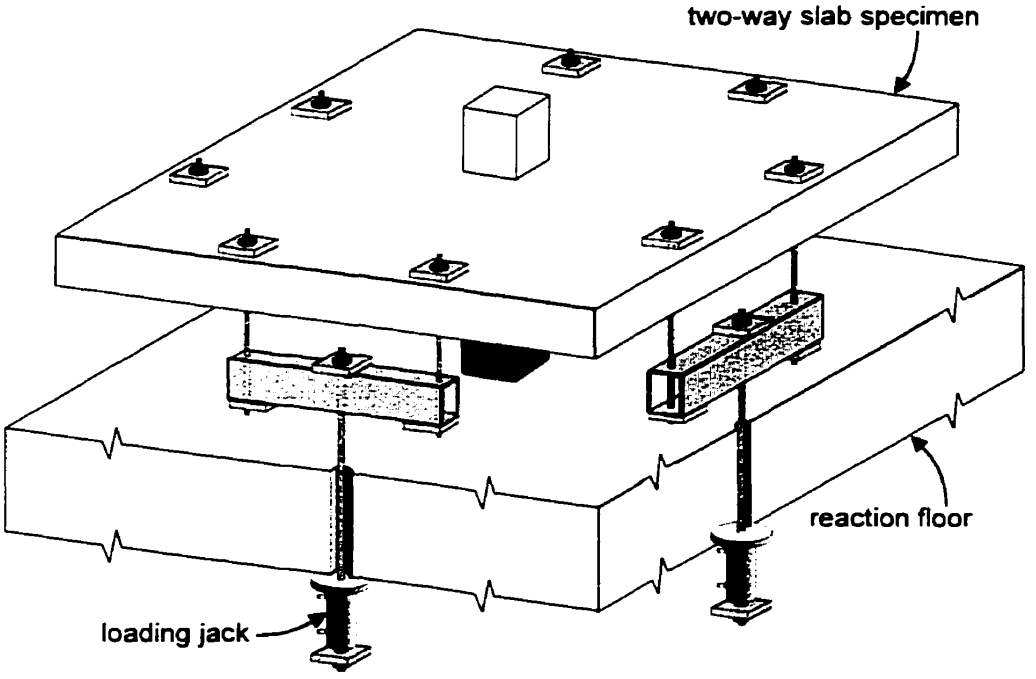

Figure 2.9 Test setup for two-way slab specimens

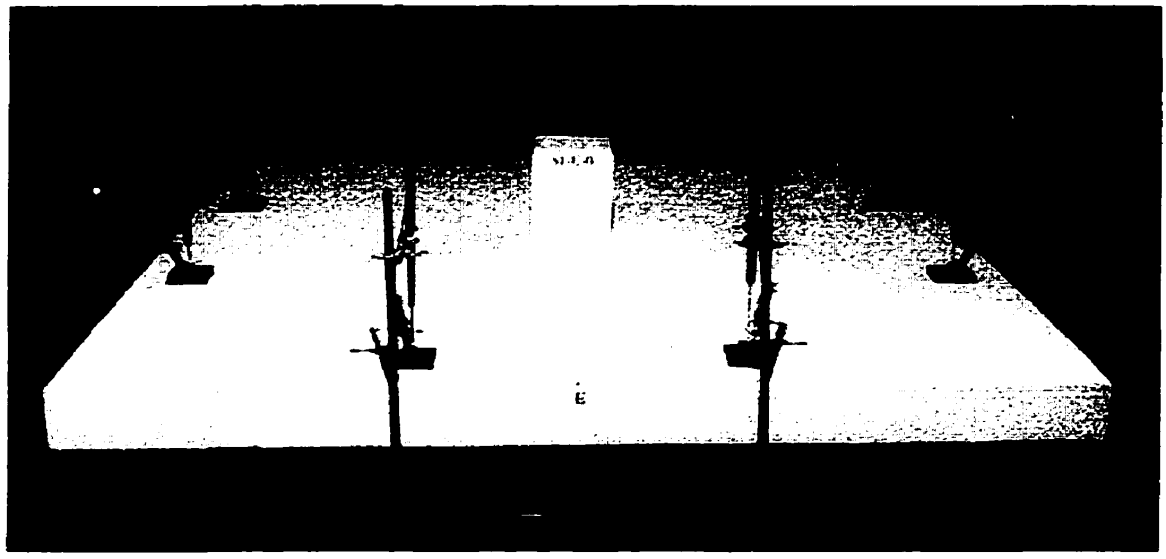

Figure 2.10 Photograph of test setup for two-way slab specimens

2.4.2 Instrumentation

Each test specimen was carefully instrumented to provide detailed data on its behaviour throughout its entire loading history. The applied loads were monitored by means of four load cells positioned at each of the four loading jacks. The vertical deflection of each loading point was measured with a linear voltage differential transformer (LVDT). Four additional LVDTs on the underside of the slab, close to the face of the column, were used to monitor the deflection of the slab relative to the column and to detect the start of a punching shear failure. Three LVDTs were also placed on the column to measure the rigid body rotation of the slab-column specimen, relative to the strong floor.

Electrical resistance strain gauges with a nominal resistance of 120 ohms and a gauge length of 5 mm were glued to the reinforcing bars in the top mat in line with the column face in the two principal directions of the slab, as illustrated in Fig. 2.11. In order to minimise the impact of the gauges on the bond characteristics of the steel, the grinding of the deformations on the reinforcement was kept to a minimum and the protection was confined to the immediate vicinity of the gauge. The steel strain measurements enabled the detection of first yielding for each bar passing through the column and the spread of yielding across the width of the test specimen.

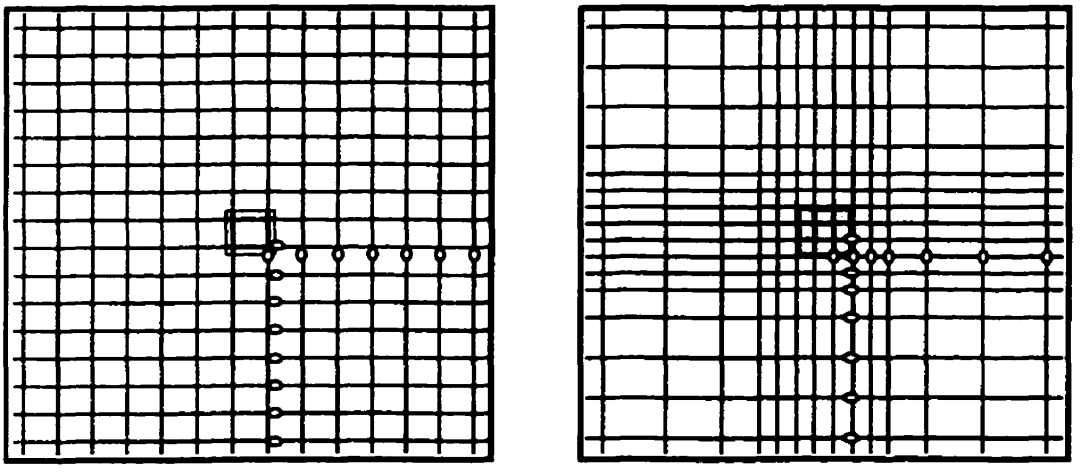

a) uniform distribution

b) banded distribution

Figure 2.11 Strain gauge locations on top mat reinforcement

Targets were glued to the top surface of the slab to determine the strains using a 203 mm gauge length mechanical extensometer. These targets are centred directly above the location of some of the electrical resistance strain gauges on the top mat of reinforcing bars, as shown in Fig. 2.12. On the bottom surface of the slab additional electrical resistance strain gauges with a gauge length of 30 mm were glued to the concrete at locations directly below the mechanical strain targets. The concrete strain readings obtained from these gauges together with the strains obtained from gauges on the steel bars enable the curvature to be determined at a number of sections. Also, another set of targets was located around the perimeter of the column to determine the average strain on this perimeter (see Fig. 2.12). All load, displacement and strain readings, except strains from the mechanical targets on the slab surface, were recorded with a computerised data acquisition system as each test proceeded.

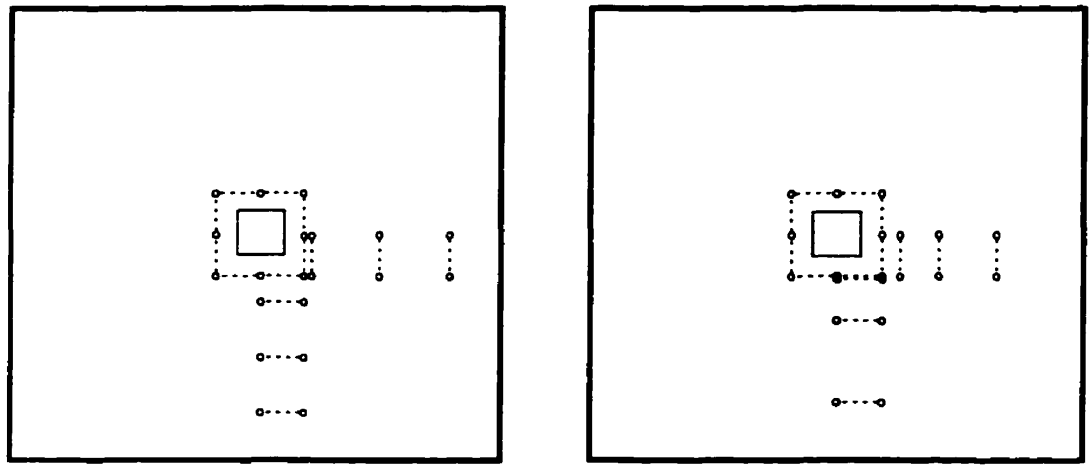

a) uniform distribution

b) banded distribution

Figure 2.12 Target locations on concrete surface of two-way slabs

Chapter 3

Response of Two-Way Slab Specimens

In this chapter, the observed experimental behaviours of the six slab-column connections are presented. Some of the experimental results that were recorded at each load increment included loads, deflections and strains. Crack patterns and crack widths were also recorded at key load stages. The most important load stages included first cracking, equivalent self-weight loading, full service load, first yielding and the failure load. The full service load was taken as the self-weight of the slab with a superimposed dead load of 1.2 kPa and a live load of 4.8 kPa, as specified by the National Building Code of Canada (NBCC, 1995). This resulted in a shear of 217 kN on the critical shear periphery of the slab specimens.

All the total loads reported in this chapter are the sum of the applied loads at the 8 loading points, the weight of the loading apparatus and the self-weight of the slab outside the critical shear periphery, d/2 from the faces of the column. The self-weight of the slab specimens outside the critical shear region, and the weight of the loading apparatus was 21.5 kN. The corresponding self-weight of the prototype structure resulted in a shear at the interior slab-column connection of approximately 85 kN. All of the deflections reported in this chapter are the average of the measured deflections at the eight loading points.

In order to establish what effect the concentration of the flexural reinforcement had on the behaviour of the slab specimens, the maximum crack widths were measured both inside the immediate column region, within a distance 1.5h from the column faces, and for the rest of the slab outside of this region.

3.1 Specimen S1-U

The total load versus deflection response of Specimen S1-U, with a concrete strength of 37.2 MPa and a uniform distribution of the top mat of reinforcement, is shown in Fig. 3.1a. As can be seen from this figure, the load-deflection curve exhibits a change in stiffness when first cracking occurs at a load of 56 kN. The first cracks occurred in the North-South direction, perpendicular to the weak direction of reinforcement and extended from the four corners of the column. First yielding occurred in one of the bars in the weak direction at a total load of 203 kN and a corresponding average deflection of 9.8 mm. This yielding occurred in the first reinforcing bar from the centre of the slab, 72 mm away from the centre. The maximum load reached was 301 kN with a corresponding average deflection of 16.9 mm, before failing abruptly in punching shear. The failure was instantaneous, with the load dropping to 195 kN and deflection increasing to 19.5 mm. The shear failure extended from the bottom slab-column intersection to the top surface of the slab at a distance of about 150 mm from the face of the column in the weak direction and at a distance of about 300 mm from the face of the column in the strong direction.

Figure 3.2a shows the measured strains in the strain gauges in the top mat of reinforcement at full service load and at the peak load. The highest strains were recorded in the weak direction in the first reinforcing bar, 72 mm away from the centre of the slab, and in the strong direction in the first reinforcing bar, 82 mm from the centre of the slab. The strains were higher in the weak direction due to the 15 mm smaller flexural lever arm. As can be seen from fig. 3.2a, the reinforcement in the weak direction reached 2188 micro-strain at full service load, which is just above the yield level of 2150 micro-strain. In general, strains decreased with distance from the column face.

Figure 3.3a shows the total load versus maximum crack width, inside and outside the "immediate column region". It can be seen that throughout the entire test, the maximum crack widths were significantly larger inside the "immediate column region" than in the remainder of the slab. The crack pattern at the full service load for Specimen S1-U is shown in Figure 3.4a. The maximum crack width at the full service load was 0.8 mm in the "immediate column region" around the column and 0.25 mm outside this region.

As shown in Fig. 3.1a, the loading was continued after the initial failure. During this loading the top reinforcing bars ripped out of the top surface of the slab. The slab reached a load of 273 mm with a corresponding deflection of 75.5 mm. Figure 3.5a shows the appearance of the slab test specimen after failure.

3.2 Specimen S1-B

The total load versus deflection response of Specimen S1-B with a concrete strength of 37.2 MPa and a banded distribution of steel is shown in Figure 3.1b. Compared to the response of Specimen S1-U, the load-deflection curve was stiffer up to the point of first cracking at a load of 58 kN. First cracking occurred in the East-West direction, perpendicular to the strong direction reinforcement. The cracks started from the edge of the test specimen and then propagated towards the column corners. First yielding in the top steel mat occurred at a load of 211 kN and a corresponding average deflection of 8.9 mm. The first bar to yield was the second bar from the centre of the column in the weak direction, 127 mm from the centre of the slab. Specimen S1-B withstood an ultimate load of 317 kN with a corresponding deflection of 15 mm, before failing abruptly in punching shear. The failure was followed by an immediate drop in load to 174 kN and an increase in deflection to 18.4 mm. The banded distribution seemed to push the failure plane away from the column. In the weak direction, the punching shear crack started at the bottom slab-column intersection and surfaced at about 350 mm from the column face. In the strong direction, the punching shear crack surfaced at distance of approximately 450 mm from the face of the column.

The measured strains in the strain gauges in the top mat of reinforcement at full service load and at the peak load are shown in Fig. 3.2b. The highest strains were recorded in the weak direction in the second bar from the column centreline, 127 mm from the centre of the slab, and in the strong direction in the third bar, 212 mm from the centre of the slab. At full service load, the second bar in the weak direction was the only bar to reach yield. The strains generally decreased with distance from the column face.

The total load versus maximum crack width for Specimen S1-B is shown in Fig. 3.3b. From this figure it can be seen that the values for the maximum crack widths inside the "immediate column region" are very close to those measured outside of this region, with the

maximum crack width being 0.15 mm larger in the "immediate column region" at the full service load. For this specimen with banded reinforcement, the cracks are of similar width across the entire surface of the slab. The crack pattern at full service load for Specimen S1-B is shown in Fig. 3.4b. The maximum crack width at full service load was 0.55 mm in the "immediate column region" and 0.4 mm outside of this region.

Upon further loading after the punching shear failure, the slab was able to resist a load greater than the full service load level (see Fig. 3.1b). Figure 3.5b shows the appearance of the slab after failure.

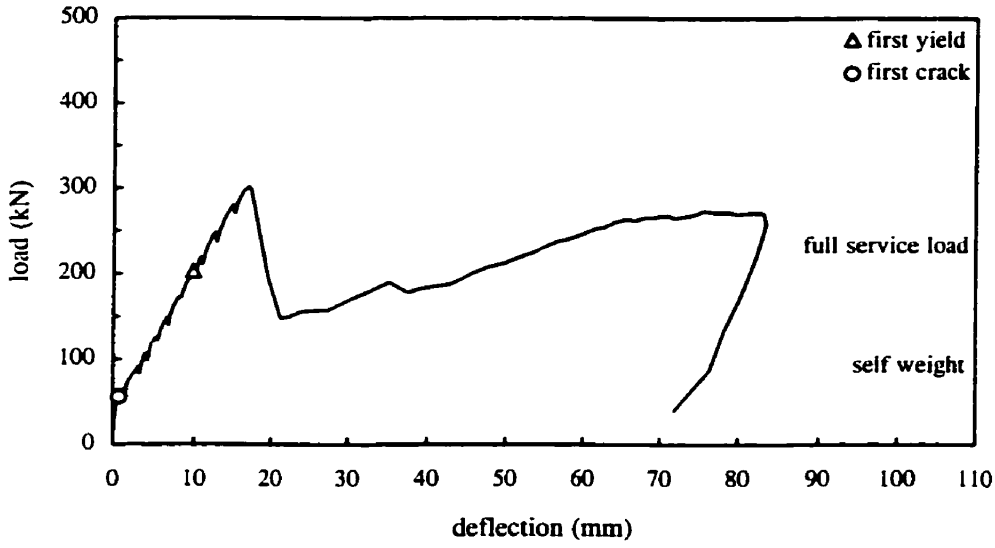

a) Specimen S1-U

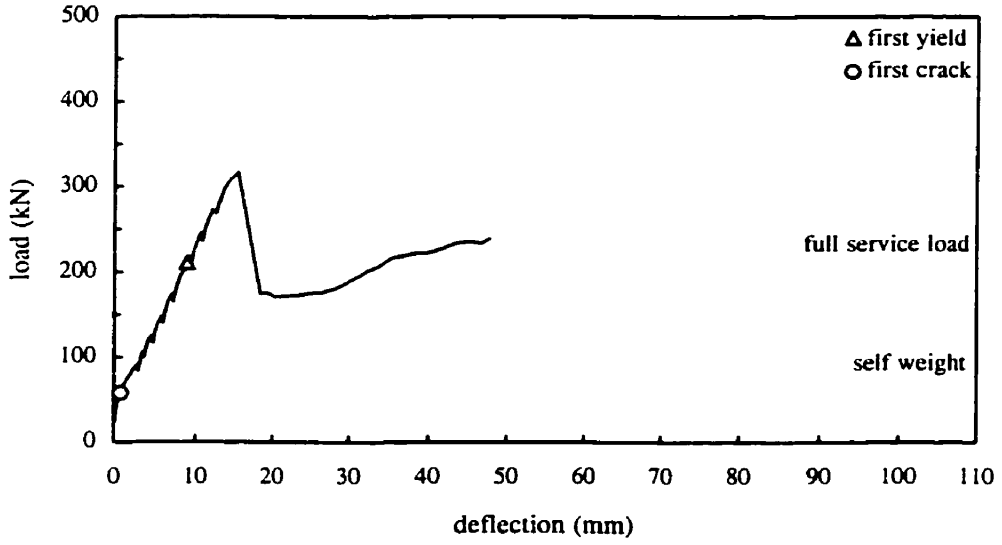

b) Specimen S1-B

Figure 3.1 Load versus average deflection responses of S1 series

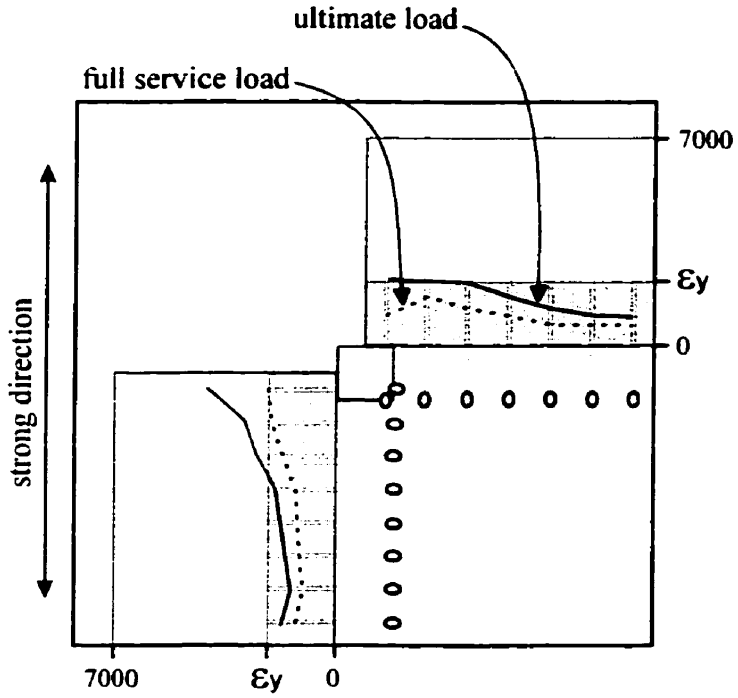

a) Specimen S1-U

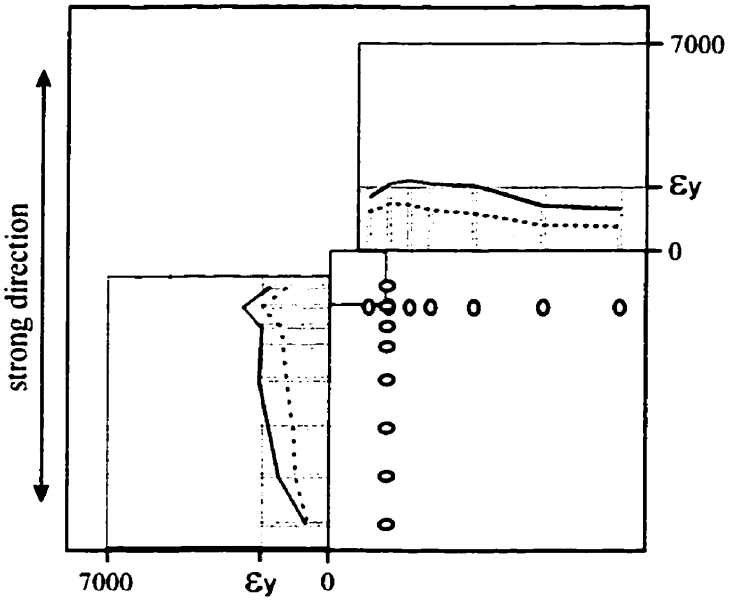

b) Specimen S1-B

Figure 3.2 Strains in top mat reinforcing bars at full service and peak load for S1 Series

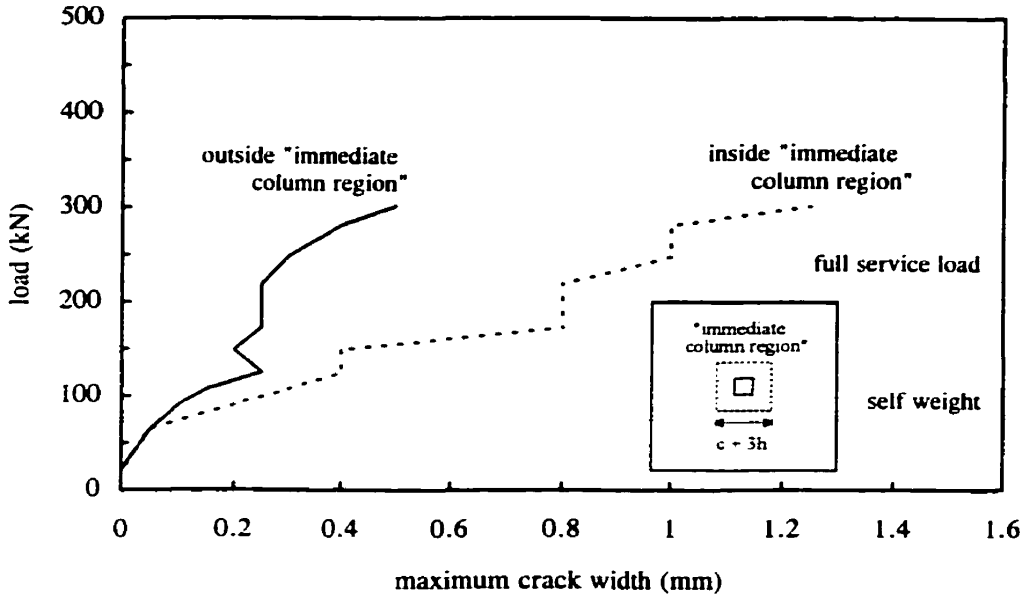

a) Specimen S1-U

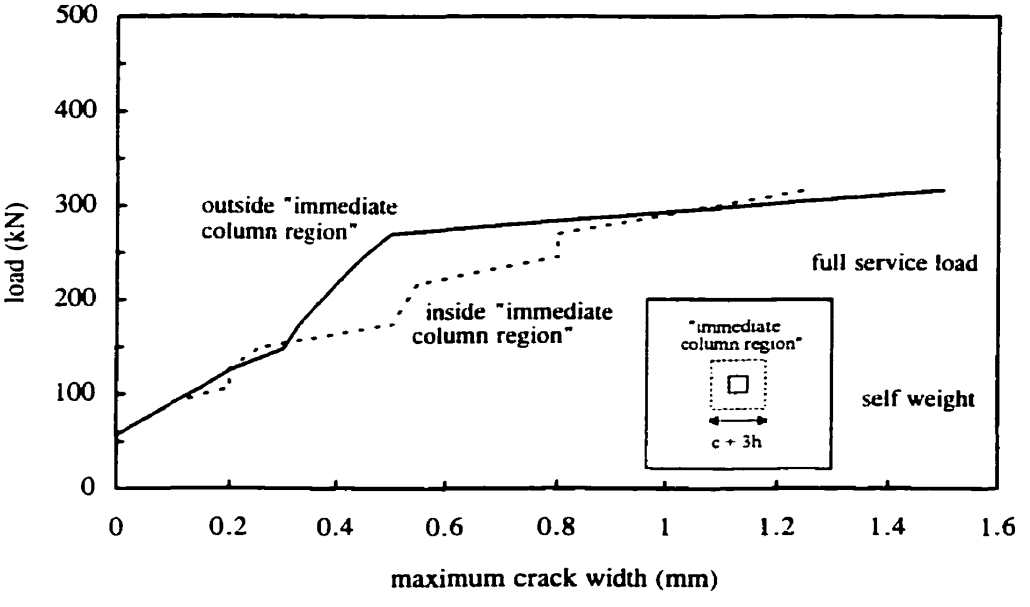

b) Specimen S1-B

Figure 3.3 Load versus maximum crack width for S1 Series

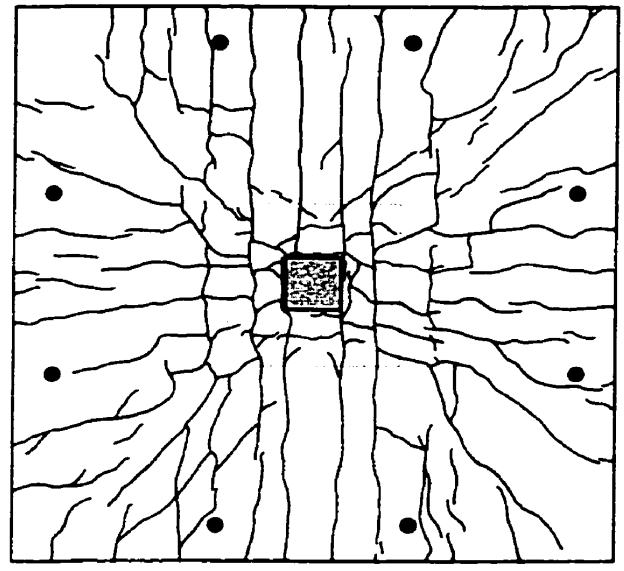

maximum crack width: inside "immediate column region" = 0.8 mm
outside "immediate column region" = 0.25 mm

a) Specimen S1-U

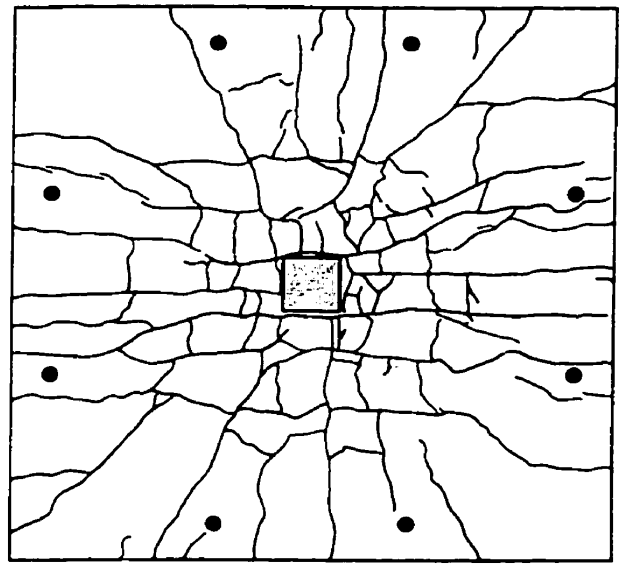

maximum crack width: inside "immediate column region" = 0.55 mm
outside "immediate column region" = 0.4 mm

b) Specimen S1-B

Figure 3.4 Crack pattern of S1 Series at full service load

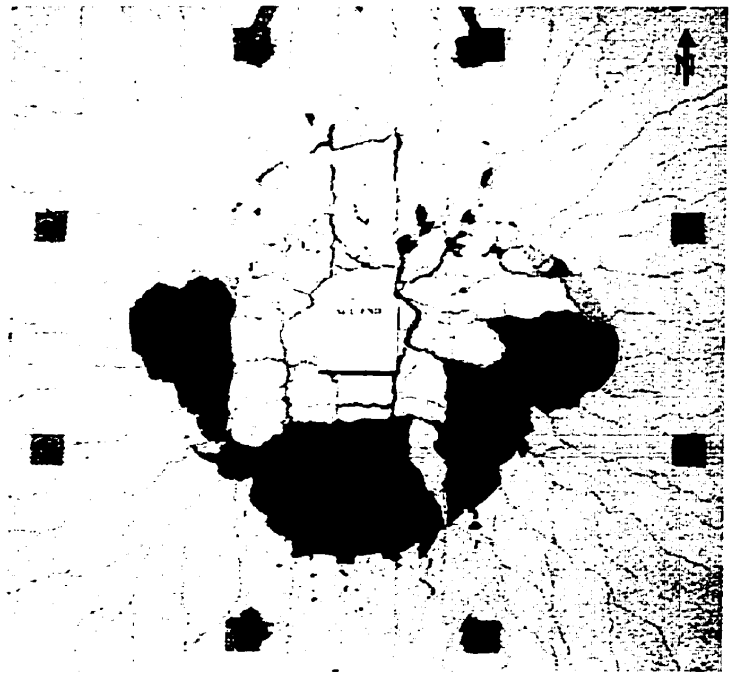

a) Specimen S1-U

b) Specimen S1-B

Figure 3.5 S1 Series at failure

3.3 Specimen S2-U

The total load versus deflection response for Specimen S2-U, having a concrete strength of 57.1 MPa and a uniform distribution of top steel, is shown in Fig. 3.6a. First cracking occurred at a load of 80 kN. As expected, the load-deflection curve was stiffer before first cracking took place. The first cracks occurred in the North-South direction, perpendicular to the weak direction reinforcement and extended from the corners of the column to the edge of the slab. The top mat of steel first yielded in the weak direction at a load of 273 kN and an average deflection of 10.9 mm. The first bar to yield was the first bar in the weak direction, located 72 mm from the centre of the slab. Specimen S2-U reached a peak load of 363 kN and a corresponding average deflection of 17.7 mm. The failure was an abrupt punching shear failure, after which the load dropped suddenly to 187 kN and the deflection increased to 22.0 mm. The failure surface extended from the bottom slab-column intersection to the top surface of the slab at a distance of approximately 2d from the column face in both the weak and the strong directions.

Figure 3.7a shows the measured strains in the strain gauges in the top steel mat at full service load and at the peak load. The first bar from the centre of the slab in the weak direction displayed the highest strain readings during the test and was the only bar to have reached yield at full service load. The strains were typically higher in the regions closer to the column face.

The total load versus maximum crack width, inside and outside the "immediate column region", are shown in Fig. 3.8a. From this figure it can be seen that the maximum crack widths were larger inside the "immediate column region" than for the remainder of the slab for the entire test. The crack pattern at full service load for Specimen S2-U is shown in Fig. 3.9a. The maximum crack width at the full service load was 0.4 mm inside the "immediate column region" and 0.2 mm outside of this region.

Upon reloading after failure, the slab was able to resist a load of 266 kN, that is, somewhat greater than the full service loading (see Fig. 3.6a). Figure 3.10a shows the appearance of the slab after failure.

3.4 Specimen S2-B

Figure 3.6b shows the total load versus deflection response for Specimen S2-B, with a concrete compressive strength of 57.1 MPa and a banded distribution of the top reinforcing steel mat. The load-deflection curve was stiffer up to the point of first cracking at a load of 88 kN. First cracking occurred in the North-South direction, perpendicular to the weak direction reinforcement. The first cracks extended from the edge of the slab specimen and then spread towards the corners of the column. First yielding of the top mat of bars occurred at a load of 316 kN and a corresponding average deflection of 11.3 mm. The first bar to yield was the third bar in the strong direction, 212 mm from the centre of the slab. The maximum load reached was 447 kN with a corresponding average deflection of 20.7 mm. Specimen S2-B failed abruptly in punching shear, after which the load dropped to 234 kN and the deflection increased to 25.9 mm. The banded distribution seemed to push the failure plane away from the column. The punching shear plane started at the intersection of the column face and bottom surface of the slab and emerged on the top surface of the slab at about a distance of 500 mm from the column face both South and West of the column.

The measured strains in the strain gauges in the top mat of reinforcement at full service load and at ultimate load are shown in Fig. 3.7b. At full service load none of the bars reached yield and the reinforcing bars throughout the entire width of the slab specimen exhibited similar strain readings. In this banded specimen, the area of steel is better distributed to resist the applied load, resulting in lower, more uniform strains in the slab reinforcement. The first bar to yield was in the strong direction due to the two additional reinforcing bars that were provided in the weak direction, resulting in a total of 16 bars in this direction and an increased strength.

The total load versus maximum crack width for Specimen S2-B is shown in Fig. 3.8b. From this figure it can be seen that the maximum crack widths were smaller inside the "immediate column region" up to full service load, after which they became smaller in the remainder of the slab, outside of this region. For Specimen S2-B with a banded distribution of reinforcement, the cracks were of similar width across the entire surface of the slab. The crack pattern at full service load for Specimen S2-B is shown in Fig. 3.9b. The maximum

crack width at full service load was 0.45 mm, both inside and outside of the "immediate column region".

After failure, the slab test specimen was reloaded. As can be seen from Fig. 3.6b, Specimen S2-B was able to withstand a load greater than the full service load of 217 kN. The slab reached a load of 298 kN with a corresponding deflection of 38.2 mm. Figure 3.10b shows the appearance of Specimen S2-B after failure.

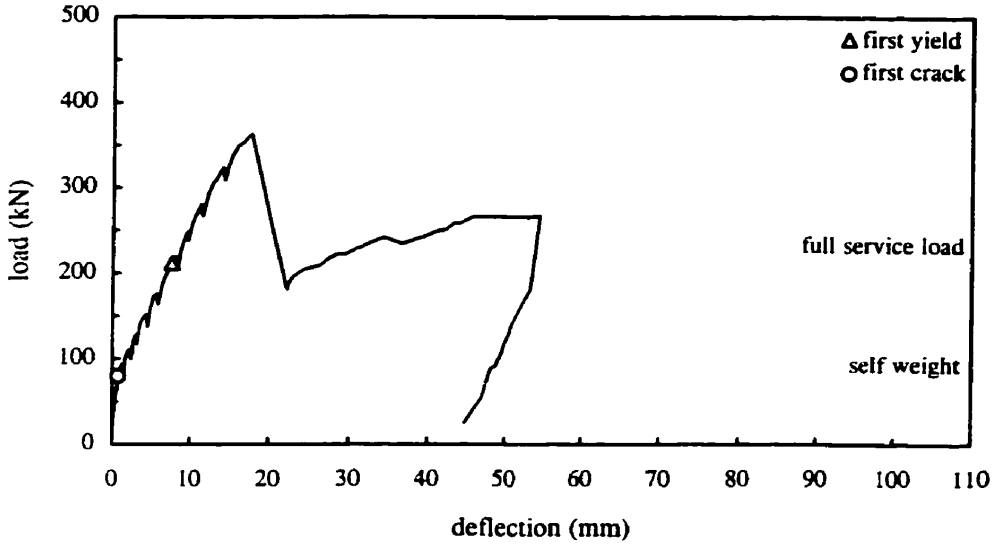

a) Specimen S2-U

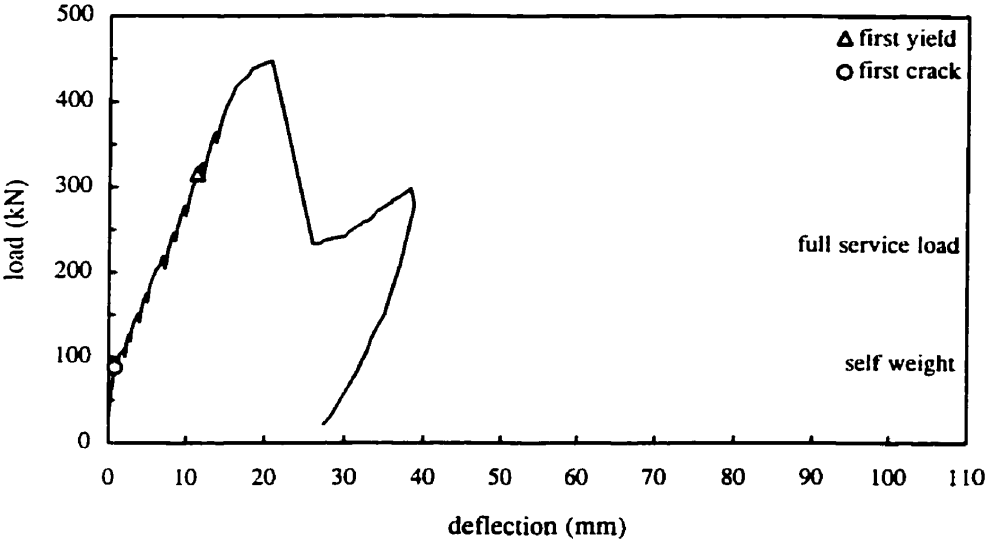

b) Specimen S2-B

Figure 3.6 Load versus average deflection responses of S2 Series

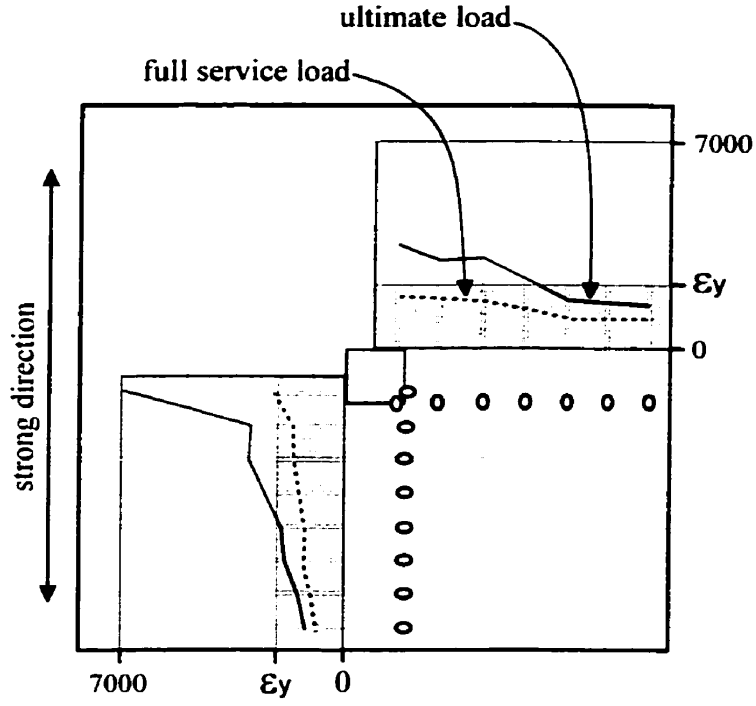

a) Specimen S2-U

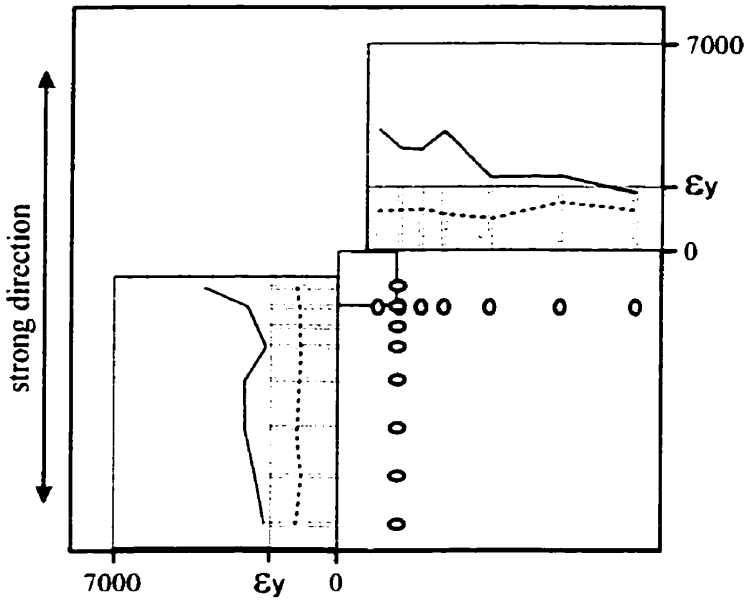

b) Specimen S2-B

Figure 3.7 Strains in top mat reinforcing bars at full service and peak load for S2 Series

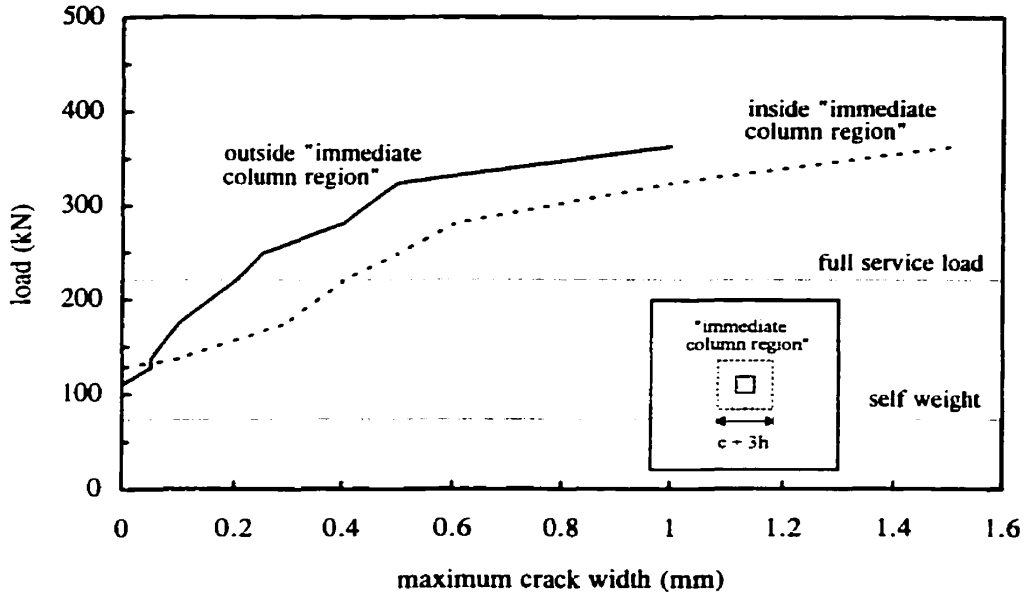

a) Specimen S2-U

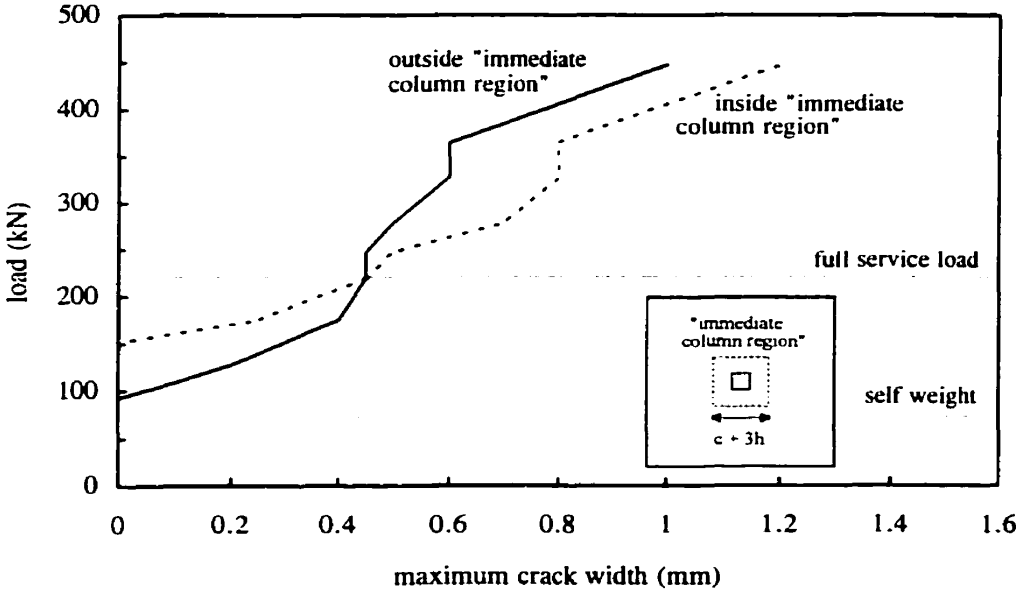

b) Specimen S2-B

Figure 3.8 Load versus maximum crack width for S2 Series

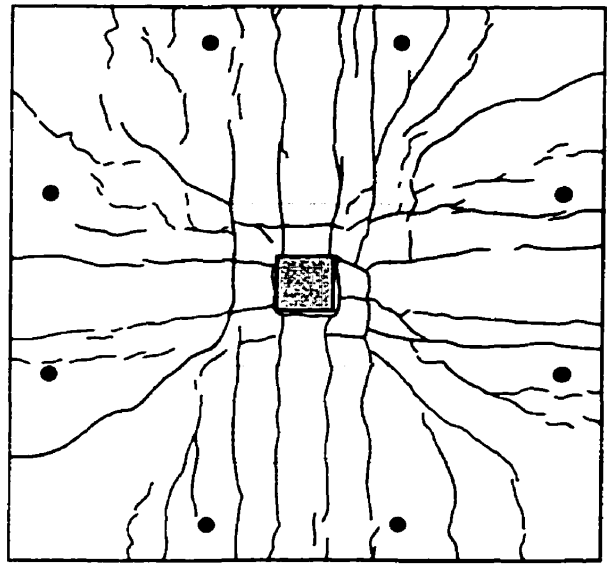

maximum crack width: inside "immediate column region" = 0.4 mm
outside "immediate column region" = 0.2 mm

a) Specimen S2-U

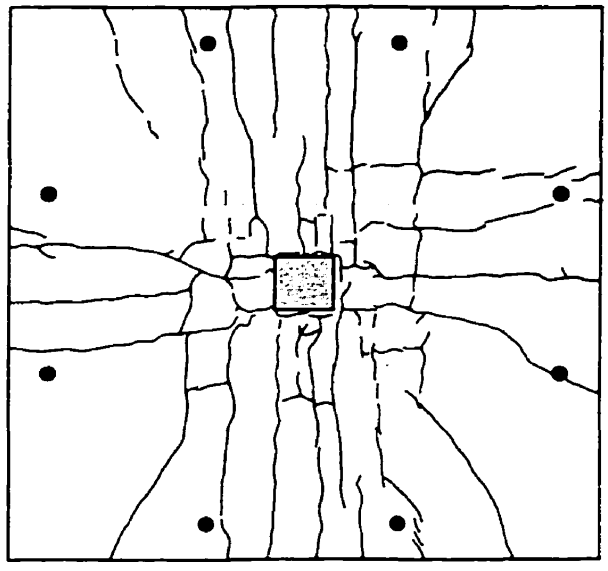

maximum crack width: inside "immediate column region" = 0.45 mm
outside "immediate column region" = 0.45 mm

b) Specimen S2-B

Figure 3.9 Crack pattern of S2 Series at full service load

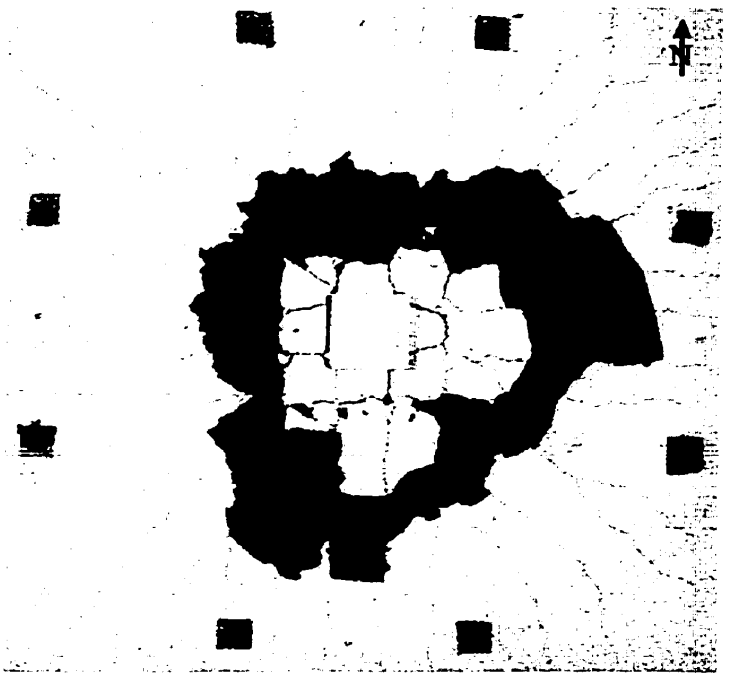

a) Specimen S2-U

b) Specimen S2-B

Figure 3.10 S2 Series at failure

3.5 Specimen S3-U

The total load versus deflection response of Specimen S3-U, with a concrete compressive strength of 67.1 MPa and a uniform distribution of top reinforcement is shown in Fig. 3.11a. As expected, the load-deflection response was stiffer up to the point of first cracking at a load of 89 kN. The first cracks occurred in the North-South direction, perpendicular to the weak direction reinforcement and extended from the corners of the column towards the edges of the slab. First yielding occurred at a load of 247 kN and a corresponding average deflection of 8.0 mm. The bar to first yield was the second bar from the centre of the specimen in the weak direction, at a distance of 297 mm from the centre of the slab. The specimen reached an ultimate load of 443 kN and a corresponding deflection of 24.7 mm, before abruptly failing in punching shear. The failure was instantaneous with a sudden drop in total load to 225 kN and an increase in deflection to 30.4 mm. It is important to note that, after failure, the slab was still able to carry the full service load of 217 kN (see fig. 3.11a). The shear failure plane started at the intersection of the column face and bottom surface of the slab and emerged on the top surface of the slab at a distance of approximately 400 mm from the face of the column North of the column and at a distance of about 300 mm from the face of the column West of the column.

Figure 3.12a shows the measured strains in the strain gauges in the top mat of reinforcement at full service load and at the peak load. At full service load none of the bars reached yield. The highest strains were in the second and third bars from the column centreline in the weak direction, located respectively at 216 mm and 359 mm from the centre of the slab specimen.

The total load versus maximum crack width, both inside and outside the "immediate column region", are shown in Fig. 3.13a. This figure shows that during the entire test, the maximum crack widths were bigger inside the "immediate column region" than in the rest of the slab. The crack pattern at full service load for Specimen S3-U is shown in Fig. 3.14a. The maximum crack width at full service load was 0.4 mm inside the "immediate column region" and 0.25 mm in the rest of the slab.

As shown in Fig. 3.11a, the loading was continued after the initial failure. The slab was able to resist a load of 281 kN with a corresponding deflection of 42.8 mm. The appearance of Specimen S3-U after failure is shown in Fig. 3.15a.

3.6 Specimen S3-B

Figure 3.11b shows the total load versus average deflection response of the test Specimen S3-B, with a concrete compressive strength of 67.1 MPa and a banded distribution of the top reinforcing bars. The drop in stiffness upon first cracking at a load of 90 kN is apparent from this figure. The first crack occurred in the North-South direction, perpendicular to the weak direction reinforcement. The first crack started from the edge of the slab and propagated towards the corner of the column. First yielding in the top mat of steel occurred in the weak direction at a total load of 339 kN with a corresponding average deflection of 12.1 mm. The first reinforcing bar to yield was the fourth bar from the centre of the column in the weak direction, 297 mm from the centre of the slab. The specimen withstood an ultimate load of 485 kN with a corresponding deflection of 26.1 mm. The punching shear failure occurred with a sudden drop in the total load to 294 kN, which is greater than the service load of 217 kN, and a corresponding increase in the deflection to 32 mm. However, the failure surface only became visible at the top surface of the slab when Specimen S3-B reached its second peak load upon further loading. The second peak load was 298 kN and had a corresponding average deflection of 40.8 mm. The failure surface started at the bottom slab-column intersection and surfaced on the top surface of the slab at a distance of approximately 600 mm from the column face both South and West of the column and at a distance of about 700 mm from the face of the column North of the column.

The measured strains in the strain gauges in the top mat of reinforcement at full service load and at the peak load are shown in Fig. 3.12b. At full service load none of the bars reached yield and all the reinforcing bars exhibited similar strains throughout the entire width of the slab. The highest strains recorded were in the third bar from the centre of the slab in the weak direction and in the first bar from the centre of the slab in the strong direction.

The total load versus maximum crack width, both inside and outside the "immediate column region", are shown in Fig. 3.13b. As can be seen from this figure, the maximum crack widths are smaller inside the "immediate column region" up to the full service load, after which they become smaller in the remainder of the slab, outside of this region. The crack pattern at full service load for Specimen S3-B is shown in Fig. 3.14b. The maximum crack width at full service load was 0.4 mm inside the "immediate column region" and 0.33 mm outside of this region.

As shown in Fig. 3.11b, the loading was continued after Specimen S3-B reached its second peak load. The slab specimen reached a load of 340 kN with a corresponding average deflection of 57.4 mm. The appearance of the slab after failure is shown in Fig. 3.15b.

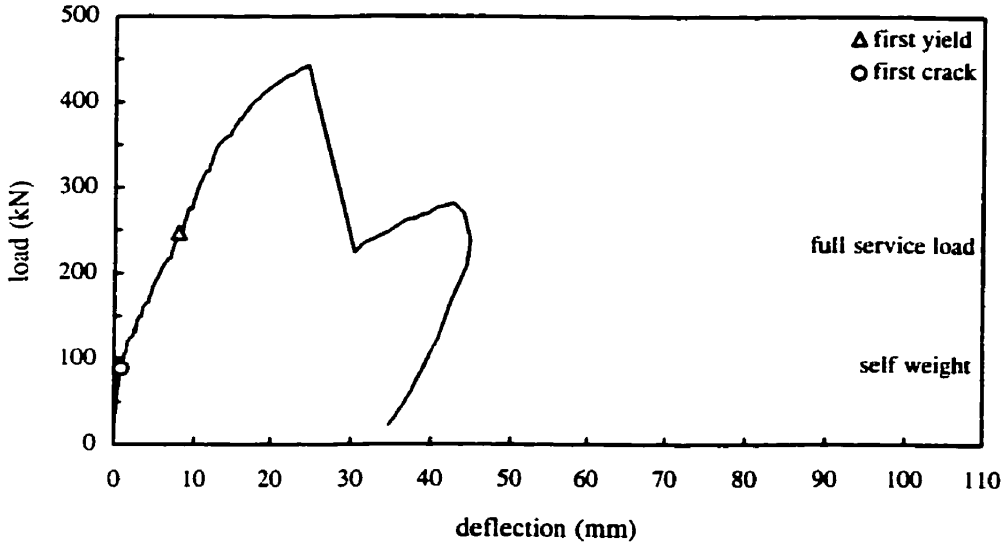

a) Specimen S3-U

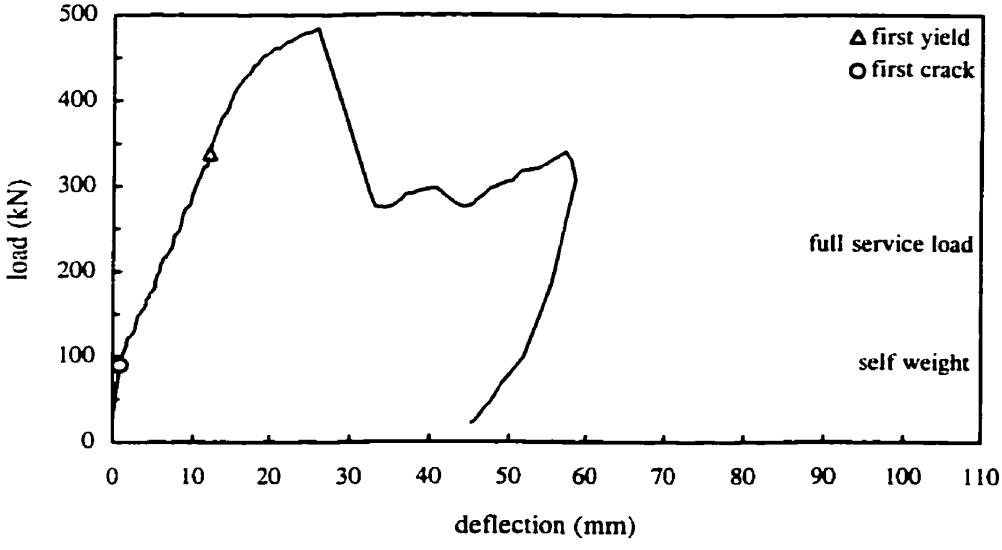

b) Specimen S3-B

Figure 3.11 Load versus average deflection responses of S3 Series

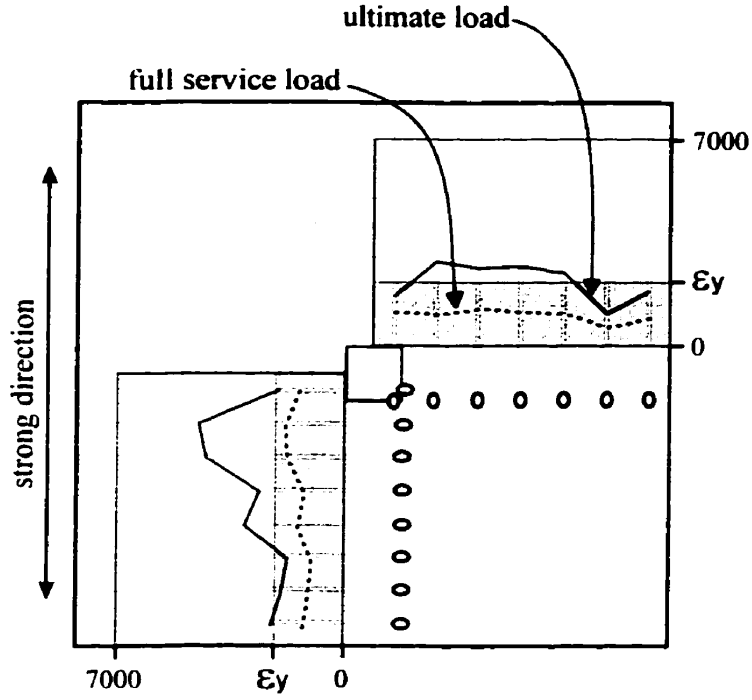

a) Specimen S3-U

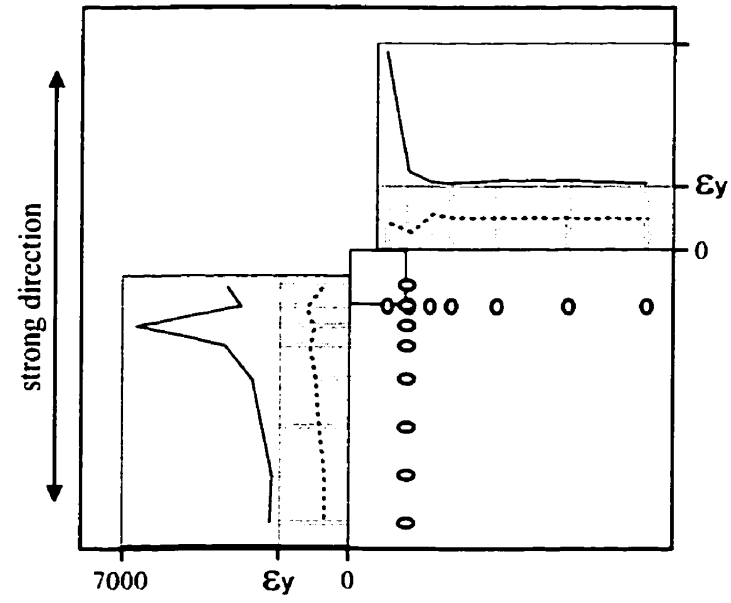

b) Specimen S3-B

Figure 3.12 Strains in top mat reinforcing bars at full service and peak load for S3 Series

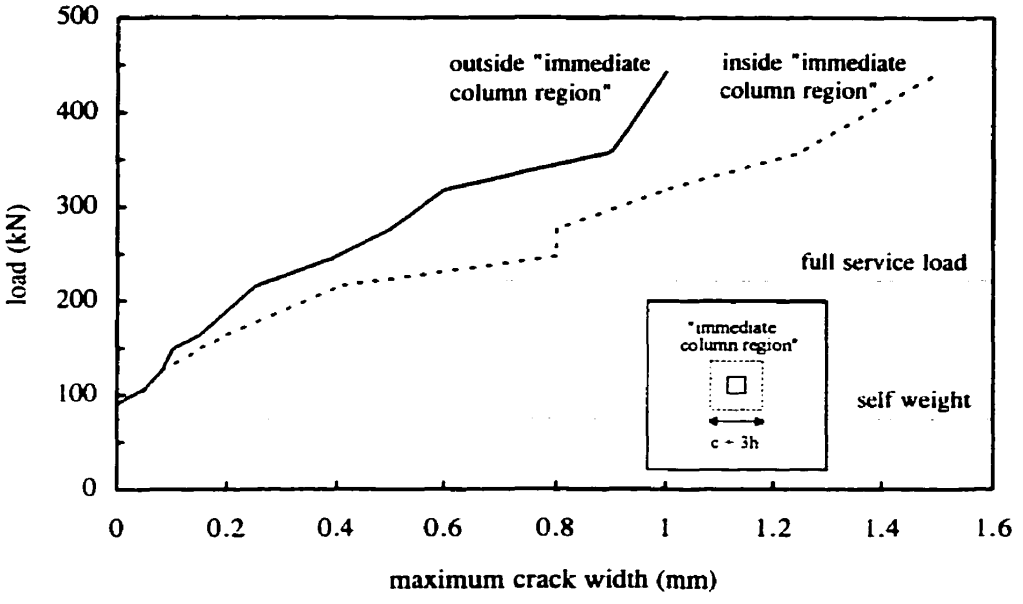

a) Specimen S3-U

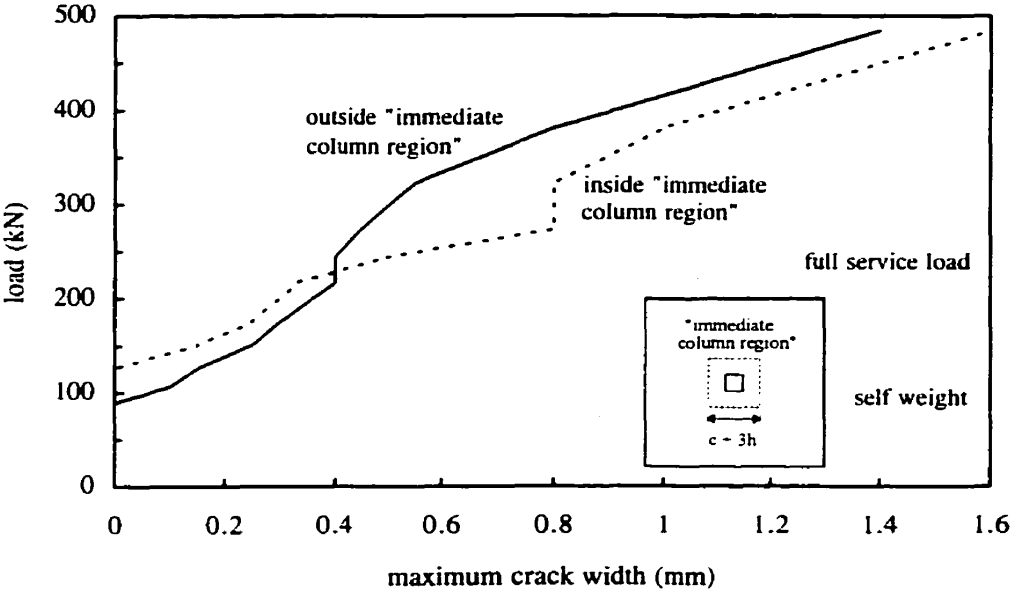

b) Specimen S3-B

Figure 3.13 Load versus maximum crack width for S3 Series

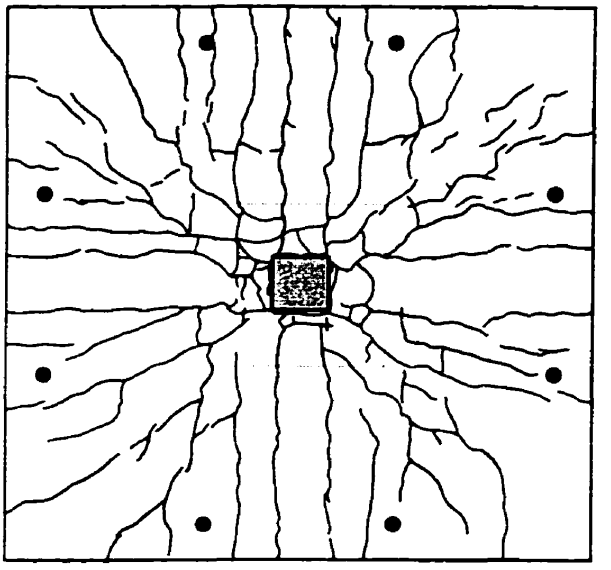

maximum crack width: inside "immediate column region" = 0.4 mm
outside "immediate column region" = 0.25 mm

a) Specimen S3-U

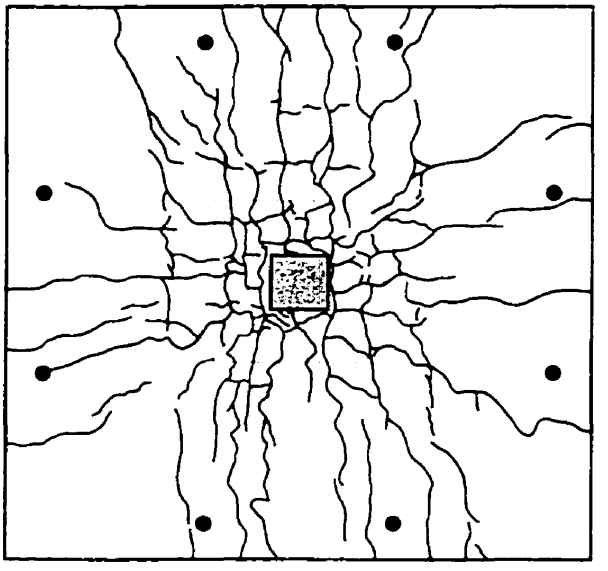

maximum crack width: inside "immediate column region" = 0.4 mm
outside "immediate column region" = 0.33 mm

b) Specimen S3-B

Figure 3.14 Crack pattern of S3 Series at full service load

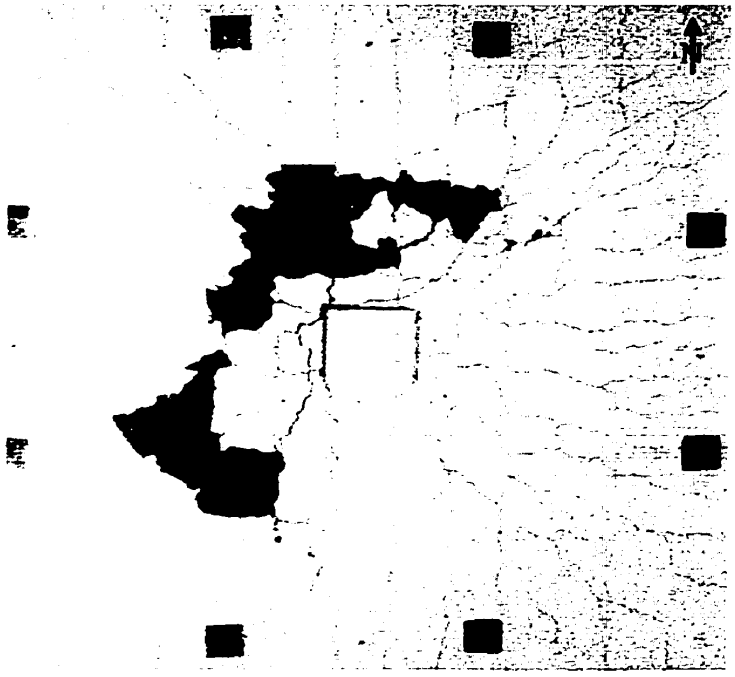

a) Specimen S3-U

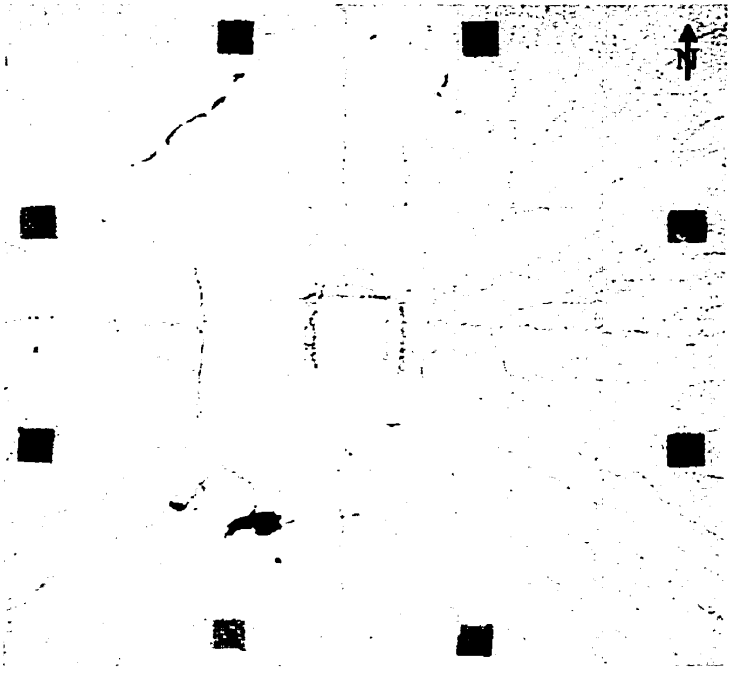

b) Specimen S3-B

Figure 3.15 S3 Series at failure

Chapter 4

Comparison of Test Results of Two-Way Slab Specimens

4.1. Comparison of Two-Way Slab Test Results

This section compares the observed behaviour of the six slab test specimens. Some of the experimental results that are compared include the load-deflection responses of the slabs, the load versus strain distribution in the reinforcing bars and the load versus maximum crack width responses.

4.1.1 Load-Deflection Responses

Figures 4.1 and 4.2 compare the total load versus average deflection responses of the six slab-column specimens. Table 4.1 provides a summary of the measured total loads and average deflections at first cracking, first yielding, full service load and peak load for the slab specimens. When comparing companion specimens with and without the banded reinforcement distribution, it can be seen from Fig. 4.1 and Table 4.1 that the specimens with the banded distribution displayed slightly larger first cracking loads due to their higher percentage of reinforcement in the region of maximum moment around the column. It is interesting to note that the first cracks in the banded specimens always started from the edges of the slab specimens where the reinforcement ratio was lower. Conversely, the first cracks in the slab specimens with the uniform distribution of reinforcement started at the column corners where the stresses were the highest and then the cracks propagated towards the edges of the slab.

From Table 4.1, it can be seen that the first cracking loads increased with the increase in the concrete compressive strength of the slab test specimens. The S1 Series,

with a concrete compressive strength of 37.2 MPa, exhibited the smallest first cracking loads. The use of a higher concrete compressive strength of 57.1 MPa in the S2 Series increased the cracking strength by 43% for the uniform specimens and by 52% for the banded specimens, over the cracking strengths of the S1 Series. For the S3 Series, with a concrete compressive strength of 67.1 MPa, the improvement in the cracking strength was of 59% for the uniform specimens and of 55% for the banded slabs, over the cracking strengths of the S1 Series.

Table 4.1 Summary of load-deflection curves for slab-column specimens

Specimen		First Cracking	Full Service Load	First Yielding	Peak Load
S1-U	load (kN)	56	217	203	301
	deflection (mm)	0.75	10.86	9.82	16.95
S1-B	load (kN)	58	217	211	317
	deflection (mm)	0.80	9.26	8.93	15.44
S2-U	load (kN)	80	217	212	363
	deflection (mm)	0.75	8.10	7.58	17.68
S2-B	load (kN)	88	217	316	447
	deflection (mm)	0.80	7.00	11.33	20.75
S3-U	load (kN)	89	217	247	443
	deflection (mm)	0.80	6.94	7.97	24.75
S3-B	load (kN)	90	217	339	485
	deflection (mm)	0.85	6.49	12.11	26.05
NSCU*	load (kN)	80	214	218	306
	deflection (mm)	1.3	9.9	9.9	17.2
NSCB*	load (kN)	78	214	273	349
	deflection (mm)	1.0	7.8	10.7	15.3

* Specimens tested by McHarg (1997)

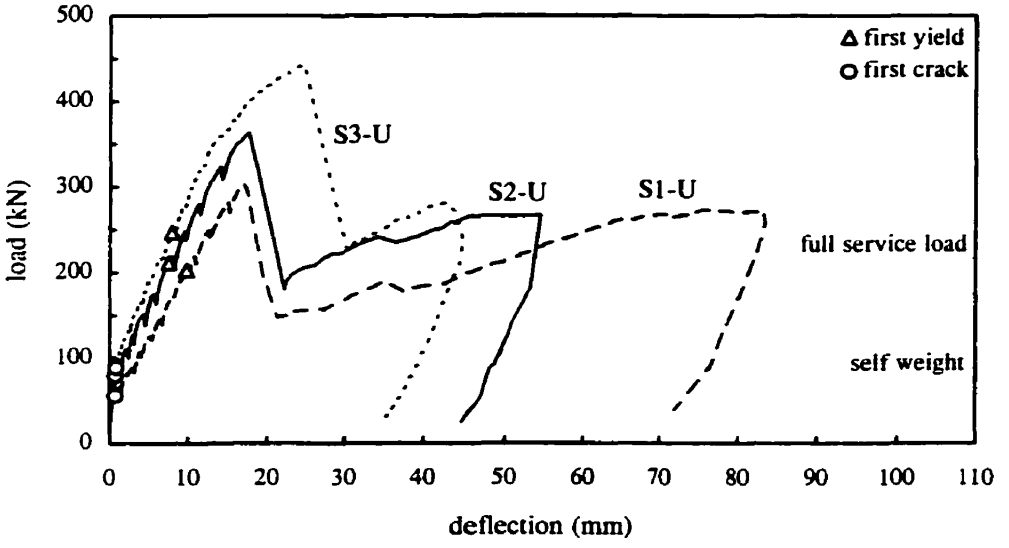

a) Uniform Specimen

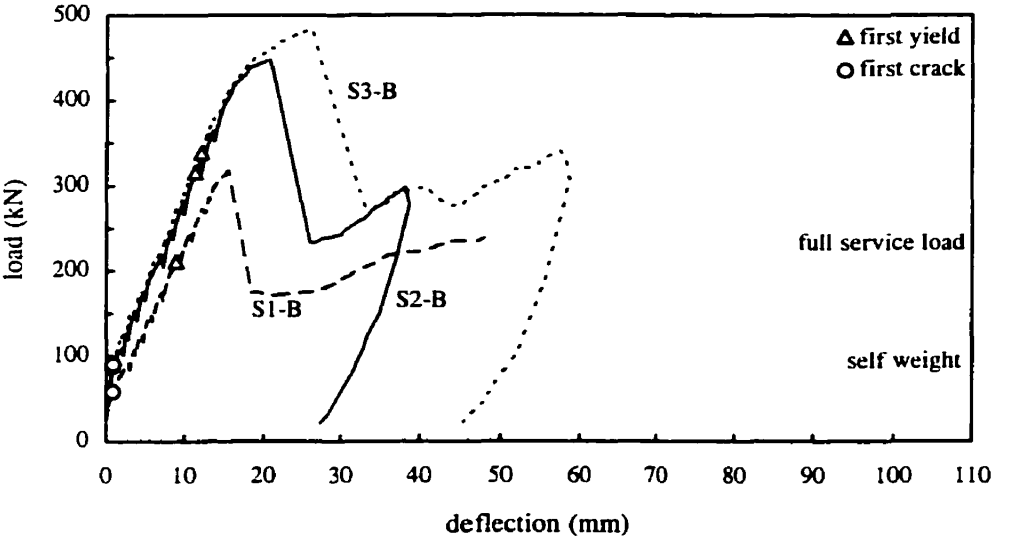

b) Banded Specimens

Figure 4.1 Influence of concrete compressive strength on the load-deflection responses

a) S1 Series

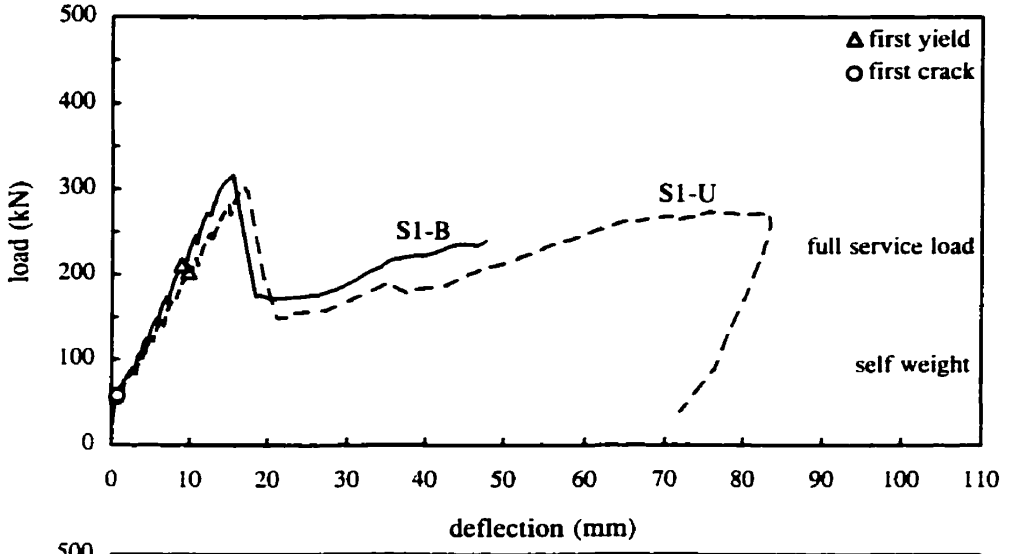

b) S2 Series

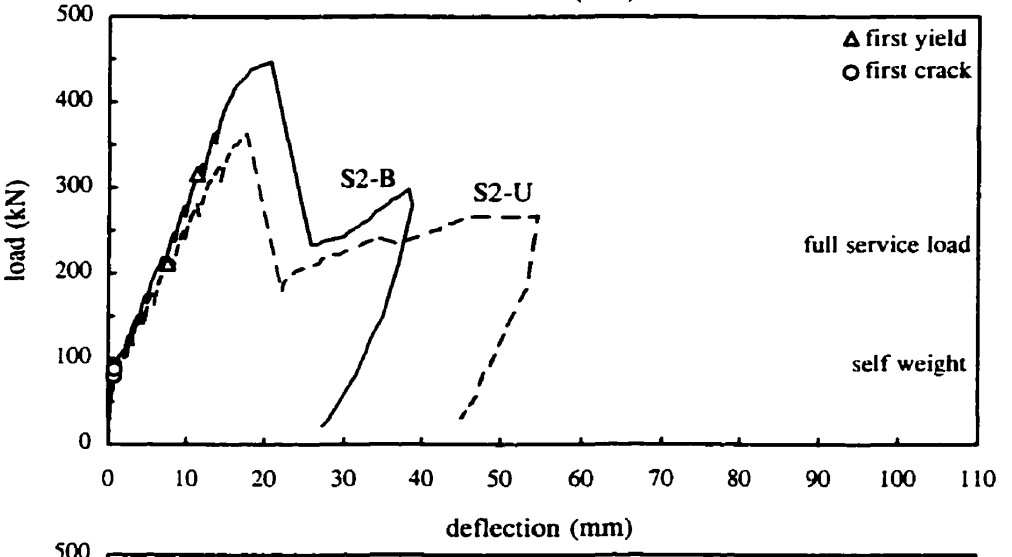

c) S3 Series

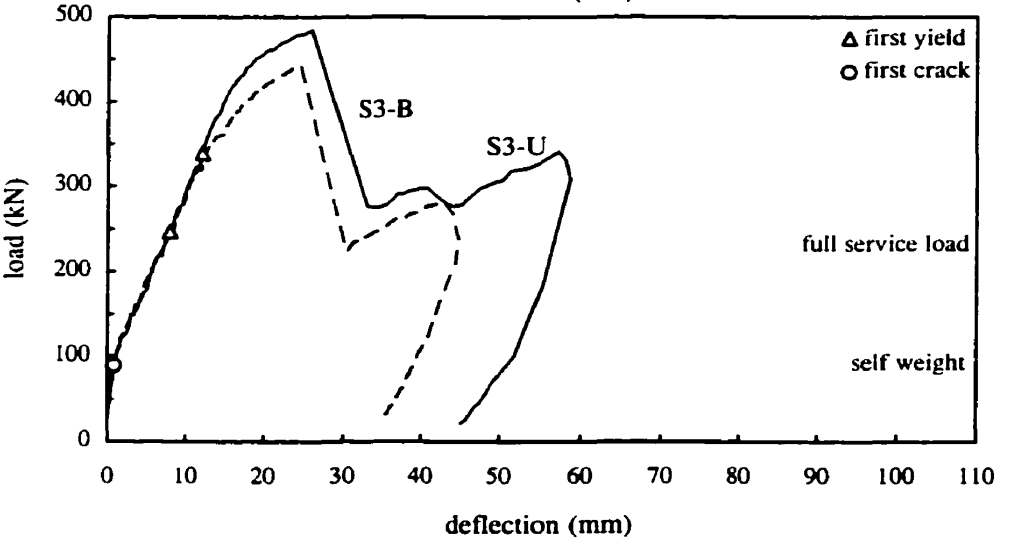

Figure 4.2 Influence of concentrating reinforcement near column on load-deflection curves

The flexural reinforcement yielded in the specimens with the uniform distribution of steel at lower loads than their companion specimens with the banded reinforcement. In the banded specimens, the area of steel was better distributed to resist the applied moments, resulting in lower, more uniform strains in the slab reinforcement. The use of the banded distribution resulted in an increase in the first yielding loads of 4%, 49% and 37% for the S1, S2 and S3 Series, respectively. Moe (1961) and Hawkins *et al.* (1975) also reported an increase in the first yielding loads when the steel reinforcement was banded. As can be seen from Table 4.1, the increase in compressive concrete strength in the slab test specimens also resulted in an increase in the load at which first yielding occurred. Specimens S1-U and S1-B exhibited the lowest first yielding loads. In the S2 Series, the first yielding load increased by 4% for Specimen S2-U and by 50% for Specimen S2-B, when compared to the S1 Series specimens. For the S3 Series, the increase in the slab first yielding loads was 22% for the specimens with the uniform steel distribution, and 61% for the specimens with the banded steel, over the S1 Series slabs.

The peak loads for the slab-column test specimens ranged from 301 kN for specimen S1-U to 485 kN for specimen S3-B. The banded specimens in each series reached higher peak loads than their companion uniform specimens. The increase was 5% for the S1 Series, 23% for the S2 Series and 9% for the S3 Series.

Elstner *et al.* (1956) and Moe (1961) reported that concentrating the flexural reinforcement near the column did not result in an increase in the punching shear strength of two-way slab systems. Whitney (1957) and Alexander *et al.* (1992), who found that banding the reinforcement does increase the shear capacity of slabs, believe that the slab specimens from previous tests with high percentages of flexural reinforcement probably failed by bond failure and not shear. Therefore, there may be a limit on the amount of flexural reinforcement that can be placed in the column vicinity. Marzouk *et al.*(1991) reported that increasing the percentage of reinforcement leads to an increase in the ultimate punching shear capacity of slabs. Gardner *et al.* (1996) and Sherif *et al.*(1996) suggested that the shear strength is a function of the cube root of the ratio of steel reinforcement.

The ultimate capacity of the slab specimens was influenced more by the increase in concrete strength than by the concentration of the flexural reinforcement in the immediate column region. The S1 Series specimens displayed the lowest peak loads. The S2 Series

exhibited an increase in the ultimate load of 21% for the uniform specimens and of 47 % for the specimens with the banded steel distribution, when compared to the peak loads of the S1 Series specimens. The increase in ultimate loads for the S3 Series was of 41% for the uniform specimens and of 53% for the banded specimens, over those of the S1 Series.

Marzouk *et al.*(1991) reported that increasing the concrete compressive strength resulted in an increase in the slab ultimate shear capacity of slabs but that this increase was at a rate of less than the square root of the slab concrete compressive strength. They suggest that the punching shear capacity of slabs is a function of the cube root of the concrete compressive strength. Gardner *et al.*(1996), and Sherif *et al.*(1996) proposed expressions for the punching shear stress of slabs, in which the relationship $v \propto \sqrt[3]{f_c'}$ was used.

All the slabs exhibited an abrupt punching shear mode of failure. The specimens failed along a sloping surface that extends from the compression surface of the slab at the face of the column to the tension surface at some distance away from the column face. After the peak loads were reached, all of the loads dropped instantaneously to approximately one-half of the load carrying capacities of the slab specimens. The higher concrete strength specimens displayed a more ductile type of failure. Before punching occurred, most of their flexural reinforcement had reached the yield stress of 2150 micro-strain, resulting in a gradual decrease in the slope of their load-deflection responses just before ultimate capacity was reached. This was especially true for specimen S3-B, which underwent a general yielding of its flexural reinforcement before failing in punching shear. Although this non-linear load-deflection behaviour is mostly due to the yielding of the flexural reinforcement, the drop in stiffness did not always correspond to the first yielding of the reinforcement. In the lower strength slab specimens, the yielding of the reinforcement was more localised in the column region.

The shear failure plane was affected by both the increase in the concrete compressive strength of the slab specimens and by the concentration of the flexural reinforcement in the column vicinity. When comparing the companion specimens in each series, it was apparent that the concentration of the flexural reinforcement in the immediate column region seemed to push the failure plane away from the column. The size of the

punching shear failure plane was also slightly increased with the increase in the concrete compressive strength.

4.1.2 Stiffness, Ductility and Energy Absorption Capacity

From Table 4.2 it can be seen that the stiffness of the specimens was a function of both the flexural reinforcement distribution and of the concrete compressive strength. In general, the load deflection responses for slabs failing in punching shear can be represented by two straight lines with different slopes . The first straight line extends up to the point of first cracking and its slope represents the stiffness of the uncracked specimen. The second line extends up to the load which caused first yielding in the top reinforcing mat. The slope of this line represents the stiffness of the cracked specimen, K.

Table 4.2 Observed stiffness, ductility and energy absorption capacity

Specimen	Concrete Strength f'_c (MPa)	Stiffness K (kN/mm)	Ductility $\frac{\Delta_u}{\Delta_y}$	Energy Absorption Capacity (kN.mm x 10^3)
S1-U	37.2	16.24	1.72	3.00
S1-B	37.2	18.89	1.68	2.85
S2-U	57.1	19.33	1.62	5.19
S2-B	57.1	21.71	1.83	5.89
S3-U	67.1	21.94	3.09	7.50
S3-B	67.1	22.13	2.16	8.59

It can be seen from Table 4.2 that the stiffness increases with an increase in the concrete strength. The S1 Series slabs, with a concrete compressive strength of 37.2 MPa, were the least stiff specimens. The use of a higher concrete compressive strength of 57.1 MPa in the S2 Series improved the stiffness by 19% for the uniform specimens and by 15% for the banded specimens, over the stiffness of the S1 Series specimens. For the S3 Series, with a concrete compressive strength of 67.1 MPa, the increase in the slab stiffness was 35% for the uniform specimens and 17% for the banded slabs, over the stiffness of the S1 Series slabs. The increase in stiffness for both the S2 and S3 Series was at a rate less than

that of the square root of the concrete compressive strength. Marzouk *et al.*(1991) also reported that the slab stiffness increased with the concrete compressive strength but at a rate less than the ratio of the square root of the concrete strength.

From Table 4.2, it can also be seen that the banded specimens were stiffer than their companion specimens without the banded steel distribution. The increase of stiffness was 16%, 14% and 1% for the S1, S2 and S3 Series, respectively. Elstner *et al.*(1956), Whitney (1957) and Moe (1961) also found that concentrating the flexural reinforcement in the column vicinity increased the stiffness of the load-deflection responses of slabs. Marzouk *et al.*(1991) reported that the slab stiffness increases as the reinforcement ratio is increased.

The ductility of each slab test specimen was calculated and the different values were included in Table 4.2. The ductility is usually quantified as the ratio of the deflection at the peak load to the deflection at first yielding of the steel flexural reinforcement. From Table 4.2, it can be seen that concentrating the steel reinforcement around the column resulted in a decrease in the ductility of the slab specimens while increasing the concrete compressive strength resulted in an increase in their ductility (specimen S2-U did not follow this trend). Marzouk *et al.*(1991) also reported that an increase in the reinforcement ratio of slabs leads to a decrease in their ductility whereas the use of higher strength concrete slightly improves the ductility. Alexander *et al.*(1992) noted that decreasing the spacing of the steel flexural reinforcement results in a decrease in ductility.

Table 4.2 also includes the energy absorption capacities of the slab specimens. The energy absorption is usually defined as the area under the load-deflection curve. From this table it can be seen that the energy absorption capacity of the slabs increased with increasing concrete compressive strength. Marzouk *et al.*(1991) reported that the effect of concrete strength on the energy absorption capacity of slabs was not very significant. The banding of the reinforcement around the column seemed to increase the energy absorption of the slab specimens for both the S2 and S3 Series, but resulted in a slight decrease in the energy absorption capacity of the specimens in the S1 Series. Marzouk *et al.*(1991) reported that the energy absorption capacity of slabs decreased with higher steel reinforcement percentages.

4.1.3 Strain Distribution of Reinforcing Steel

Figure 4.3 shows the strain distributions recorded for the flexural steel reinforcement at full service load for both the uniform and the banded specimens. The reinforcement in the uniform specimens exhibited higher strains near the column than did the reinforcement in the companion specimens with the banded distribution of steel. Due to the two-way action of slabs, applied moments in the specimens are the highest at the column face. The specimens with a uniform distribution of reinforcement displayed high strains near the column due to the larger stiffness of this region. The strains in banded specimens were more uniform across the slab width as the reinforcement was more closely spaced in the region of maximum applied moment around the column. Elstner *et al.*(1956) reported that the steel strains near the columns in slabs with banded reinforcement were lower than those in the companion specimens with uniform steel distribution.

As can be seen from Fig. 4.3a, the effect that the increase in the concrete compressive strength had on the service-load behaviour of the uniform specimens was not evident. The three uniform specimens had very similar strain distributions (see Fig. 4.3a). The behaviour of the banded specimens at full service load however was improved by the increase in the concrete compressive strength. As shown in Fig. 4.3b, the strains in the reinforcement decreased as the concrete strength increased.

4.1.4 Maximum Crack Widths

Table 4.3 shows the maximum crack widths at full service load for all the slab specimens. In the uniform specimens, the maximum crack width inside the "immediate column region" was greatly affected by the increase in concrete strength. As can be seen from Table 4.3 and from Fig. 4.4a, at the full service load of 217 kN, the maximum crack widths inside the "immediate column region" in specimens S2-U and S3-U, with concrete compressive strengths of 57.1 MPa and 67.1 MPa, were reduced by half as compared to those of specimen S1-U, with a concrete strength of 37.2 MPa. Also from Fig. 4.4b it can be seen that for total loads up to full service load, the crack widths outside the "immediate column region" were slightly smaller in specimen S1-U than they were in specimens S2-U and S3-U. In the specimens with the banded distribution of steel reinforcement, the crack widths at service-load inside and outside the "immediate column region" were slightly

smaller for the higher strength specimens. Figure 4.5 shows the maximum crack widths measured for the banded specimens at the different load stages.

Table 4.3 Maximum crack width at full service load for slab-column specimens

Specimen	Maximum crack width at full service load (mm)	
	inside the "immediate column region"	outside the "immediate column region"
S1-U	0.80	0.25
S1-B	0.55	0.40
S2-U	0.40	0.20
S2-B	0.45	0.45
S3-U	0.40	0.25
S3-B	0.40	0.33

From Fig. 3.4, Fig. 3.9 and Fig. 3.14, which present the crack patterns for the slab specimens at full service load, it can be seen that the banded specimens have more cracks inside the "immediate column region" as compared to their companion specimens with the uniform distribution of reinforcement. Although the banded specimens displayed more cracks, their maximum crack widths were smaller than those of the uniform specimens up to full service load, as can be seen from Fig.4.6. Also the average tensile strains on the surface of the slab around the column were always less for the banded specimens (see Fig. 4.7). The average tensile strain around the column versus total load are presented in Fig. 4.8 for both the uniform and the banded specimens. As can be seen from this figure, the tensile stresses around the column were lower for the S2 and S3 Series than they were for the S1 Series. These results display a similar trend to the maximum crack widths values presented in Table 4.3. The use of higher strength concrete, therefore, resulted in a slight increase in the first cracking strength of the slab specimens and helped limit their crack growth as the load was increased. The slabs with the high-strength concrete would thus be expected to have a greater durability than those built with normal strength concrete.

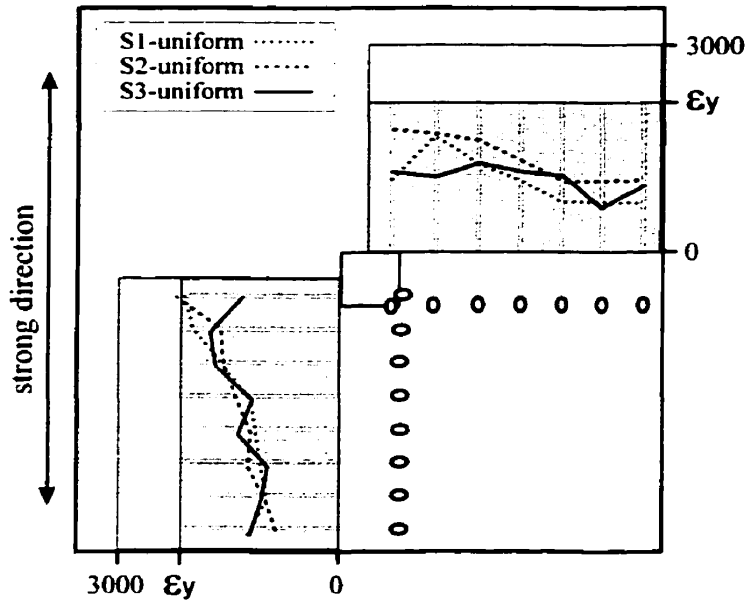

a) uniform specimens

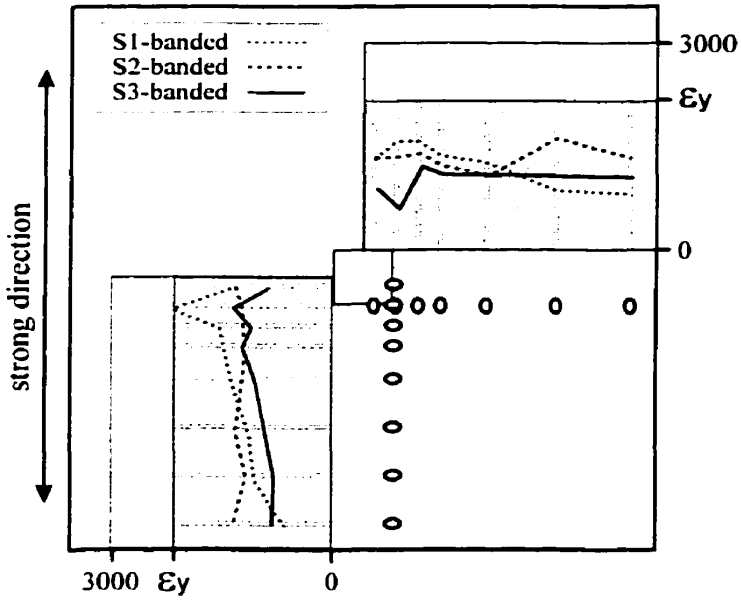

b) banded specimens

Figure 4.3 Strains in top reinforcing bars at full service load

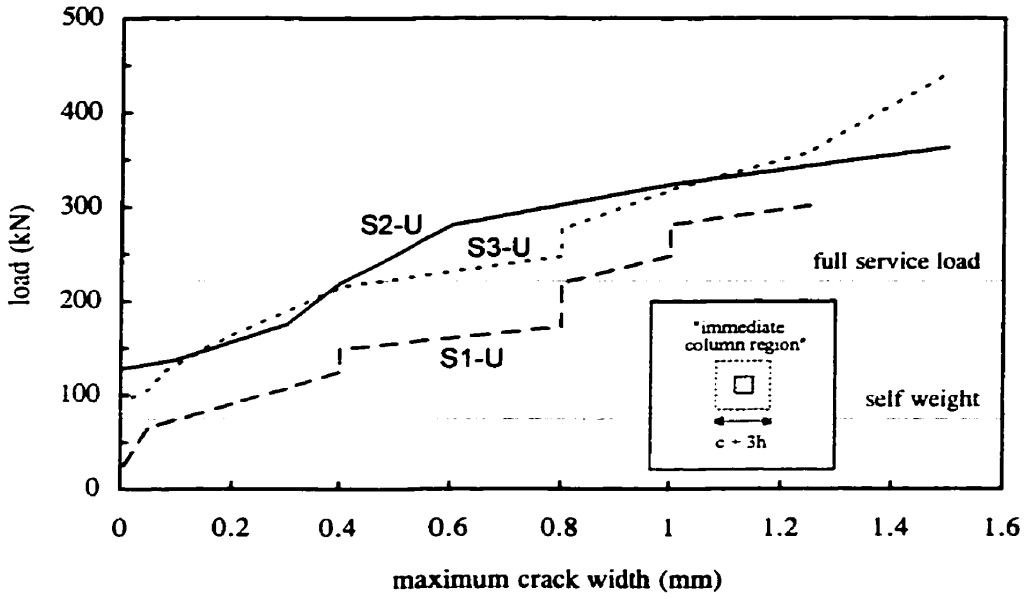

a) within "immediate column region" 1.5h from column face

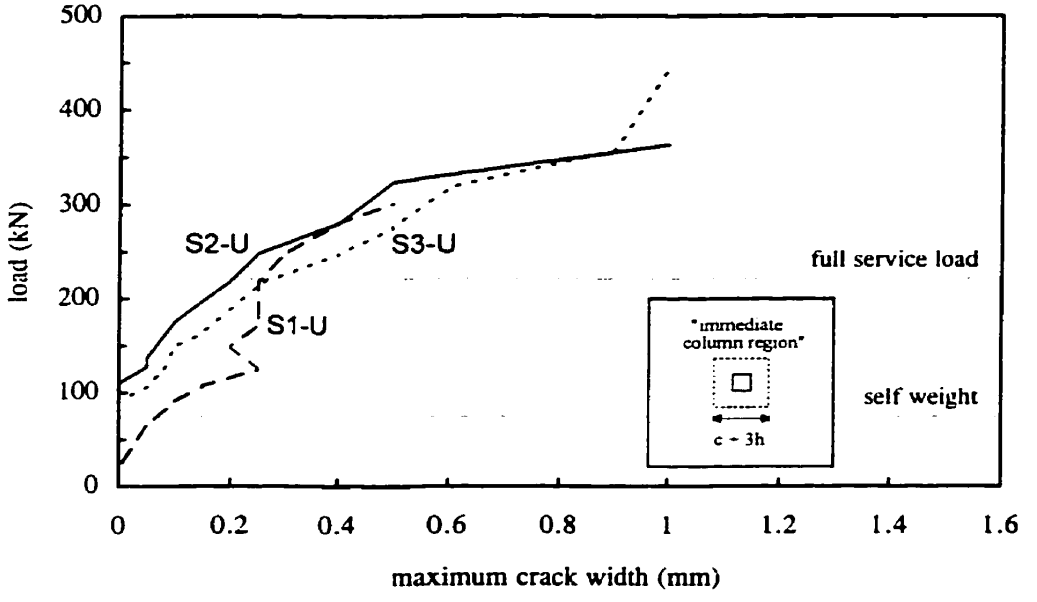

b) outside "immediate column region" 1.5h from column face

Figure 4.4 Load versus maximum crack width for uniform specimens

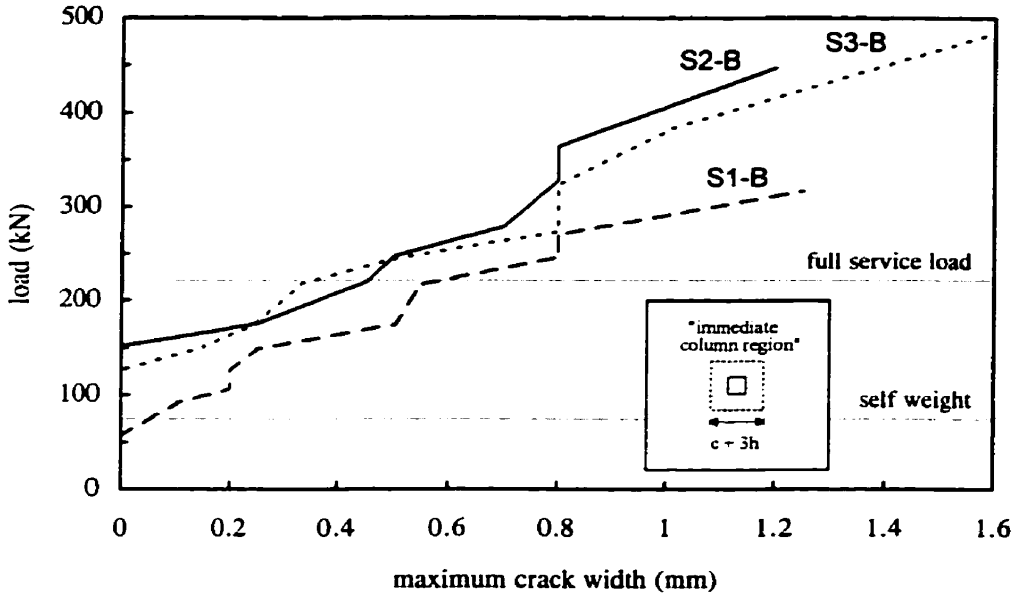

a) within "immediate column region" 1.5h from column face

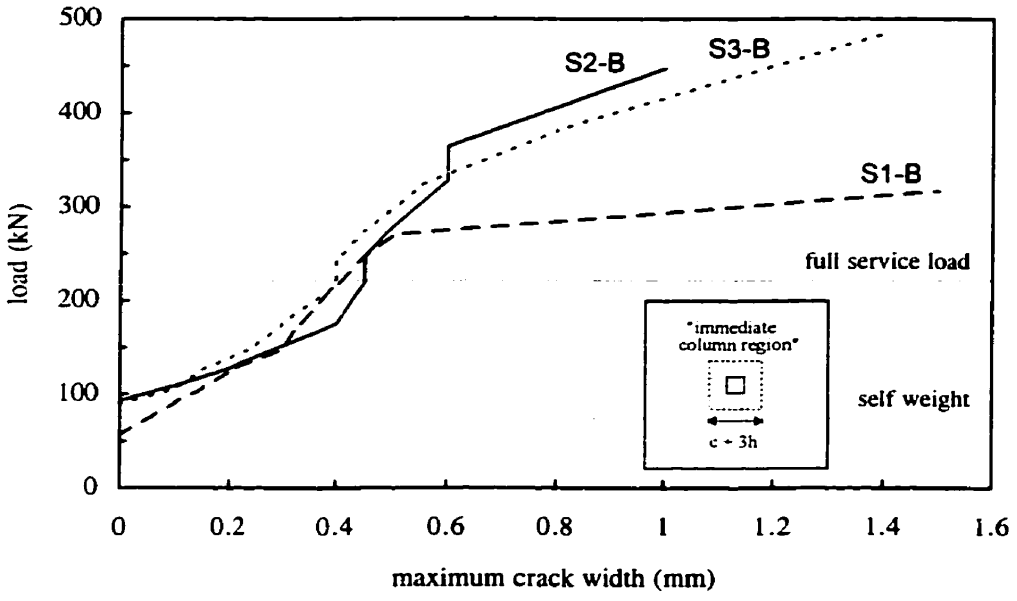

b) outside "immediate column region" 1.5h from column face

Figure 4.5 Load versus maximum crack width for banded specimens

a) S1 Series

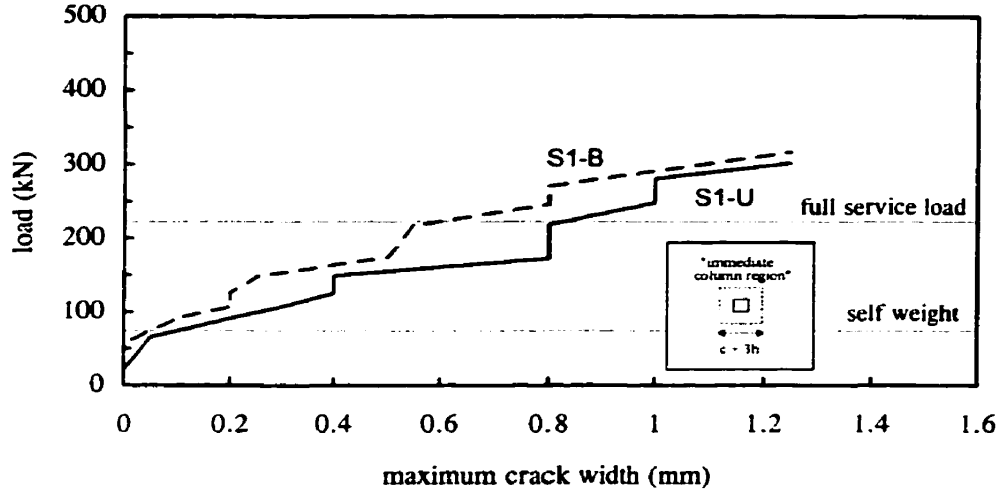

b) S2 Series

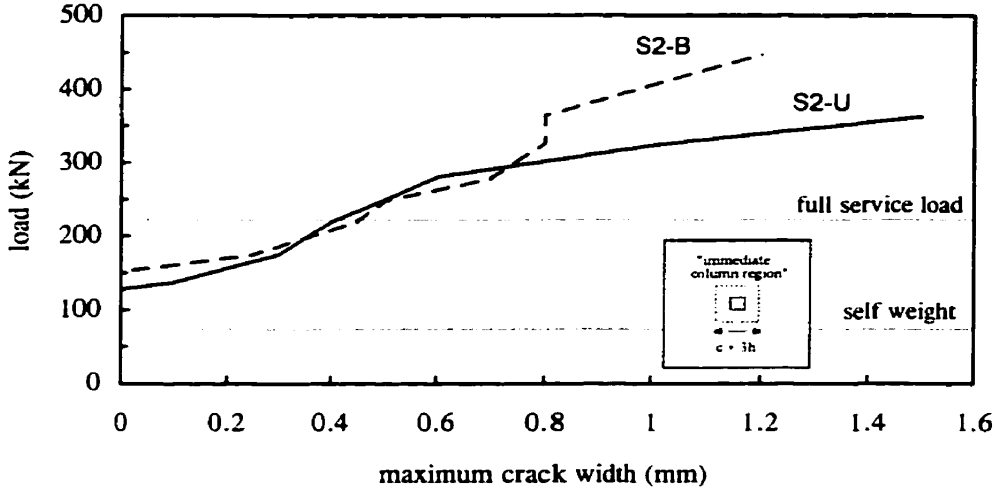

c) S3 Series

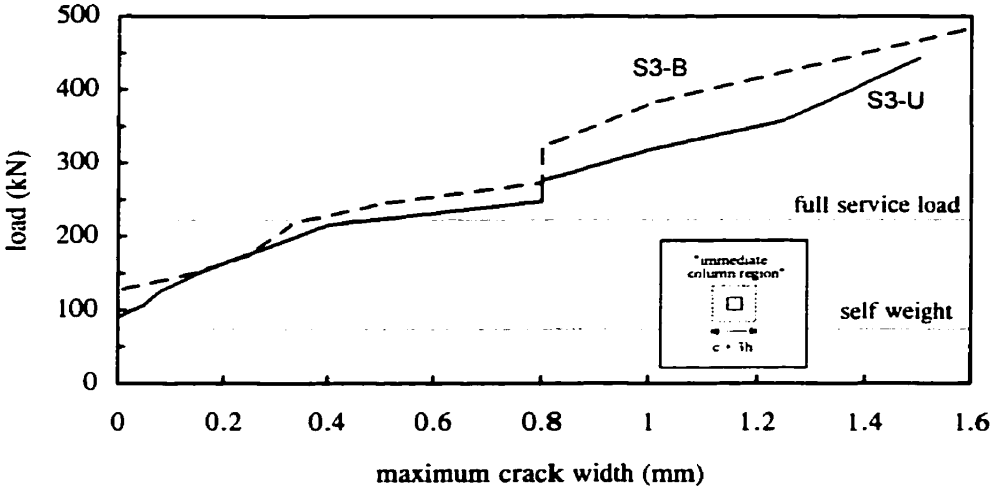

Figure 4.6 Load versus maximum crack width inside "immediate column region"

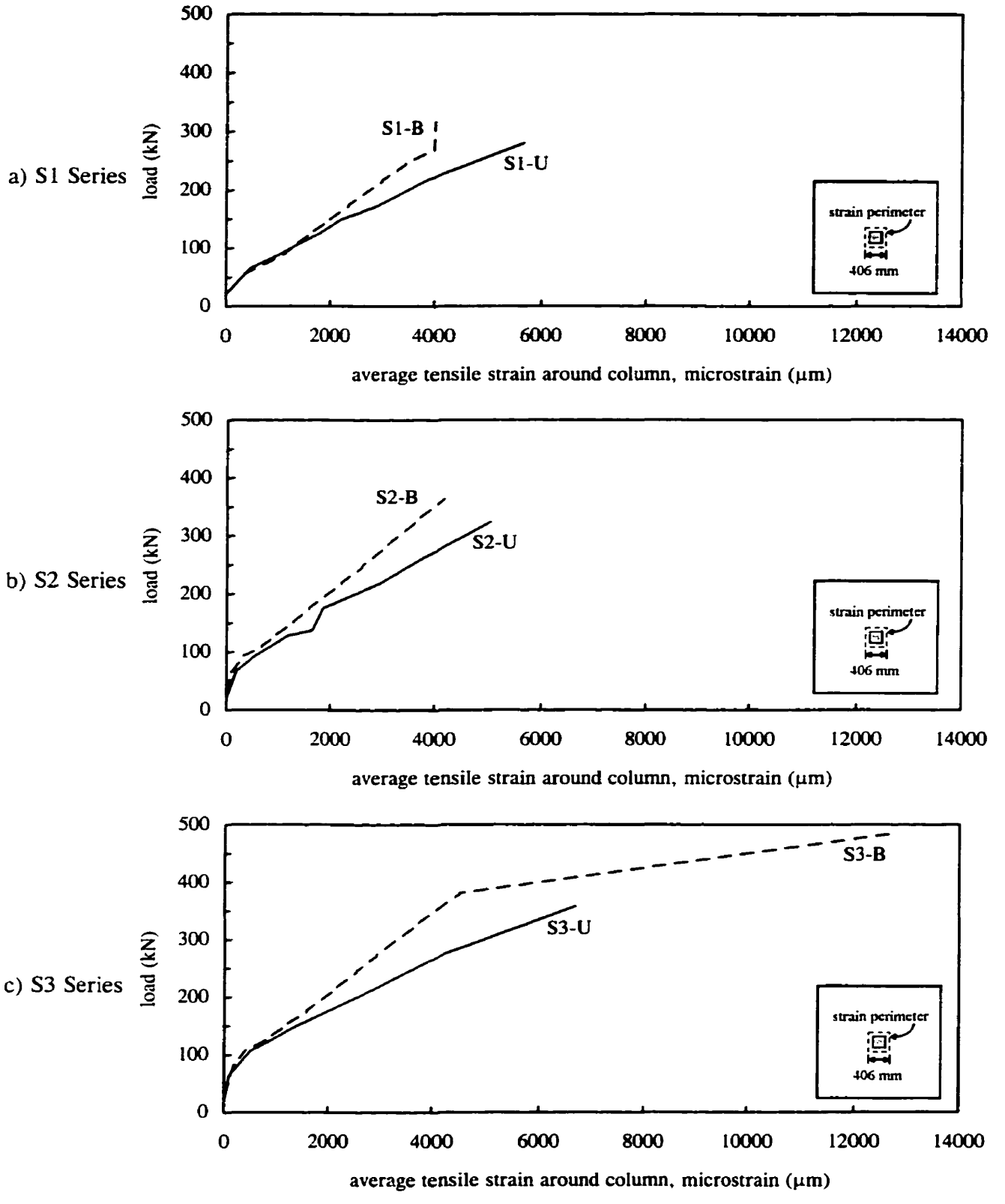

Figure 4.7 Load versus average tensile strain around column of slab-column specimens

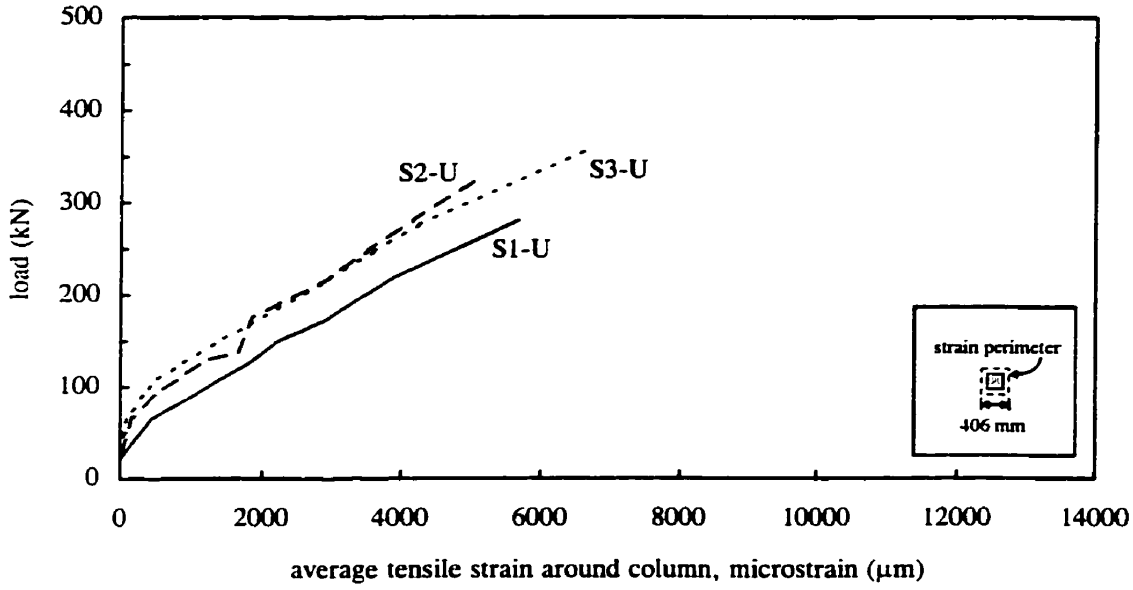

a) uniform specimens

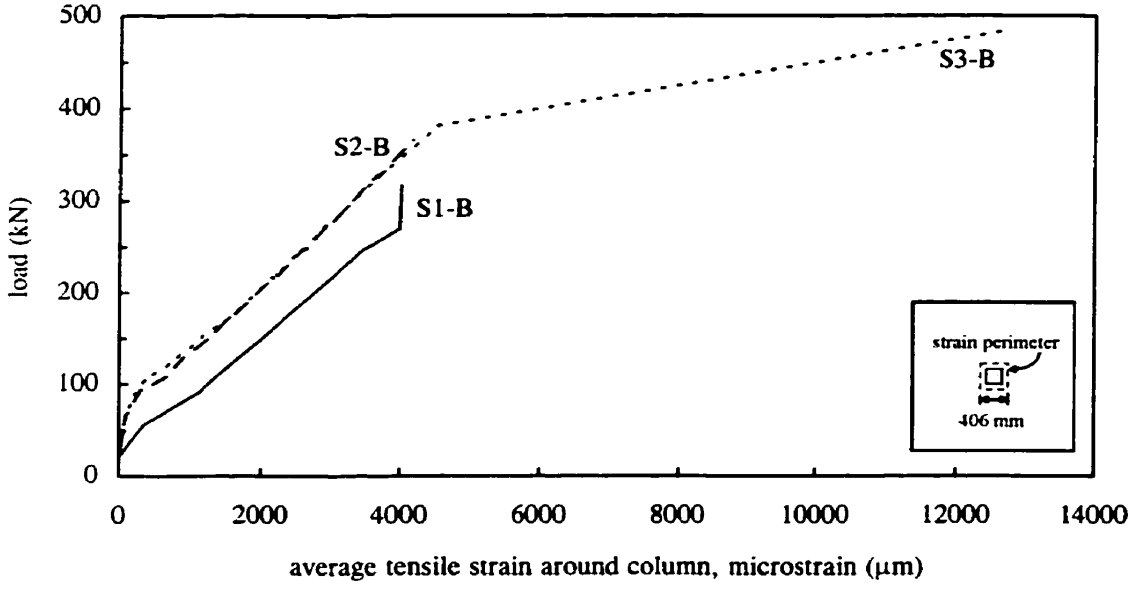

b) banded specimens

Figure 4.8 Influence of concrete compressive strength on the load versus average tensile strain around column

4.2 Comparison of Failure Loads with Predictions

In this section the experimental results obtained for the punching shear strength of the slab specimens will be compared to the predicted failure loads using different code equations and other expressions proposed by a number of investigators. Table 4.4 provides a summary of the nominal shear stress values for the six test specimens as predicted by the ACI Code (1995), the CSA Standard (1994), the BS Standard (1985) and the CEB-FIP Code (1990). All of the code expressions used to determine the values in Table 4.4 are given in Table 1.1. Figure 4.9 also compares the experimentally determined failure loads with the failure loads predicted using the three different code expressions.

Table 4.4 Comparison of failure loads to code predictions for slab specimens

			Shear Resistance (kN)			
Specimen	f'_c **(MPa)**	ρ **(%)**	**Experimental Results**	**ACI 318-95 & CSA A23.3-94**	**BS 8110 (1985)**	**CEB-FIP (1990)**
S1-U	37.2	0.96	**301**	297	300	233
S1-B	37.2	1.92	**317**	297	378	294
S2-U	57.1	0.96	**363**	368	307	257
S2-B	57.1	1.92	**447**	368	387	324
S3-U	67.1	0.96	**443**	398	307	257
S3-B	67.1	1.92	**485**	398	387	324
NSCU*	30.0	0.96	**306**	266	279	217
NSCB*	30.0	1.92	**349**	266	352	273

* Specimens tested by McHarg (1997)

The punching shear strength expressions of the ACI Code and CSA Standard do not include a reinforcement ratio term. As they do not acknowledge the beneficial effects of concentrating the flexural reinforcement in the immediate column region, they both underestimate the shear strength of the banded specimens (see Table 4.4 and Fig. 4.9). For the uniform specimens, with a reinforcement ratio of less than 1%, the predictions of the American and Canadian codes slightly underestimate the punching shear strength of

Specimens S1-U and S3-U but slightly overestimate the strength of specimen S2-U (see Table 4.4 and Fig. 4.9). Sherif *et al.*(1996) noted that the shear strength provisions of the American and the Canadian codes can be unsafe under certain conditions, particularly for slabs with low reinforcement ratios ($\rho < 0.01$). They suggested that the code expressions for the punching shear stress be modified to include the steel reinforcement ratio.

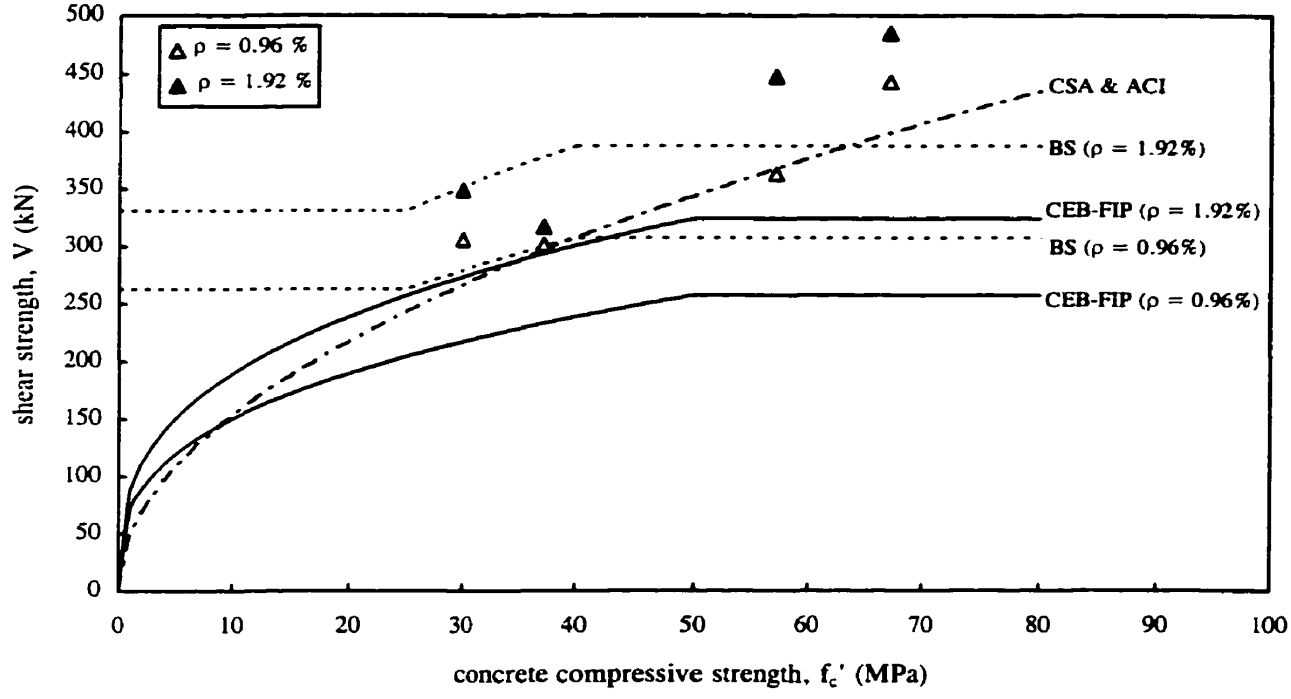

Figure 4.9 Comparison of experimental and predicted failure loads

The expressions for the punching shear strength of the BS Standard and the CEB-FIP Code are both a function of the cube root of the reinforcement ratio and of the concrete compressive strength. Both the British and the European codes have an upper limit for the values of f_c' used in computing the punching shear strength of slabs. The BS Standard specifies that f_c' should not be taken as greater than 40 MPa while the CEB-FIP Code sets its limit on f_c' to 50 MPa. As can be seen from Table 4.4 and Fig. 4.9, the BS Standard is conservative in its predictions of the punching shear strengths of all the test specimens, except for that of Specimen S1-B. Due to the limit on f_c', the shear strengths of the slab specimens of Series S2 and Series S3 are significantly underestimated by the punching shear strength expression of the British Standard. The CEB-FIP Code expression

is also very conservative as it results in shear strength values that are significantly smaller than the experimental results recorded for the punching shear strengths of all the slab test specimens.

Table 4.5 provides a summary of the nominal punching shear strength values for the six test specimens as predicted by Rankin *et al.*(1987), Gardner *et al.*(1996) and Sherif *et al.* (1996). The equations used to evaluate the punching shear strengths in Table 4.5 can be found in Chapter 1 (see Equations 1.7, 1.8 and 1.9).

Table 4.5 Comparison of failure loads to equations proposed by various investigators

			Shear Resistance (kN)			
Specimen	f'_c **(MPa)**	ρ **(%)**	**Experimental Results**	**Rankin *et al.* (1987)**	**Gardner *et al.* (1996)**	**Sherif *et al.* (1996)**
S1-U	37.2	0.96	**301**	369	248	340
S1-B	37.2	1.92	**317**	439	312	428
S2-U	57.1	0.96	**363**	458	286	392
S2-B	57.1	1.92	**447**	544	360	494
S3-U	67.1	0.96	**443**	496	302	414
S3-B	67.1	1.92	**485**	590	380	521
NSCU*	30.0	0.96	**306**	332	231	316
NSCB*	30.0	1.92	**349**	394	290	398

* Specimens tested by McHarg (1997)

Rankin *et al.*(1987) proposed Equation 1.7 for the punching shear strength of slabs. In their expression, the shear stress is assumed to be a function of the square root of the concrete compressive strength and a function of $\sqrt[4]{\rho}$. As can be seen from Table 4.5, the use of Equation 1.7 results in shear strength predictions that are significantly higher than the experimental results obtained for the six slab test specimens.

Gardner *et al.*(1996) suggested that the punching shear load is approximately proportional to the cube root of the concrete strength, steel ratio, and steel yield stress. They proposed Equation 1.8 for the shear stress of slabs. From Table 4.5 it can be seen that Equation 1.8 underestimates the shear strength of all the slab specimens.

Sherif *et al.*(1996) proposed Equation 1.9 for the shear strength of slabs. In this equation, the shear strength is assumed to be a function of the cube root of both the concrete compressive strength and of the steel reinforcement ratio. It can be seen from Table 4.5 that, except for specimen S3-U, Equation 1.9 overestimates the shear capacity of all the slab test specimens.

Chapter 5

Comparison of Test Results with Code Predictions

In this chapter, the punching shear predictions of the American ACI 318-95 Code and the Canadian CSA A23.3-94 Standard are compared to the experimental results obtained for the punching shear strength of a number of slab-column connections tested in this experimental program and tested by various investigators. The connections that will be investigated are interior slab-column connections without shear reinforcement and subjected to monotonic, concentric loading. In the tests reported in this chapter, the influence of the concrete compressive strength, f'_c, and the steel flexural reinforcement ratio, ρ, were the two parameters studied. The effective depth, d, of the test specimens had a range between 75 and 473 mm and the perimeter-to-thickness ratio (b_o/d) had a maximum value of 17. The objective of this chapter is to determine whether the shear provisions of the ACI Code and the CSA Standard provide conservative punching shear strength predictions for interior slab-column connections.

5.1 Comparison of Experimental Results with Code Predictions

In the following section, the experimental data published by the various investigators will be presented. The different properties and test results of the slab specimens are summarized in Tables 5.1 through 5.4. Also, plots comparing the punching shear predictions of the ACI Code and the CSA Standard with the experimental results obtained by the various investigators are provided (see Fig. 5.1, 5.2 and 5.3).

Table 5.1 is a summary of the properties and test results of some of the slab specimens tested by Graf (1938), Narasimhan (1971), Petcu *et al.* (1973), Base (1968), Criswell (1970) and Tolf (1988). As mentioned previously, only the interior slab-column connections without shear reinforcement and subjected to concentric loading were included in this comparison. It is important to note that failure in all of these tests occurred before the flexural capacities of the slab specimens were reached. From Fig. 5.1 and Table 5.1, it can be seen that the ACI Code and the CSA Standard provide conservative punching shear strength predictions for all the slabs except for some of the specimens with very low reinforcement ratios ($\rho < 0.8\%$).

Table 5.1 Experimental data for slab tests performed by a number of investigators

Investigators	Specimens	f_c' (MPa)	ρ (%)	ρ' (%)	d (mm)	b_o/d	P_u (kN)	v (MPa)
Graf (1938)	1362	13.9	1.04	0	271	8.4	1157	1.88
	1375*	**15.5**	**0.6**	**0**	**473**	**6.5**	**1648**	**1.13**
Narasimhan (1971)	L9	30.4	1.11	1.11	143	12.5	588	2.30
	L7	33	1.11	1.11	143	12.5	687	2.69
Petcu et al. (1973)	**A-1***	**20.9**	**0.37**	**0**	**120**	**10.7**	**186**	**1.21**
	B-4	32.6	0.4	0	216	7.7	696	1.94
	B-5*	**32.8**	**0.4**	**0**	**220**	**7.6**	**666**	**1.81**
Base (1968)	A1/M3	14.2	1.85	0	121	10.7	301	1.92
	A1/T1	14	1.01	0	124	10.6	254	1.56
	A2/M1	35.4	1.01	0	124	10.6	401	2.46
	A2/M3	32.5	1.25	0	121	10.7	422	2.69
	A2/T1	39.3	1.01	0	124	10.6	411	2.52
	A3/M1	18.8	1.01	0	124	10.6	242	1.48
	A3/T1	20.6	1.03	0	121	10.7	322	2.06
Criswell (1970)	**S2075-1***	**32.4**	**0.79**	**0**	**122**	**12.3**	**290**	**1.58**
	S2075-2*	**29**	**0.78**	**0**	**122**	**12.3**	**273**	**1.49**
	S2150-1	29.6	1.54	0	124	12.2	464	2.47
	S2150-2	30.1	1.56	0	122	12.3	440	2.40
Tolf (1988) (circular columns)	S2.1	30.3	0.8	0	200	7.1	603	2.12
	S2.2	28.6	0.8	0	199	7.1	600	2.13
	S2.3*	**31.7**	**0.34**	**0**	**200**	**7.1**	**489**	**1.72**
	S2.4*	**30.2**	**0.35**	**0**	**197**	**7.1**	**444**	**1.61**

*** ACI/CSA punching shear strength predictions were unconservative for these specimens**

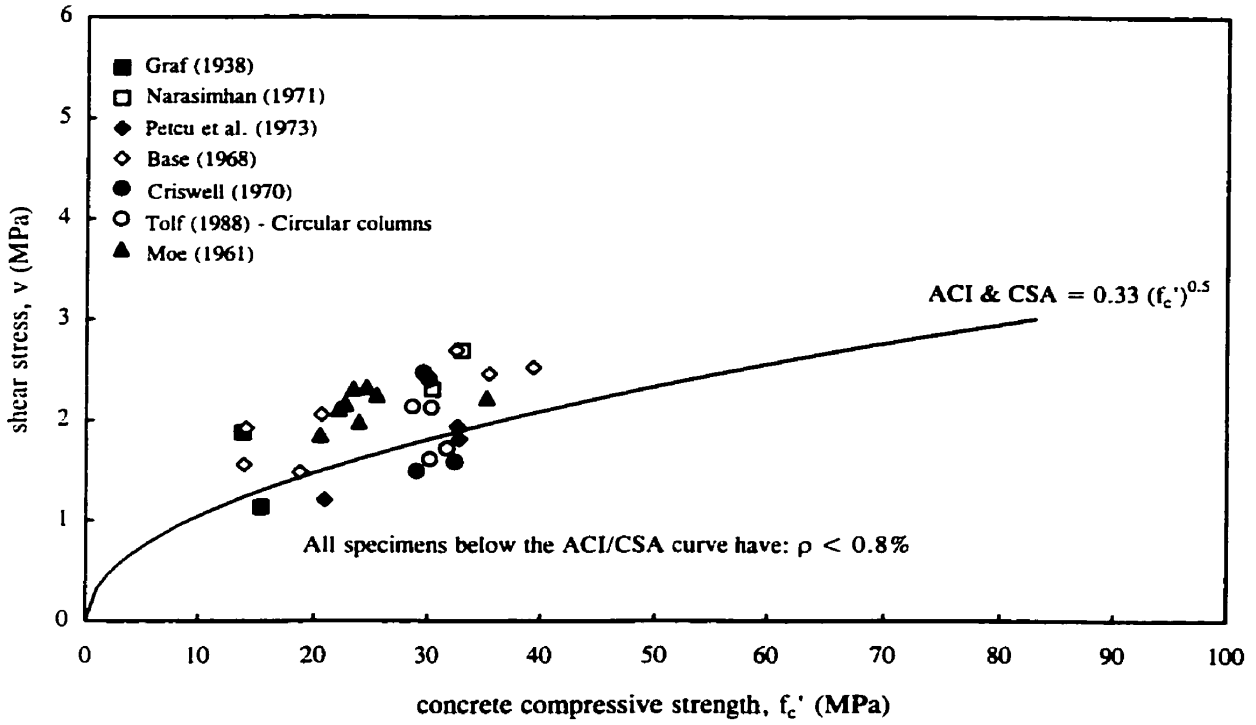

Figure 5.1 Comparison of shear failure predictions and experimental results by various investigators

Table 5.2 summarizes the different properties and punching shear test results of the thirty eight slabs tested by Elstner *et al.* (1956). In 1957, Whitney studied the failure mechanisms of these 38 specimens and concluded that some of the slabs with high reinforcement ratios had actually failed in bond failure and not shear. He believed that the close spacing of the rebars in those specimens resulted in the failure of the anchorage of the steel bars in the concrete thus leading the specimens to fail in a bond type of failure. All the specimens with very high reinforcement ratios ($\rho > 7\%$) were, therefore, not included in this study. Also, specimens B-1, B-2 and B-3 ($\rho < 1\%$) were not included as they failed in flexure.

Table 5.2 Experimental data for slab tests performed by Elstner *et al.* (1956)

Specimen	f_c' (MPa)	f_y (MPa)	ρ (%)	ρ' (%)	d (mm)	c (mm)	b_o/d	P_u (kN)	v (MPa)
TESTS AT UNIVERSITY OF ILLINOIS, 1952									
A-1a	14.07	332.58	1.15	0.56	118	254	12.64	302.48	1.73
A-1b	25.24	332.58	1.15	0.56	118	254	12.64	364.75	2.09
A-1c	29.03	332.58	1.15	0.55	118	254	12.64	355.86	2.04
A-1d*	**36.82**	**332.58**	**1.15**	**0.56**	**118**	**254**	**12.64**	**351.41**	**2.01**
A-1e	20.27	332.58	1.15	0.56	118	254	12.64	355.86	2.04
A-2a	13.65	321.54	2.47	1.15	114	254	12.89	333.62	1.98
A-2b	19.51	321.54	2.47	1.15	114	254	12.89	400.34	2.38
A-2c	37.44	321.54	2.47	1.15	114	254	12.89	467.06	2.77
A-7b	27.92	321.54	2.47	1.15	114.3	254	12.89	511.54	3.04
A-3a	12.77	321.54	3.7	1.15	114.3	254	12.89	355.86	2.11
A-3b	22.63	321.54	3.7	1.15	114.3	254	12.89	444.82	2.64
A-3c	26.57	321.54	3.7	1.15	114.3	254	12.89	533.78	3.17
A-3d	34.57	321.54	3.7	1.15	114.3	254	12.89	547.13	3.25
A-4	26.13	332.58	1.15	0.56	118	355.6	16.10	400.34	1.80
A-5	27.79	321.54	2.47	1.15	114	355.6	16.44	533.78	2.48
A-6	Unusual behaviour reported (Whitney, 1957). Not included in graphs								
A-7	28.48	321.54	2.47	1.15	114	254	12.89	400.34	2.38
A-8	21.93	321.54	2.47	1.15	114	355.6	16.44	435.92	2.03
A-7a*	**27.92**	**321.54**	**2.47**	**1.15**	**114**	**254**	**12.89**	**280.24**	**1.66**
A-9 & A-10	Concentrated reinforcement: flexural steel ratio > 7%. Not included in graphs								
A-11 & A-12	Eccentric thrust on column								
A-13	Unusual behaviour reported (Whitney, 1957). Not included in graphs								
TESTS AT PCA LABORATORIES, 1954									
B-1**	14.20	324.30	0.50	0	114.3	254	12.89	178.37	1.06
B-2**	47.58	320.85	0.50	0	114.3	254	12.89	200.17	1.19
B-4**	47.71	303.60	0.99	0	114.3	254	12.89	333.62	1.98
B-9	43.92	341.55	2.00	0	114.3	254	12.89	504.87	3.00
B-11	13.51	409.17	3.00	0	114.3	254	12.89	329.17	1.95
B-14	50.54	325.68	3.00	0	114.3	254	12.89	578.27	3.43
B-3 to B-17	Shear reinforcement provided.								

***ACI/CSA punching shear predictions were unconservative for these specimens**

** Specimens failed in flexure. Not included in graphs

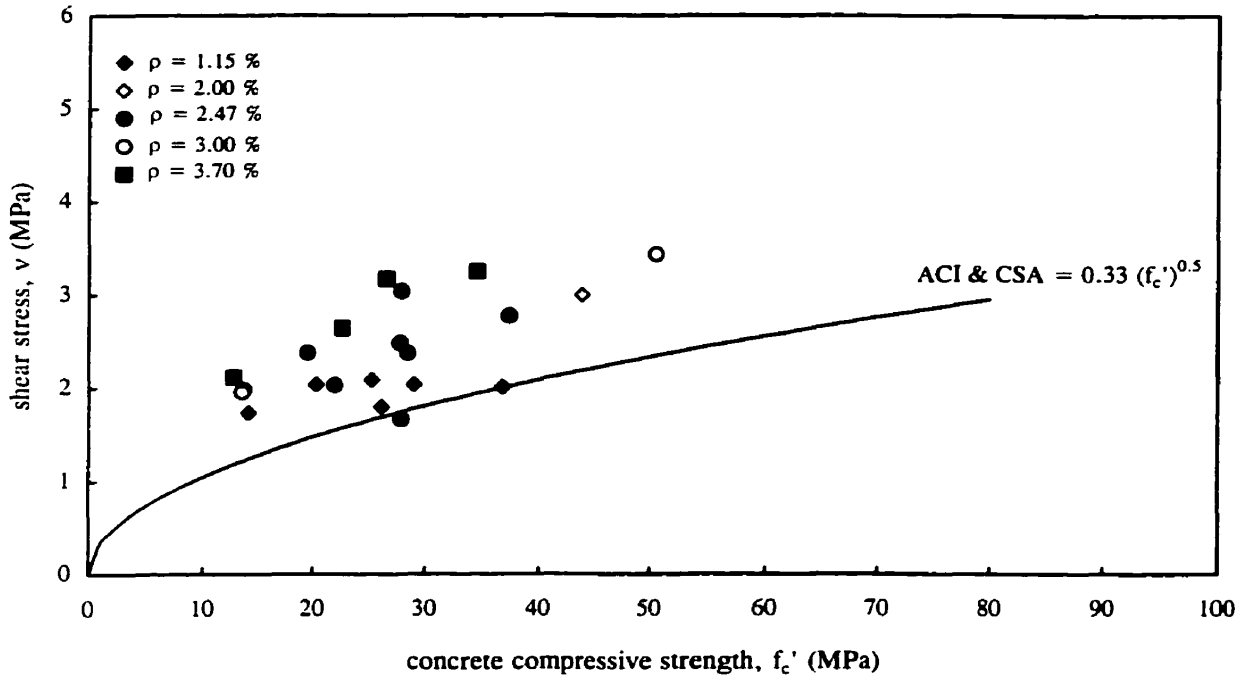

Figure 5.2 Comparison of shear failure predictions and experimental results by Elstner *et al.* (1956)

Figure 5.2 compares the shear failure predictions of the ACI Code and the CSA Standard to the experimental results obtained by Elstner *et al.* (1956). It can be seen from Fig. 5.2 and Table 5.2 that the American and the Canadian codes give conservative shear strength predictions for all the specimens except for specimen A-7a (ρ = 2.47%).

In 1961, Moe carried out experiments that were designed to complement those of earlier tests (especially those of Elstner *et al.*). He tested forty three, 6 ft by 6 ft, 6 in. thick, slabs of which only the 8 slabs of Series SA were interior slab-column connections without shear reinforcement and loaded concentrically. Moe designed this series of slabs to determine the effect that concentrating the flexural reinforcement in narrow bands across the column would have on the punching shear capacity of the slabs. The eight slabs, thus, displayed varying degrees of concentration of the flexural reinforcement near the column. The properties and test results of these slabs are summarized in Table 5.3. A comparison of the punching shear code predictions with the experimental results obtained by Moe can be found in Fig. 5.1. From this figure, it can be seen that the ACI Code and the CSA Standard provide conservative predictions for the punching shear strength of the slabs tested by Moe.

Table 5.3 Experimental data for slab tests performed by Moe (1961)

Series SA - Concentration of Tensile Reinforcement									
Specimen	f_c' (MPa)	f_y (MPa)	ρ (%) inner bands	ρ (%) outer bands	d (mm)	c (mm)	b_o/d	P_u (kN)	v (MPa)
S1-60	23.32	399.44	1.06	1.06	114.3	254	12.89	389.22	2.31
S2-60	22.08	399.44	1.53	0.84	114.3	254	12.89	355.86	2.11
S3-60	22.63	399.44	2.3	0.54	114.3	254	12.89	363.64	2.16
S4-60	23.84	399.44	3.45	0.265	114.3	254	12.89	333.62	1.98
S1-70	24.5	482.72	1.06	1.06	114.3	254	12.89	392.33	2.33
S3-70	25.39	482.72	2.3	0.54	114.3	254	12.89	378.1	2.25
S4-70	35.19	482.72	3.45	0.265	114.3	254	12.89	373.65	2.22
S4A-70	20.49	482.72	3.45	0.265	114.3	254	12.89	311.37	1.85

Marzouk *et al.*(1991) tested 17 high-strength, interior slab-column connections. The concrete strength, f_c', and the reinforcement ratio, ρ, were the two parameters that were varied in their tests. Table 5.4 summarizes the characteristics and the test results of the seventeen slab specimens. Figure 5.3 is a comparison of the shear failure predictions of the American and Canadian codes with the experimental results obtained by Marzouk *et al.* It can be seen from this figure that the ACI Code and the CSA Standard are conservative in their predictions, except for the slabs with low reinforcement ratios ($\rho < 0.9\%$).

Table 5.4 Experimental data for slab tests performed by Marzouk *et al.* (1991)

Specimen	f_c' (MPa)	ρ (%)	Bar Size (mm)	d (mm)	slab thickness (mm)	c (mm)	b_o/d	P_u (kN)	v (MPa)
NS1	42	1.474	M 10	95	120	150	10.32	320	3.44
NS2	30	0.944	M 10	95	150	150	10.32	400	4.30
HS1*	**67**	**0.491**	**M 10**	**95**	**120**	**150**	**10.32**	**178**	**1.91**
HS2*	**70.2**	**0.842**	**M 10**	**95**	**120**	**150**	**10.32**	**249**	**2.67**
HS3	69.1	1.474	M 10	95	120	150	10.32	356	3.82
HS4	65.8	2.37	M 15	95	120	150	10.32	418	4.49
HS5*	**68.1**	**0.64**	**M 10**	**125**	**150**	**150**	**8.80**	**365**	**2.65**
HS6	70	0.944	M 10	95	150	150	10.32	489	5.25
HS7	73.8	1.193	M 10	95	120	150	10.32	356	3.82
HS8	69	1.111	M 15	125	150	150	8.80	436	3.17
HS9	74	1.611	M 15	125	150	150	8.80	543	3.95
HS10	80	2.333	M 15	125	150	150	8.80	645	4.69
HS11	70	0.952	M 10	75	90	150	12.00	196	2.90
HS12	75	1.524	M 10	75	90	150	12.00	258	3.82
HS13	68	2	M 10	75	90	150	12.00	267	3.96
HS14	72	1.474	M 10	95	120	220	13.26	498	4.16
HS15	71	1.474	M 10	95	120	300	16.63	560	3.73

*** ACI/CSA punching shear predictions were unconservative for these specimens**

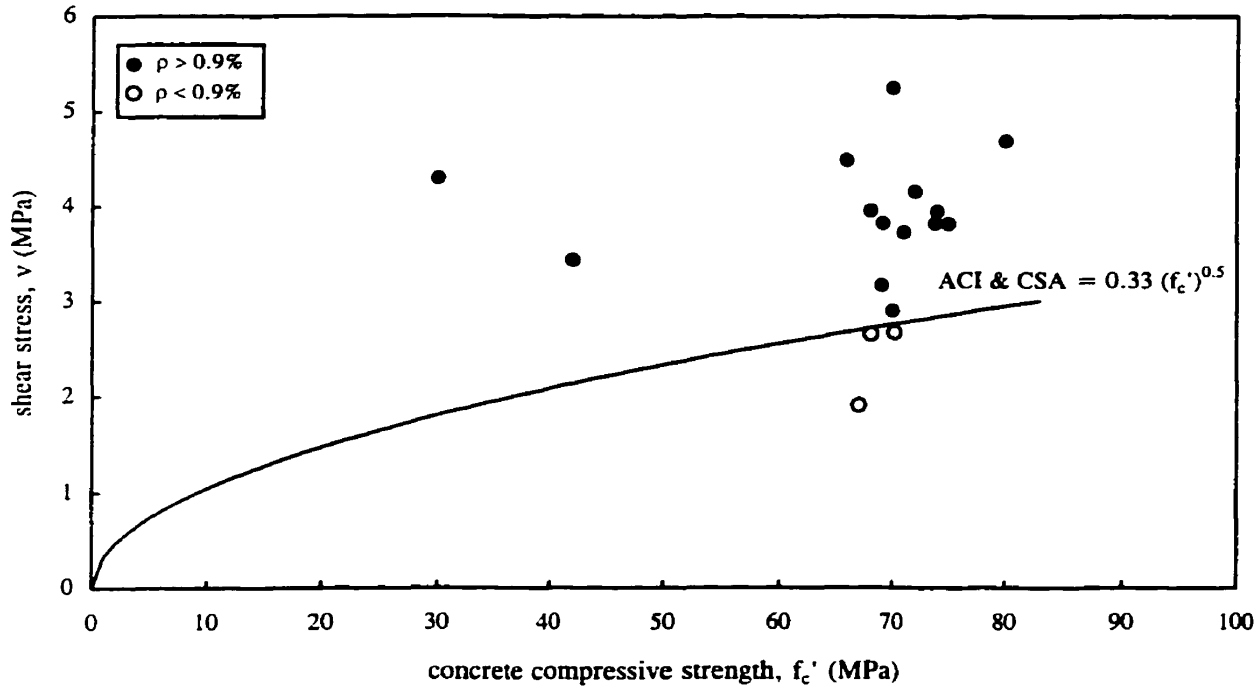

Figure 5.3 Comparison of shear failure predictions and experimental results by Marzouk *et al.* (1991)

5.2 Summary of Code Predictions

From the test results presented in the previous section, it was shown that the ACI Code and the CSA Standard provide conservative punching shear predictions for interior slab-column connections, except for certain slabs in which the reinforcement ratio was low ($\rho < 0.9\%$). This can also be seen from Fig. 5.4 which compares the shear failure predictions of these codes to the various experimental punching shear test results published in the literature.

Figure 5.5 shows a plot of $v/\sqrt{f_c'}$ versus the steel flexural reinforcement ratio, ρ. From this figure, it can be seen that the American and the Canadian codes seem to be in good agreement with the experimental results, for a reinforcement ratio of about 1%. However, their expressions for punching shear are somewhat unconservative for $\rho < 1\%$, and are conservative for $\rho > 1\%$.

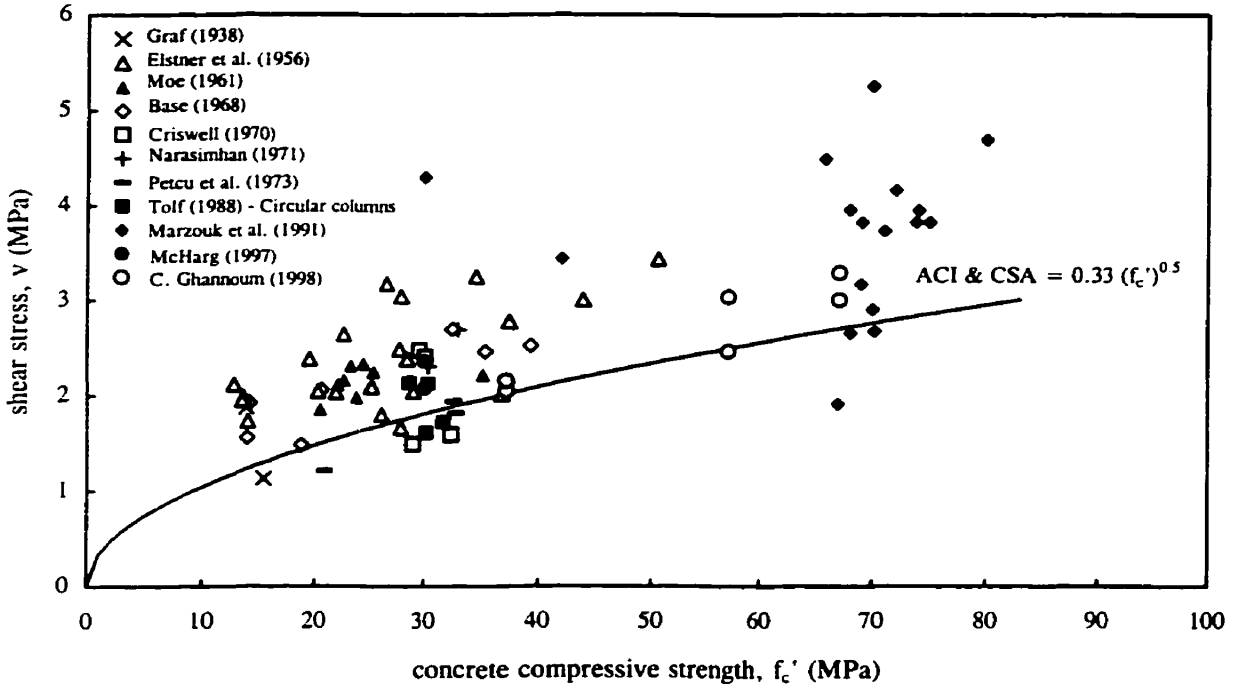

Figure 5.4 Effect of concrete strength on shear strength: Comparison with the ACI Code and the CSA Standard

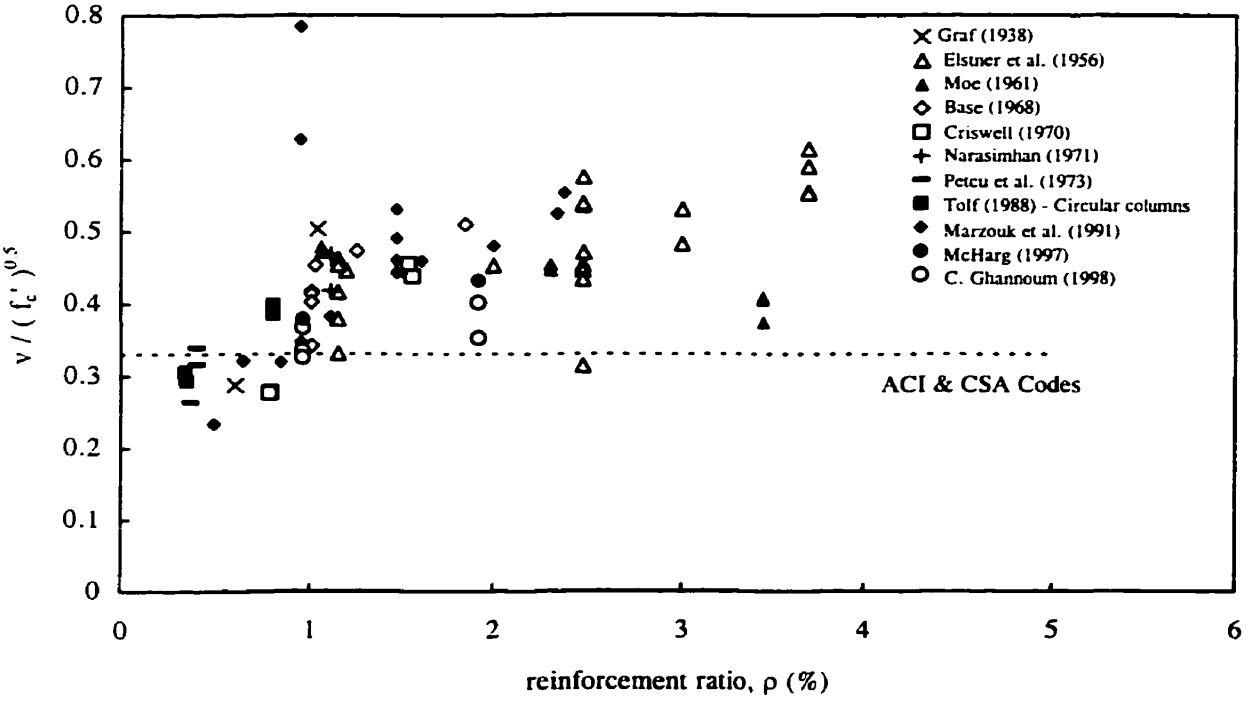

Figure 5.5 Effect of flexural reinforcement ratio on shear strength: Comparison with the ACI Code and the CSA Standard

It is concluded that the punching shear strength of slabs is a function of the flexural reinforcement ratio, ρ. As the ACI Code and the CSA Standard do not include the amount of flexural reinforcement in their shear strength calculations it is recommended that their punching strength expressions be modified to take into account the effect that the flexural reinforcement ratio has on the punching shear capacity of interior slab-column connections.

Chapter 6

Conclusions

6.1 Conclusions of this Experimental Program

The following conclusions were drawn from the results of the experimental program on the two-way slab specimens and from a similar experimental study by McHarg (1997):

1. Concentrating the top mat of flexural reinforcement in slabs, as required by the 1994 CSA Standard, results in a higher punching shear strength, a greater post-cracking stiffness, a more uniform distribution of the strains in the top flexural bars and smaller crack widths up to and including full service loading. The increase in the punching shear strength, due to the concentration of the top reinforcing bars in the "immediate column region", was 5% for the S1 Series, 23% for the S2 Series and 9% for the S3 Series.
2. Increasing the concrete compressive strength of slabs results in an improvement in their performance, with an increase in the punching shear strength, an increase in the post-cracking stiffness, a greater ductility and smaller crack widths. Also, for the specimens with a banded distribution of top reinforcing bars, the increase in concrete strength results in smaller strains in the flexural steel reinforcement at full service load. The increase in the punching shear resistance of slabs due to the use of high-strength concrete was 21% and 41% for Specimens S2-U and S3-U, with the uniform distribution of top bars, and was 47% and 53% for Specimens S2-B and S3-B, with the banded flexural reinforcement distribution, over the punching shear resistance of the S1 Series.
3. The ACI Code (1995) and the CSA Standard (1994) give conservative strength predictions for the punching shear of the two-way slabs tested. The BS Standard (1985)

and the CEB-FIP Code (1990) expressions result in conservative predictions of the punching shear strength for all but one of the slab specimens tested. The BS Standard is unconservative for Specimen S1-B.

4. The punching shear strength expressions proposed by Rankin *et al.* and Sherif *et al.* both overestimate the punching shear capacity of the slabs tested. The equation proposed by Gardner *et al.* for computing the shear strength of slabs results in very conservative strength predictions.

Significance of results

It has been determined that concentrating the flexural reinforcement in the immediate column region, together with the use of high-strength concrete results in an improvement in the performance of two-way slabs.

6.2 Other Conclusions

The following conclusions were drawn from this experimental program and from test results for the punching shear strength of interior slab-column connections published in the literature:

1. The punching shear predictions of the American Code and the Canadian Standard seem to be in good agreement with experimental results for a reinforcement ratio, ρ, of about 1%. However, the code expressions for punching shear are somewhat unconservative for $\rho < 1\%$, and are very conservative for $\rho > 1\%$.
2. The punching shear strength of slabs is a function of the flexural reinforcement ratio, ρ.
3. The ACI 318-95 Code and the CSA A23.3-94 Standard expressions for the punching shear strength of interior slab-column connections should be modified to take into account the effect that the flexural reinforcement ratio, ρ, has on the punching shear strength of slabs.

References

CODES

American Concrete Institute (ACI) 1989. Building Code Requirements for Reinforced Concrete and Commentary (ACI 318-89 and ACI 318R-89). Detroit, Michigan, 353 pp.

American Concrete Institute (ACI) 1995. Building Code Requirements for Reinforced Concrete and Commentary (ACI 318-95 and ACI 318R-95). Detroit, Michigan, 369 pp.

Canadian Standards Association (CSA) 1984. CSA A23.3-M84. Code for the Design of Concrete Structures for Buildings. CSA, Rexdale, Ont., 281 pp.

Canadian Standards Association (CSA) 1994. CSA A23.3-94. Design of Concrete Structures. CSA, Rexdale, Ont., 220 pp.

Comité Euro-International du Béton et Fédération Internationale de la Précontrainte (CEB-FIP) 1990. Model Code for Concrete Structures (MC90 model code). Lausanne, Switzerland.

British Standard Institution (BSI) 1985. Structural Use of Concrete (Standard BS-8110). London, United Kingdom.

Associate Committee on the National Building Code (NBC) 1995. National Building Code of Canada 1995 (NBCC), National Research Council of Canada, Ottawa, 571 pp.

ACI / ASCE

ACI-ASCE Committee 426. 1974. " The Shear Strength of Reinforced Concrete Members-Slabs", Proceedings, ASCE, V. 100, ST8, August, pp. 1543-1591.

ACI-ASCE Committee 426. 1977. "Suggested Revisions to Shear Provisions for Building Codes", Journal of the American Concrete Institute, Proceedings, V. 74, No. 9, September, pp. 458-468.

ACI-ASCE Committee 352. 1988. "Recommendations for Design of Slab-Column Connections in Monolithic Reinforced Concrete Structures", Journal of the American Concrete Institute, V. 85, No. 6, November-December, pp. 675-696.

ACI Committee 363. 1984. "State-of-the-art Report on High-Strength Concrete", Journal of the American Concrete Institute, V. 81. No. , July-August, pp. 364-411.

OTHER REFERENCES

Alexander, S.D.B. and Simmonds S.H. 1988. " Shear-Moment Interaction of Slab-column Connections", Canadian Journal of Civil Engineering, Vo. 15, March, pp. 828-833.

Alexander, S.D.B. and Simmonds S.H. 1992. "Tests of Column-Flat Plate Connections", ACI Structural Journal, V. 89, No. 5, September-October, pp. 495-502.

Canadian Portland Cement Association (CPCA) 1991. "Analysis and Design of Slab Systems" (ADOSS), Ottawa.

Elstner, R.C. and Hognestad, E. 1956. "Shearing Strength of Reinforced Concrete Slabs", Journal of the American Concrete Institute, Vol. 53, No.1, July, pp. 29-58.

Gardner, N.J. and Shao, X. 1996. "Punching Shear of Continuous Flat Reinforced Concrete Slabs", ACI Structural Journal, V. 93, No. 2, March-April, pp. 218-228.

Graf, O. 1933. "Tests of Reinforced Concrete Slabs Under Concentrated Loads Applied Near One Support", (In German), Deutscher Ausschuss für Eisenbeton, berlin, Heft 73, 2 pages.

Graf, O. 1938. "Strength Tests of Thick Reinforced Concrete Slabs Supported on All Sides Under Concentrated loads", Deutscher Ausschuss für Eisenbeton, No. 88, Berlin, Germany.

Hawkins, N.M and Mitchell, D. 1979. "Progressive Collapse of Flat Plate Structures", Journal of the American Concrete Institute, Proceedings V.76, No. 7, July, pp. 775-808.

Hawkins, N.M, Mitchell, D. and Hanna S. 1975. "The Effects of Shear Reinforcement on the Reversed Cyclic Loading Behavior of Flat Plate Structures", Canadian Journal of Civil Engineering, Vo.2, August, pp. 572-582.

Hussein, A. 1990. "Behavior of Two-Way Slabs Made with High-Strength Concrete", M.Eng. Thesis, Memorial University of Newfoundland, St. John's, Newfoundland, August, 145 pp.

Joint Committee of 1924. 1924. "Standard Specification for Concrete and Reinforced Concrete. Joint Committee", Proceedings, American Society for Testing Materials, 24, Part I, pp. 312-385.

Kinnunen, S. and Nylander, H. 1960. "Punching of Concrete Slabs Without Shear Reinforcement", Transactions of the Royal Institute of Technology, Stockholm, No. 158, March, 112 pp.

Marzouk, H.M. and Hussein, A. 1991 a. "Experimental Investigation on the Behavior of High-Strength Concrete Slabs", ACI Structural Journal, V. 66, No. 6, pp. 701-713.

Marzouk, H.M. and Hussein, A. 1991 b. "Punching Shear Analysis of Reinforced High-Strength Concrete Slabs", Canadian Journal of Civil Engineering, V. 18, No. 6, pp. 954-963.

McHarg, P.J. 1997. "Effect of Fibre-Reinforced Concrete on the Performance of Slab-Column Specimens", M.Eng. Thesis, Mc Gill University, Quebec, July, 87 pp.

Moe, J. 1961. "Shearing Strength of Reinforced Concrete Slabs and Footings Under Concentrated Loads", Development Department Bulletin D47, Portland Cement Association, Skokie, Ill., April, 130 pp.

Rankin, G.I.B. and Long, A.E. 1987. "Predicting the Punching Strength of Conventional Slab-Column Specimens", Proceedings of the Institution of Civil Engineers (London), V. 82, Part 1, April, pp. 327-346.

Regan, P.E. 1971. "Behaviour of Reinforced and Prestressed Concrete Subject to Shear Forces", Paper 7441S, Proceedings of the Institution of Civil engineers, Vol. 50, London, England, December, p. 522. Supplement (xvii), pp. 337-364.

Regan, P.E. 1974. "Design for Punching Shear", Structural Engineer (London), V. 52, No. 6, pp. 197-207.

Regan, P.E. and Braestrup, M.W. 1985. "Punching Shear in Reinforced Concrete: A State of Art Report", Bulletin D'information No. 168, Comité Euro-International de Béton, Lauzanne, 232 pp.

Richart, F.E. 1948. "Reinforced Concrete Wall and Column Footings", Journal of the American Concrete Institute, October and November, Proc. V. 45, No. 2 and 3, pp. 97-127 and 237-260.

Shehata, I.M. and Regan, P. 1989. "Punching in Reinforced Concrete Slabs", ASCE Journal of the Structural Division, V. 115, ST7, pp. 1726-1740.

Sherif, A.G. and Dilger, W.H. 1996. "Critical Review of the CSA A23.3-94 Punching Shear Strength Provisions for Interior Columns", Canadian Journal of Civil Engineering, V. 23, March, pp. 998-1101.

Talbot, A.N. 1913. "Reinforced Concrete Wall Footings and Column Footings", Bulletin No.67, University of Illinois, Engineering Experiment Station, Urbana, Ill., March, 114 pp.

Whitney, C.S. 1957. "Ultimate Shear Strength of Reinforced Concrete Flat Slabs, Footings, Beams, and Frame Members Without Shear Reinforcement", Journal of the American Concrete Institute, Vol. 54, No. 4, October, pp. 265-298.

Zsutty, T.C. 1968. "Beam Shear Strength Prediction by analysis of Existing data", Proceedings of the American Concrete Institute, V. 65, November, p. 943.

Appendix A

Design of Test Specimens

This appendix describes the design of the interior region of the flat plate structure described in Chapter 2 and shown in Fig. 2.1. This typical flat plate was a four bay by four bay structure, with 4.75 m square panels. The small column size (225 x 225 mm) used in this structure was chosen to produce high punching shear stresses in the slab around the column and to, thus, ensure that a punching shear mode of failure will occur.

The slab was designed for assembly area use as specified by the National Building Code of Canada (NBCC, 1995). The applied loads on this structure were, thus, a superimposed dead load of 1.2 kPa and a specified live load of 4.8 kPa.

As the slab specimens tested in this experimental program were to be compared to the similar normal strength concrete slabs tested by McHarg (1997), a specified 28-day concrete compressive strength of 30 MPa was used for this design. The steel yield stress was 400 MPa.

The design was according to the CSA A23.3-94 Standard. The key steps of this design are given below:

a) Choice of Slab Thickness (Clause 13.3.3)

$$h_s \geq \frac{l_n}{30}\left(0.6 + \frac{f_y}{1000}\right)$$

$$\geq \frac{(4750 - 225)}{30}\left(0.6 + \frac{400}{1000}\right)$$

$$\geq 150.8 \text{ mm}$$

Use $h_s = 150$ mm.

b) Critical Shear Section (Clause 13.4.3)

$$d = h - \text{cover} - d_b$$

$$= 150 - 25 - 15 = 110 \text{ mm}$$

$$b_o = 4 \times (d + c)$$

$$= 4 \times (110 + 225) = 1340 \text{ mm}$$

c) Maximum Shear Stress Resistance (Clause 13.4.4)

Nominal Shear Stress Resistance, V_n,

$$V_n = 0.33\sqrt{f_c'}\, b_o d$$
$$= 0.33\sqrt{30}\,(1340)(110)$$
$$= 266.4 \text{ kN}$$

Factored Shear Stress Resistance, V_r,

$$V_r = 0.4\phi_c\sqrt{f_c'}\, b_o d$$
$$= 0.4(0.6)\sqrt{30}\,(1340)(110)$$
$$= 193.8 \text{ kN}$$

d) Applied Shear Stress (Clause 13.4.5)

Factored Shear Stress, V_f,

$$V_f = \text{T. A.} \times w_f$$

where: T.A. is the tributary area, calculated as:

$$\text{T. A.} = (4.75 - 0.225 - 0.110)^2 = 19.5 \text{ m}^2$$

The self weight of the slab, s. w., is:

$$\text{s. w.} = \frac{2400(9.81)(0.150)}{1000} = 3.53 \text{ kPa}$$

Superimposed dead load = 1.2 kPa

live load = 4.8 kPa

$$\therefore \quad w_f = (3.53 + 1.2) \times 1.25 + (4.8) \times 1.5 = 13.1 \text{ kPa}$$

Now,

$$V_f = \text{T. A.} \times w_f$$
$$= 19.5 \times 13.1$$
$$= 255.3 \text{ kN}$$

e) Determination of Applied Factored Moments

The determination of the total negative factored moment was done with the computer programme ADOSS:

$M_{f(total)} = 94.0$ kNm

Factored Moments in Column Strips (Clause 13.12.2)

Multiply by factor within 0.6 and 1.0 for negative moment at interior column

Choose 0.75, therefore: $M_{f(total)}(75\%) = 70.5$ kNm, for column strip, and,

$M_{f(total)}(25\%) = 23.5$ kNm, for middle strip.

f) Factored Moment Resistance

$$M_r = \phi_s (A_s \cdot f_y) \left[d - \frac{a}{2} \right]$$

$$= \phi_s (A_s \cdot f_y) \left[d - \frac{\phi_s (A_s \cdot f_y)}{2 \alpha_1 \phi_c f_c' b} \right]$$

where,

$\alpha_1 = 0.85 - 0.0015 f_c' \geq 0.67$ (clause 10.1.7)

$= 0.805$

$$M_r = 0.85 (A_s \cdot 400) \left[102.5 - \frac{0.85 (A_s \cdot 400)}{2 \cdot 0.805 \cdot 0.6 \cdot 30 \cdot 2160} \right]$$

for column strip, where $M_r = M_f = 70.5$ kNm, gives $A_{s(required)} = 2254.3$ mm^2

Try $A_s = 2800$ mm^2 (14-No.15 bars)

for middle strip, where $M_r = M_f = 23.5$ kNm, gives $A_{s(required)} = 696.4$ mm^2

Try $A_s = 800$ mm^2 (4-No.15 bars)

minimum flexural steel, $A_{s(min)} = (200) \times 2500/450 = 1112$ mm^2

Therefore use $A_s = 1200$ mm^2 for middle strip (6-No.15 bars)

g) Reinforcement for Interior Slab-Column Connections (Clause 13.12.2.1)

At least one-third of the reinforcement for total factored negative moment at interior columns shall be located in a band with a width extending a distance $1.5h_s$ from the side faces of the column.

Band width, b.w. is:

$$\begin{aligned} b.w. &= 3 \cdot h + c \\ &= 3 \cdot 150 + 225 \\ &= 675 \text{ mm} \end{aligned}$$

One-third of the total steel must be in the band width, that is:

$$\begin{aligned} A_{s\,(b.w.)} &= \frac{1200 + 2800}{3} \\ &= \frac{4000}{3} \\ &= 1333.3 \text{ mm}^2 \end{aligned}$$

Use $A_s = 1600 \text{ mm}^2$ (8-No.15 bars)

Spacing, s = 675/8 = 84.4 mm

h) Curtailment of Reinforcement (Clause 13.12.5.1)

Without drop panels (from Figure 13-1)

top bars:

minimum % of A_s	**minimum distance bar must extend into slab from column face:**
50 %	$0.30l_n = 0.30(4525) = 1357.5$ mm
remainder	$0.20l_n = 0.20(4525) = 905$ mm

maximum length available in specimen is 0.5 (2300-225) = 1037.5 mm

therefore weld steel plates to the end of half of the bars.

i) Minimum Reinforcement for Structural Integrity (Clause 13.11.5)

The summation of the area of bottom reinforcement connecting the slab to the column on all faces of the periphery of the column shall be:

$$\Sigma A_{sb} \geq \frac{2V_{se}}{f_y}$$

where: V_{se} = shear transmitted to column due to specified loads, but not less than the shear corresponding to twice the self-weight of the slab.

$$\therefore A_{sb} = \frac{2\,(3.53 + 1.2 + 4.8)\,.\,(1000)}{400}$$

$$= 1170 \text{ mm}^2$$

A_{sb} required for one face = 1170/4 = 292.5 mm^2

Therefore use 3-No. 10 bars in each direction.